Doctoral Dissertation

博士論文

Development of Fire Sprinklers and Extinguishing System for Residential Application

一般住宅用スプリンクラーと消火システムの開発

Juhwan OH

呉 周煥

Graduate School of Science and Engineering

Yamaguchi University

山口大学理工学研究科

March 2014

ABSTRACT

Development of Fire Sprinklers and Extinguishing System

for Residential Application

Three related studies are presented in this dissertation.

Firstly, the practicality of direct connection to domestic water supply line with additional auxiliary water tank and booster pump to guarantee successful operation of the residential sprinkler system is investigated. The investigation was done by surveying the conditions of domestic water supply system in terms of water pressure, flow rate and piping network. Furthermore, actual fire tests were conducted to verify the performance of the system against varied water pressure, flow rate and sprinkler K-factors. It was found that additional water tank with booster pump is required if the pressure at the sprinkler is lower than 0.1 MPa. The findings have led to the design and development of a compact package-type fire sprinkler system for residential fire protection application.

Secondly, an analytical model for predicting the assembly loads and structural response of the sprinkler is developed. Equilibrium force system equations are derived considering load transfer mechanics within several contacting components for the two-step assembly process. Components integration and downsizing which have enabled an innovative design of the deflector with equally-sized spray ports uniformly located around the circumference are proposed. The size of the rectangular ports and the gap between the heat collector and deflector are taken as design parameters for improving water spray distribution pattern and response time index (RTI) characteristics of the sprinkler. Design parameters are explored and

corresponding prototypes are tested to verify water spray distribution pattern and RTI performance. The analytical model for predicting assembly loads is verified with experimental testing. Tests revealed that the proposed analytical model agrees significantly with test data. The proposed sprinkler exhibits even spray distribution patterns when tested at different water pressures with RTI that meets standard regulations for residential application. Moreover, the proposed sprinkler is relatively slimmer with seven-piece less components resulting to an over 32% weight reduction compared to existing design.

Lastly, the ubiquitous technology is implemented for the purpose of ensuring fire safety in residential buildings through wireless fire detection and extinguishing system. This system also aimed at reducing installation cost due to space restriction and promoting ease and practicality of installation in existing residential buildings. The main ideas of the proposed fire detection and extinguishing system were: firstly, in housing condition where it is not easy or impractical to install conventional fire detection equipment, a smart fire sensor network using wireless communication system that activates and sends warning alarm within the building, to the building residents, and the fire department was developed. Secondly, to implement an improved, compact water-based fire sprinkler system with higher discharge so that the fire can be effectively controlled or extinguished at the early stage. The compactness of the sprinkler system is believed to cut the total installation cost. The two systems were integrated for the development of practical wireless fire detection and sprinkler system for residential building applications. Experimental tests were conducted to verify the system performance.

要　旨

一般住宅用スプリンクラーと消火システムの開発

近年、住宅火災が建物火災の約 60%にのぼる。また、死者数で見ると住宅火災による死者数が火災による総死者数の 55%を占め、65 歳以上の高齢者の死者数が住宅火災による死者数の 60%も占め、一般者より 2.7 倍も高い。これは高齢者が体の不自由で逃げ遅れのためと考えられる。特に高齢者や障害者のための福祉施設での火災における多数の犠牲者が問題となっている。これらの被害を減らすため、福祉施設や住宅などに安価で簡便に設置できる住宅用スプリンクラー消火システムの開発が求められている。最近、スプリンクラー消火システムを住宅に導入しやすくするため、コスト面を配慮した消防法の改正によりで水道管に直結することが認められている。しかし実際運用しようとすると様々な問題がある。例えば、地域における水道水の圧力変動や家庭用水道管の太さの違いなどで直結できないこと場合がある。そのほか衛生面などの問題もある。本研究では、低コストかつ設置容易なスプリンクラー消火装置を開発すると共に、本装置にも適応可能な低コストで高性能なスプリンクラーヘッドの設計開発、さらに、ICT 技術を活用した火災・ガス漏れ等の自動通報と自動消火システムの開発を目指す。

本論文は緒論・結言を含め 6 章から構成されている。第 1 章は研究の背景、既存のスプリンクラーシステム設計の考え方及び本論文の概要について述べている。第 2 章では既存のスプリンクラーシステムの概要、火災実験や評価方法を説明し、研究の方向性を述べている。第 3 章では低コストで住宅に簡単に設置できるコンパ

クトスプリンクラー消火装置の開発を行った。コストを下げるため、水道の圧力変動や水道管の太さの違いを十分に考慮し最低必要の補助水タンクの容量を実験的に求めた。また、停電時にも対応できるようバディリーに自動切り替える駆動システムも開発した。さらに、本装置に対して実環境下の火災実験を行い、本装置の有効性、日本ならびに韓国の消防法の要件基準を満たすことを確認できた。第 4 章においては、散水分布性能の向上とコスト削減を目指した新しいスリムタイプスプリンクラーヘッドの設計開発を行った。スプリンクラーヘッドは、内部プレート、外部プレート、保持リング、フレーム、可溶片、デフレクターなどから構成され、構造的に非常に複雑のため、スプリンクラーヘッドの設計開発は実験と経験に頼っている。本研究では、内部プレート、外部プレート、保持リング、フレームなどの重要な部品に対する力学モデルを立て、スプリンクラーヘッドを組み立てる際に応力解析方法を提案した。実証実験により理論結果が非常に合致することを確認できた。また、新しく設計したヘッドはスリム化し、部品数も 6 つ減らすことができ、既存のものより重さを 32%軽くすることができた。また、水圧の異なる環境下で散水分布実験を行い、現在市販の数種類のスプリンクラーヘッドの特性と比較検証をした。本開発したスプリンクラーヘッドは既存のものに比べ散水分がかなり改善された。第 5 章では Zigbee 無線デバイスと警報器を内蔵した火災検知器とガス漏れ検知器を設計開発し、ICT 技術を活用した遠隔・自動通報システムを開発した。検知器が異常を検知するとまたは火災が発生すると、その情報をすぐに消防署に通報すると同時、あらかじめ登録されている家族や友人へ連絡する。さらに、実住宅環境下において火災実験を行い、無線警報器とスプリンクラーの配置の最適化も考慮して、本システムの有効性と実用性が確認された。第 6 章はまとめである。

TABLE OF CONTENTS

CONTENT Page

LIST OF FIGURES

LIST OF TABLES

Chapter 1

INTRODUCTION

Numerous fires occur in residential buildings almost every year worldwide. Even in many advanced countries, the number of fatalities, injury, and loss or damage of properties due to residential fire is alarming and triggers great concern. Concerns over life safety, property protection against fire, and advances in fire sprinkler system technology have driven international consensus on the use and installation of fire sprinkler system in residential building and facilities. The present challenge is seemingly focused on meeting the demands with the most innovative and economical residential automatic fire sprinkler system.

In residential installation, methods for supplying water to the sprinkler system include direct connection to the domestic water supply, use of high pressure water tank or storage tank with booster pump. Direct connection to the domestic water supply line is generally popular in most residential homes consisting of up to two floors. However, in case where the residential structure is situated in elevated location or away from the domestic water supply line, the significant drop in water pressure and flow may reduce the capability of fire sprinklers to extinguish a fire. In this study, the practicality of direct connection to domestic water supply line with additional auxiliary water tank and booster pump to guarantee successful operation of the sprinkler system is investigated. The investigation was done by first surveying the conditions of domestic water supply system in terms of water pressure, flow rate and piping network. Actual fire tests were conducted to verify the performance of the system against varied water pressure, flow rate and sprinkler K-factors. The findings

have led to the design and development of a compact package-type fire sprinkler system for residential fire protection application.

A relatively large number of individual components for an existing fusible link, flush type pendent residential sprinkler render complexity of the assembly process. For such type of sprinkler, knowledge of the assembly mechanics is critical for ensuring proper and reliable operation over its intended service life. However, analytical method for predicting the assembly loads and structural response of such sprinkler has neither been well-established nor published in scholarly literature. Furthermore, the existing sprinkler was observed to spray water unevenly due to its tripod-mounted deflector. The impress screw that is used to provide the required force to seal the nozzle and prevent water leakage is manipulated from the interior of the sprinkler making it difficult to visually check the structural condition during and after assembly process. The large number of individual components also contributes to increased product cost, product rejection rate and high probability of activation malfunction. In this study, an analytical model for predicting the assembly loads and structural response of the sprinkler is developed. Equilibrium force system equations are derived considering load transfer mechanics within several contacting components for the two-step assembly process. Components integration and downsizing which have enabled an innovative design of the deflector with equally-sized spray ports uniformly located around the circumference are proposed. The size of the rectangular ports and the gap between the heat collector and deflector are taken as design parameters for improving water spray distribution pattern and response time index (RTI) characteristics of the sprinkler. Design parameters are explored and corresponding prototypes are tested to verify water spray distribution

pattern and RTI performance. The analytical model for predicting assembly loads is verified with experimental testing. Tests revealed that the proposed analytical model agrees significantly with test data. The proposed sprinkler exhibits even spray distribution patterns when tested at different water pressures with RTI that meets standard regulations for residential application. Moreover, the proposed sprinkler is relatively slimmer with seven-piece less components resulting to an over 32% weight reduction compared to existing design.

In modern residential houses, nursing homes for elderly and physically-impaired persons, a fully automatic fire protection system is seen to be necessary to ensure safety against the hazards brought by fire. While the current communication technology within the fire-fighting industry is mostly still based on wired system, there is a growing need for the application of wireless communication between fire protection system components with the capability of home network integration. Zigbee-equipped wireless smoke sensors along with IT technology can activate alarms if a fire occurs. In this study, the ubiquitous technology is implemented for the purpose of ensuring fire safety in residential buildings through wireless fire detection and extinguishing system. This system also aimed at reducing installation cost due to space restriction and promoting ease and practicality of installation in existing residential buildings. Unlike wired interconnection which may only be practical for use in new construction, especially if the wires are laid out without cutting walls and ceilings (or floors in multi-story residence) the wireless interconnected sensors can be conveniently retrofitted in buildings without costly wire installations. In effect, the building interior design is not compromised and total installation cost can be significantly reduced. The main ideas of the proposed fire

detection and extinguishing system were: firstly, in housing condition where it is not easy or impractical to install conventional fire detection equipment, a smart fire sensor network using wireless communication system that activates and sends warning alarm within the building, to the building residents or owner, and the fire department was developed. Secondly, to implement an improved compact water-based fire extinguishing sprinkler system with higher discharge so that the fire can be effectively extinguished at the early stage. The compactness of the extinguishing system is believed to cut the total installation cost. The two systems were integrated for the development of practical wireless fire detection and extinguishing system for residential building applications. Experimental equipment for water supply with specific type of sprinklers and wireless communication were developed and tested to verify the system performance.

The thesis is organized as follows: Chapter 2 presents the review of related studies and formulation of the research objectives. Chapter 3 describes the development of package type fire extinguishing system for residential use. Chapter 4 presents the analysis and design of fusible, flush pendent sprinkler. Chapter 5 presents the implementation of embedded system for the development of smart automatic residential fire extinguishing system. Finally, Chapter 6 contains the conclusions. References and Appendix are found at the end of this dissertation.

Chapter 2

RELATED LITERATURE

2.1 Background

Fire sprinkler system is a fire extinguishing or suppression system consisting of a network of overhead pipes fitted with sprinklers that automatically open when the predetermined temperature has been reached and release water at adequate pressure and flowrate. It is extensively used worldwide with great majority in factories and large commercial buildings but its use for homes and small building is expanding rapidly. Statistics show that in buildings completely protected by fire sprinkler systems, over 99% of fires were controlled by fire sprinklers alone [1, 2].

2.1.1 Fire sprinklers

Fire sprinklers or simply sprinkler are orifices that direct a jet of water onto a deflector plate which defuses over a large area. The water is held back by a glass bulb or fusible link that holds an orifice plug in place. When heat is applied from a fire below, the glass bulb will burst, due to expansion of the liquid in the bulb, or the fusible link made of fusible alloy such Wood's alloy (metal) will melt, which then releases the plug and water flows through the sprinkler orifice

The hot gases from a fire will raise the temperature at ceiling level and when the area adjacent to the sprinkler reaches a specific temperature that sprinkler will actuate and spray water on to a fire. Only the sprinklers over the fire will open and the others will remain closed. This limits any damage to areas where there is no fire and reduces the amount of water needed. Sprinklers can be placed in enclosed roof

spaces. For residential application, sprinklers heads can be installed in almost all interior areas of the building.

Sprinklers can be generally classified according to the manner to which they are activated – *glass bulb type* and *fusible link type* (as mentioned above). Moreover, sprinklers are commonly further classified according to their intended use and installation – *pendent sprinkler* in which water jet is directed downward against the deflector, *sidewall sprinkler* in which water is discharged away from the wall resembling a quarter sphere and *upright sprinkler* in which water jet is directed upward against the deflector. Standardized classification of sprinklers are defined in NFPA 13 [3]. Figure 2.1 shows examples of some sprinkler and an illustration of the activation process of a fusible flush pendent type sprinkler during fire.

Glass bulb type Fusible link type

(a) Sprinkler types

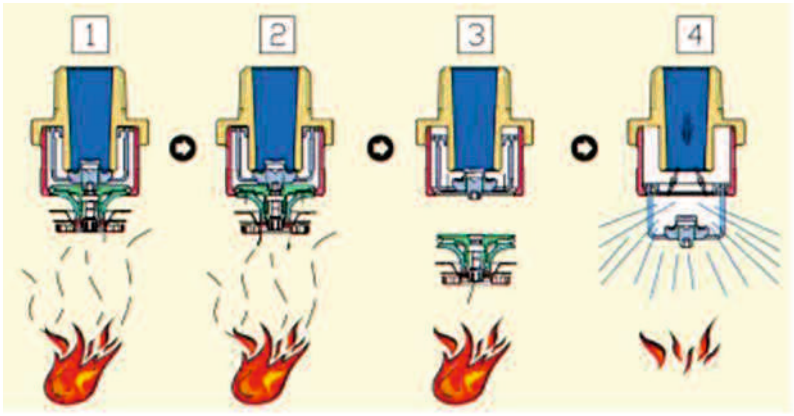

(b) Heat from fire reaches the sprinkler (1), fusible link melts at predefined temperature (2), fusible link ejects and releases orifice plug (3) and deflector descends with water discharging into the area (4)

Figure 2.1 (a) Examples of some sprinklers (b) activation of a fusible link type sprinkler.

The sprinkler orifice is designed to provide a known water flow rate at a design water pressure. Sprinkler orifices conform to Bernoulli's orifice equation, which states that the velocity of the water through the orifice is proportional to the water pressure, P [3]. For sprinkler design applications the volumetric flow rate, Q, is commonly used than the velocity. Therefore for design applications, Bernoulli's orifice equation is rewritten as

$$Q = K\sqrt{P} \tag{2.1}$$

The orifice flow coefficient, K, is known as the sprinkler "K-factor". It is nearly constant for the range of operating pressures used in sprinkler applications. The K-Factor is nominally proportional to the square of the orifice diameter [4]. The units used for the K-Factor are $\text{liters} \cdot \text{minute}^{-1} \cdot \text{bar}^{-1/2}$ or $\text{gallons} \cdot \text{minute}^{-1} \cdot \text{psi}^{-1/2}$.

2.1.2 Residential sprinkler

Residential sprinkler is a type of fast-response sprinkler having a thermal element with response time index (RTI) of $50\,(\text{m} \cdot \text{s})^{1/2}$ or less, that has been specifically investigated for its ability to enhance survivability in the room of fire origin, and that is listed for use in the protection of dwelling units [5]. In many advanced countries, residential sprinkler system is required in property that is used as a shared residence with shared access and living space [1, 6-9] . This applies to homes for the elderly, care homes and some student accommodation.

Residential sprinkler systems offer advantages to the homebuilder: (a) low-cost reliable safety option that would attract many buyers (b) trade-offs between sprinklers and code requirements that can result in lower construction costs, more

units per area of land, etc. (5 to 15 percent). For homeowners, the advantages include assurance of a safer environment for their families, protection of their investment and irreplaceable family possessions, and lower insurance rates 5 to 15 percent [10].

Modern residential sprinklers are small, neat and unobtrusive and visitors are seldom able to spot them. They are available in a variety of finishes and colors to suit any decor, and are even available in concealed versions.

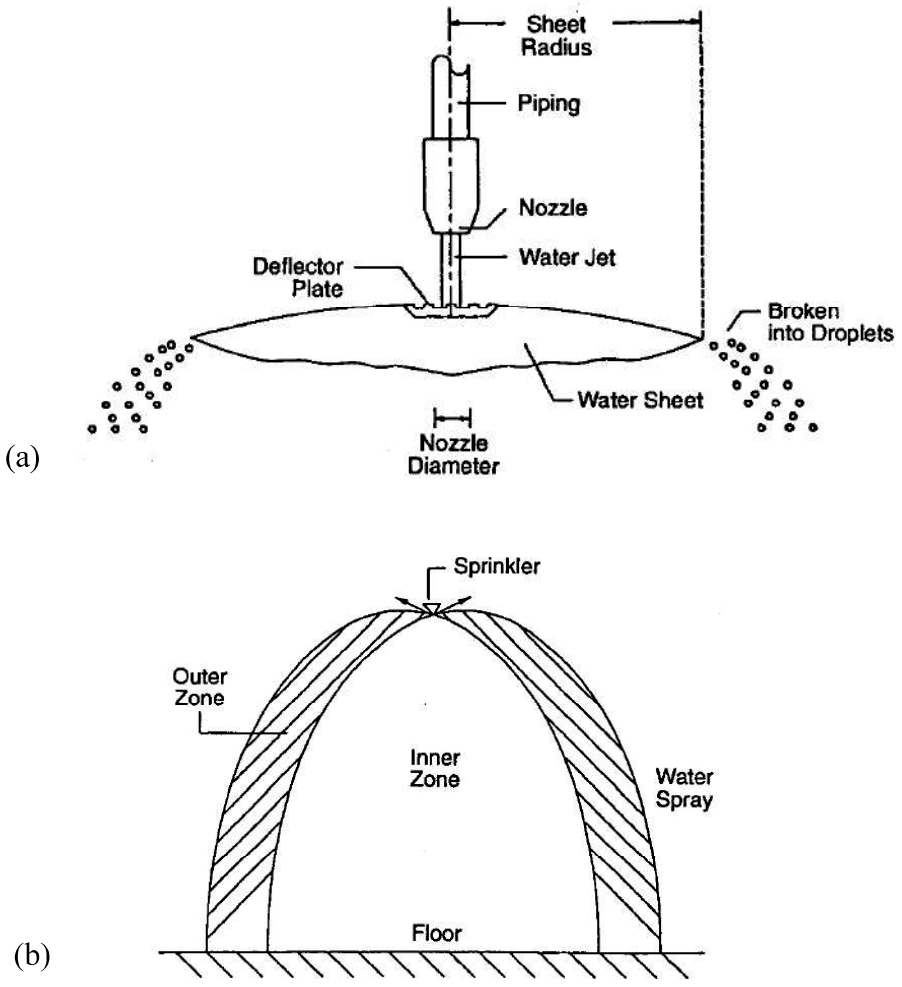

Figure 2.2 (a) Sprinkler water sheet and (b) typical sprinkler spray (adopted from [11])

2.1.3 Fire sprinkler performance

2.1.3.1 Sprinkler spray patterns

Most sprinklers are designed to alter the overall fire environment by lowering temperatures and controlling flame spread by wetting combustible materials to prevent their ignition [4, 11-16]. Residential sprinklers are intended to control fire growth and prevent flashover in the space where fire starts. When they operate, residential sprinklers are designed to distribute water in a flat pattern to wet the specified areas of the walls and the entire ceiling of the space where the fire occurs. This wetting action is intended to prevent flashover from the high temperatures that accumulate near the ceiling. Typical water sheet and spray pattern are illustrated in Figure 2.2 [11].

2.1.3.2 Method for determining sprinkler spray patterns

Spray profile or pattern. For the Spray Profile method, water is collected at a variety of elevations below the representative sprinkler via a turntable apparatus similar to the "10 Pan Distribution Test" described in UL199 [17]. Consequently, the profiles are radial averaging that tends to negate the normal unevenness of the actual sprinkler spray pattern (due for example to frame arm shadow and/or pipe line shadow). This technique most reasonably lends itself to standard spray upright and pendent sprinklers, since it provides information as to how the sprinkler's applied density varies from its center towards its theoretical outside diameter.

Cross sectional pattern. For the Cross Sectional method, and as the name implies, the data provides spray patterns at various sections through the representative sprinkler's spray distribution. This technique allows for documenting

complex spray distribution patterns, as in the case of standard coverage horizontal sidewall sprinklers. Studying these patterns reveals the actual contour of the upper limit of spray as opposed to the typical spray representation of a single line on a two-dimensional graph.

Wall wetting pattern. For the Wall Wetting method, the representative sprinkler sample is sprayed within rooms that were equivalent in size to various coverage areas, and at corresponding flow rates. The wetting of the walls was then documented. While this type of data requires interpolation between coverage areas and flow rates, it is considered to be the best way to portray the intricacies of extended coverage and residential type sprinkler spray patterns.

Average Applied Density. For the Average Applied Density method, water was collected at a variety of elevations below the representative sprinkler via a turntable apparatus similar to the "10 Pan Distribution Test" described in UL199. However, because certain sprinklers do not discharge all of the water in a downward direction, such as Conventional "Old Style" Sprinklers that spray approximately 40% of their discharge pattern in an upward direction, the data as collected could not be used to generate traditional spray profiles. Therefore, the data is presented in a tabular fashion that documents the cumulative Average Applied Density of both the water directed downward and the water returning downward after having initially been discharged upward.

One effect of the difference in water distribution pattern is the importance of sprinkler spacing. Internationally, the spacing rules established by the sprinkler listing, or the National Fire Protection Association (NFPA) standards (13, 13R, and 13D), are intended to assure adequate coverage by the water distribution. In other

countries, the application of residential sprinklers must comply with at least domestic fire safety standards like Korea Fire Institute of Industry and Technology (KFI) in Korea and Japan Fire Equipment Inspection Institute (JFEII) in Japan.

Korea and Japan have similar testing standards for water spray distribution testing. The sprinkler is supplied with water at specific pressure. After one minute, water supply is shut and water from catch pans arranged in a prescribed manner is collected and measured. The schematic for water spray pattern testing is illustrated in Figure 2.3.

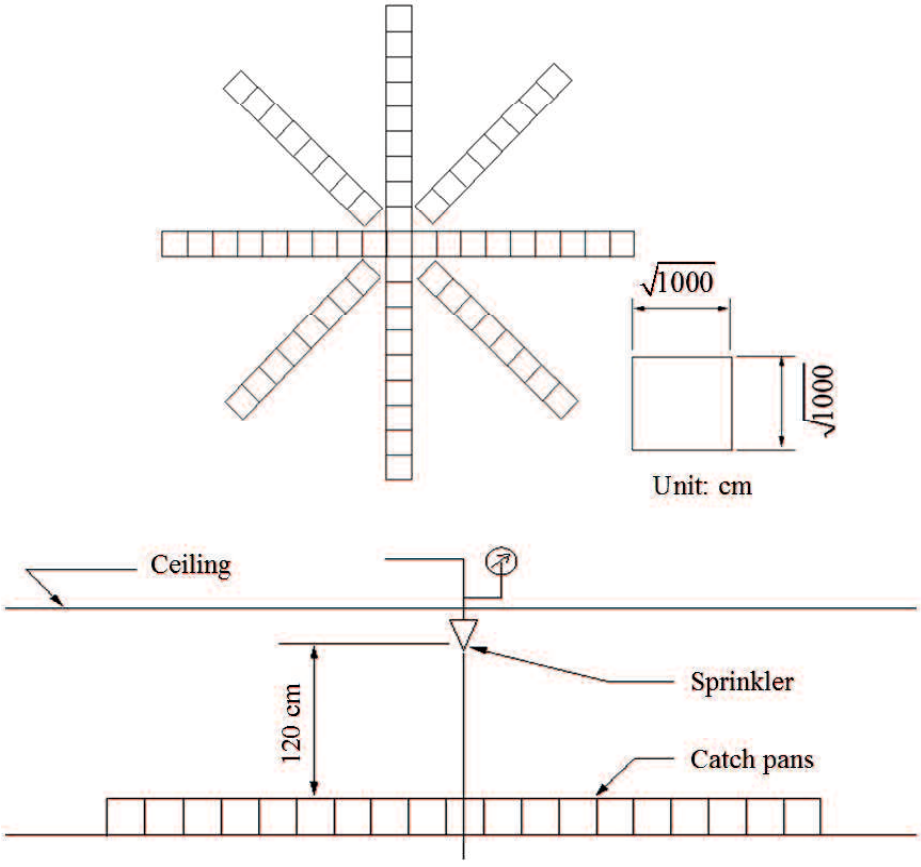

Figure 2.3 Setup for water spray pattern distribution test in accordance with Korean and Japanese standards

2.1.3.3 Response time index (RTI)

The response time index (RTI) is a measure of the sensitivity of the sprinkler's thermal element as installed in a specific sprinkler. The RTI of a sprinkler is highly influenced by the thermal characteristics of its thermal element (glass bulb or fusible alloy) [18]. It is usually determined using test oven whereby hot air is introduced into the sprinkler under controlled conditions. Figure 2.4 shows the schematic of test setup for determining the RTI of a sprinkler.

For a sprinkler to qualify for residential application, as pointed out earlier must be of quick-response which have an RTI of $50\,(\text{meters}\cdot\text{seconds})^{1/2}$ or less. The RTI of sprinkler is calculated using

$$RTI = \frac{-t_r\sqrt{u}}{\ln\left[1-\left(\frac{|T_m - T_u|}{T_g - T_u}\right)\right]} \tag{2.2}$$

RTI: Response Time Index $[(\text{m}\cdot\text{s})^{1/2}]$

t_r: Operating time of the sprinkler [s]

u: Nominal gas velocity in the test section of the wind tunnel [2.54 m/s]

T_m: Marked temperature rating of the sprinkler [°C]

T_g : Nominal gas temperature [°C]

T_u : Nominal ambient air temperature [24°C]

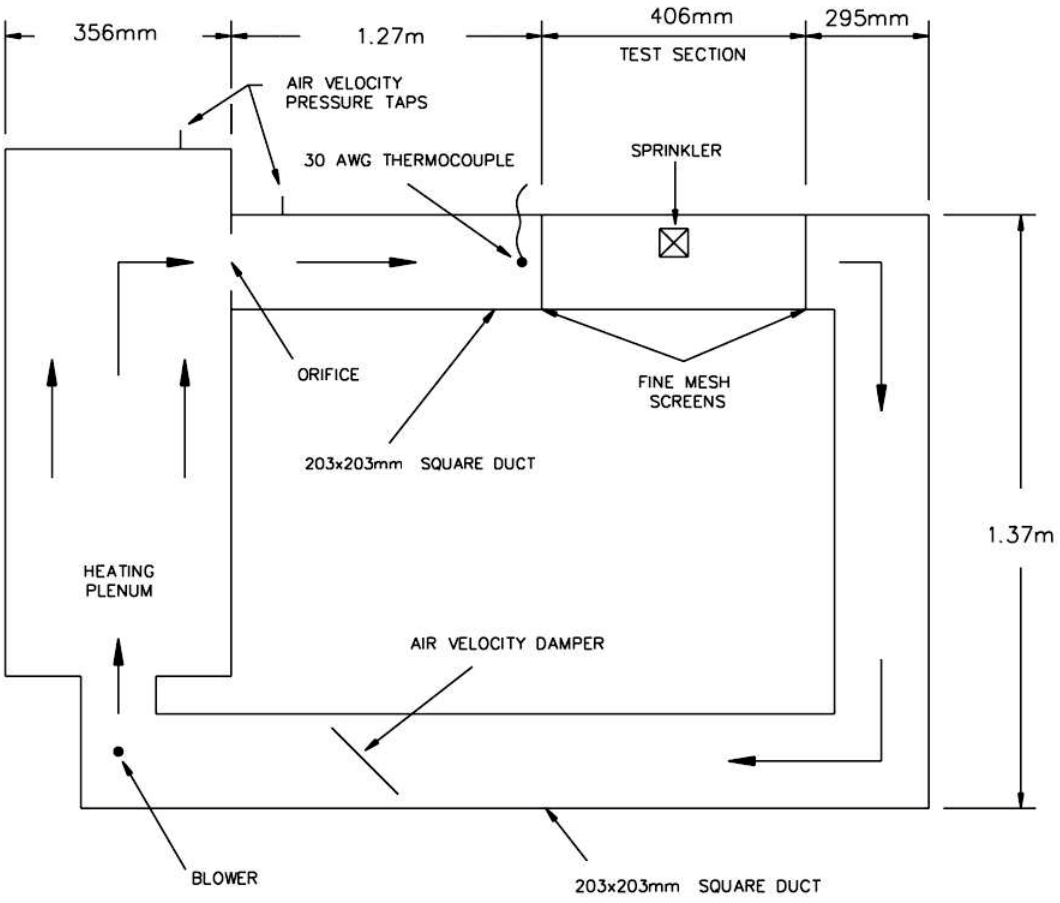

Figure 2.4 Schematic diagram of test oven used for determining RTI of sprinklers

2.2 Related studies

Every year residential fires occur practically around the world [19-22]. For example in the USA, recent estimates showed an average yearly of 371,700 residential structures fires causing 2,590 civilian deaths, 12,910 civilian injuries, and $7.2 billion in direct property damage. Majority (71%) of the reported residential fires occurred in one- or two-family homes with the remaining occurred in apartments or other multi-family housing [21, 23, 24]. In the UK, 43,500 residential (dwelling) fires were reported for the year 2011-2012. These fires caused 287 fatalities and 11,300 non-fatal casualties [25]. The damages to property, injuries and

loss of lives caused by residential fires have great impact on the economy and society. This impact has continuously encouraged the promotion and implementation of stricter fire safety requirements particularly in industrialized and advanced countries. For example, in 1991, the Japanese fire prevention department had published technical guidelines for the installation of fire alarm and sprinkler equipment on residential buildings. According to the guidelines, automatic detection of heat, smoke or flames as indicators of fire together with water-based glass bulb or fusible type sprinkler systems must be installed covering the entire area of the residential building including living room so that fire can be effectively suppressed. In short, the function of fire protection system is not only for fire suppression but should be able to warn residents at the early stage of fire for evacuation.

In an event of residential fire, smoke alarm can save lives and reduce the loss to properties by providing early warning alarms to residents. In many cases, smoke alarms are combined with other detection technologies (such as gas and heat sensors) to ensure an efficient and reliable detection of the early indicators of fire occurrence [26-31]. For extra protection against fire however, in addition to smoke alarms installation of fire sprinklers is recommended. It is reported that the risk of dying and property loss decreases by about 80% and 71%, respectively when sprinklers are installed [24]. A wise approach therefore, is to combine smoke alarms (and other sensors) with fire sprinkler system to obtain a reliable and more efficient fire protection system. Recently, the addition of fire sprinkler has become part of the building requirements for residential structures [9, 32].

In Japan, after learning lessons from a horrific fire accident in Omura, Nagasaki that have taken seven human lives, major revisions in the fire protection

guidelines were made leading to the creation of Japan's Fire Services Act in the following year. Subsequently, in 2009 the act mandated technical standards for the installation of fire escape accessible to physically impaired person in social welfare facilities (with floor area over 275 m^2 but less than 1,000 m^2) and installation of particular type of sprinkler equipment for a specific residential facility and were made clear. The standards include specifications for sprinkler minimum performance which are 0.02 MPa at 15 L/min or 0.05MPa at 30 L/min,

The Fire Services Act in Korea specifies that sprinkler should be able to discharge water at 0.1 MPa at the rate of 50 L/min continuously for more than 10 minutes. In Japan and Korea the installation of fire sprinkler equipment in residential houses although optional is increasing. The continuous expansion of home fire sprinkler installation will consequently reduce sprinkler equipment and installation cost.

In residential installation, methods for supplying water to the sprinkler system include direct connection to the domestic water supply and use of high pressure water tank or storage tank with booster pump. Direct connection to the domestic water supply line is generally popular in most residential homes consisting of up to two floors. However, in case where the residential structure is situated in elevated location or away from the domestic water supply line, the significant drop in water pressure and flow rate may reduce the capability of fire sprinklers to control or extinguish a fire. Additionally, most sprinkler systems are too costly to install and maintain; which makes homeowners uncertain of adopting the technology despite its life saving capabilities. It is therefore essential to develop a system that is reliable against water supply conditions and affordable to homeowners.

As been pointed earlier, one of the key components of sprinkler system in controlling or extinguishing fire is the sprinkler. In a designer's viewpoint, understanding of the functionality of such device is essential in ensuring its performance for intended use. The performance of sprinkler can include cost-effectiveness and ability to discharge or spray water in a manner effective for fire control or extinguishment. For an existing fusible link, flush type pendent residential sprinkler, a relatively large number of individual components render complexity of the assembly process. For such type of sprinkler, knowledge of the assembly mechanics is critical for ensuring proper and reliable operation over its intended service life. However, analytical method for predicting the assembly loads and structural response of such sprinkler has neither been well-established nor published in scholarly literature. Furthermore, the existing sprinkler was observed to spray water unevenly due to its tripod-mounted deflector. The impress screw that is used to provide the required force to seal the nozzle and prevent water leakage is manipulated from the interior of the sprinkler making it difficult to visually check the structural condition during and after assembly process. The large number of individual components also contributes to increased product cost, product rejection rate and high probability of activation malfunction. Therefore, it important to develop an analytical model for predicting the assembly loads and structural response of the sprinkler that will enable quick, easy and cost-effective design exploration for obtain optimum product.

Recently, wireless system has also received attention for its application in the fire early detection system [33-35]. This system is becoming more attractive to housing which accommodates elderly couple or elderly person living alone because it

is perceived to be more secured. The fire alarm system using wireless technology is seen to be necessary in modern society as part of the fire-fighting equipment. In addition, inspired by the era of communication and data sharing the wireless home network applications are now freely available. While the current communication technology within the fire-fighting industry is mostly still based on wired system, there is a growing need for the application of wireless communication between fire-fighting system components with the capability of home network integration. Zigbee-equipped wireless smoke sensors along with IT technology can activate alarms if a fire occurs. These technologies can be implemented for the purpose of ensuring fire safety in residential buildings through wireless fire detection and extinguishing system

2.3 Research objectives

The objectives for this study are summarized as follows:

- To investigate the practicality of direct connection to domestic water supply line with additional auxiliary water tank and booster pump to guarantee successful operation of the residential sprinkler system. Based on findings, develop a compact and affordable package type residential fire extinguishing system that can accommodate varying water pressure from local supply line. The proposed system must be tested for real fire extinguishing performance.

- To develop analytical approach for understanding the physics involved in the fusible, flush pendent sprinkler. Such approach shall be useful for quick and easy design exploration such as component reduction and downsizing. Furthermore, the analytical approach shall facilitate design of alternative sprinklers that possess better

spray pattern performance under a variety of water pressures. The RTI of the alternative sprinkler should comply with standards related to residential fire sprinkler system.

- To implement ubiquitous technology for ensuring safe and reliable fire protection system in residential buildings and facilities through wireless fire detection and extinguishing system. This system should be able to promote ease and practicality of installation in existing residential buildings and facilities.

Chapter 3

DEVELOPMENT OF RESIDENTIAL FIRE SPRINKLER SYSTEM

3.1 Overview

Experimental study for determining the minimum requirements for the design of a low-cost residential fire sprinkler system and their effect on the system fire suppression performance is conducted. At first, several basic experiments with different water pressure conditions were carried out to investigate the minimum requirements for fire suppression. Next, fire extinguishing tests on a residential sprinkler experimental system were performed. The results from experiments have pointed out several important facts. Finally, a compact residential fire extinguishing system is designed based from the experimental results.

3.2 Experiment setup

3.2.1 Residential fire sprinklers

The installation of residential fire sprinkler system requires identification of the method for supplying water with suitable pressure and flow as specified in the fire sprinkler operation standard. Methods for supplying water to the sprinkler system include direct connection to the domestic water supply, use of high pressure water tank or use of storage tank with booster pump. Direct connection to the domestic water supply line is generally popular in most residential homes consisting of up to two floors. This popularity is due to the fact that direct connection is easy to install, maintain and does not require systematic management and inspection. However, in case where the residential structure is situated in elevated location or away from the domestic water supply line, the significant drop in water pressure and flow may

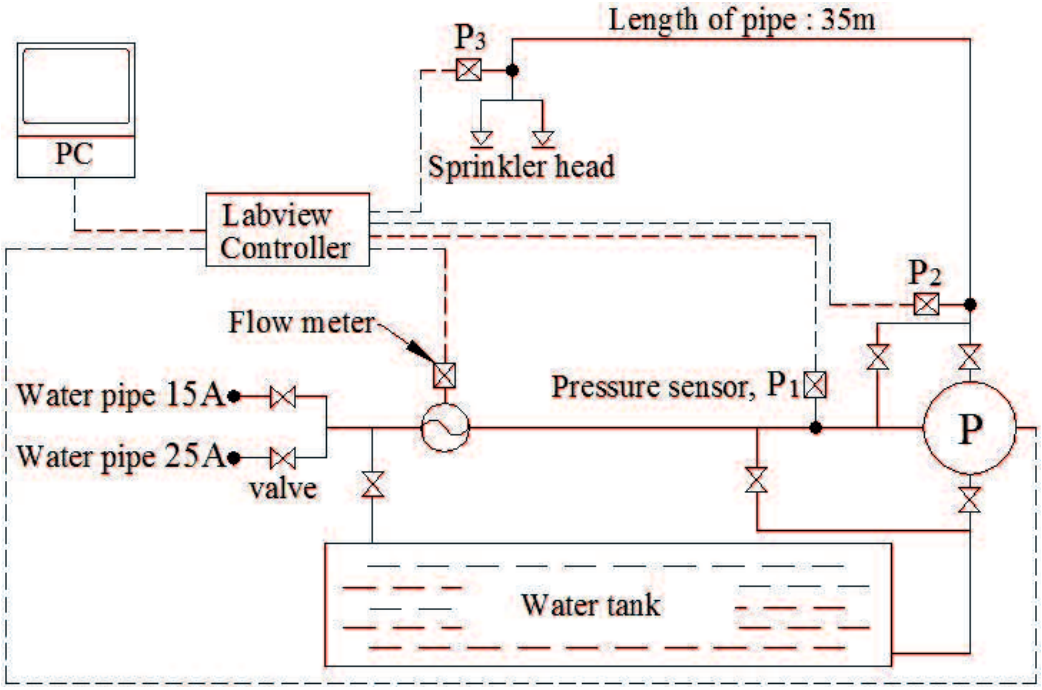

(a)

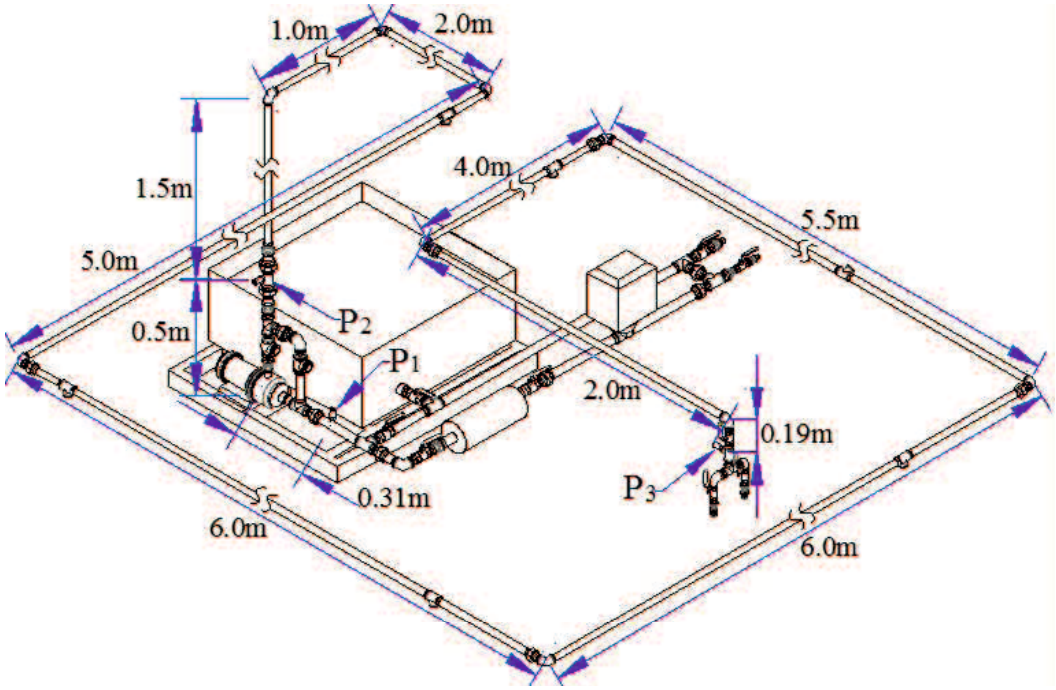

(b)

Figure 3.1 Experimental setup of residential sprinkler fire extinguishing system: (a) Schematic diagram (b) Piping layout

reduce the capability of fire sprinklers to fully suppress fires. In this study, the practicality of direct connection to domestic water supply line with additional auxiliary water tank and booster pump to guarantee that suitable water pressure and flow for sprinkler systems are maintained all the time is investigated.

For the purpose of this study, the condition of domestic water supply particularly water pressure and plumbing in regular household was surveyed. In Japan, water pressure in the domestic water supply ranges from 0.1-0.8 MPa with 0.3 MPa found to be common. Water pressure drop was observed depending on the distance and altitude of the location of a household. Also, less pressure drop was observed for larger pipes. Consequently using larger pipe to alleviate pressure drop entails higher material and labor costs. Either 15A or 25A pipes were commonly used in the surveyed houses with a few using 32A pipe.

In this study, fire sprinkler system for use in residential or home environment is considered. Specifically, pump performance testing and validation are performed to verify the suitability of the equipment against the restrictions imposed by law in Japan and Korea. A schematic of the experiment setup is shown in Figure 3.1. In this experiment, the effects of pipe size and type of sprinklers on the changes in water supply pressure are investigated. Two pipe sizes 15A and 25A commonly used at household pipelines were installed and fitted with manual valves for easy manipulation during experiments. Water pressure at the main water supply line (at the inlet joint with 15A and 25A pipes) was actually measured as 0.157 MPa. As been pointed out earlier, to ensure that the fire sprinkler system will have continuous supply of water during suppression, a direct connection with the domestic water supply is maintained with bypass into the auxiliary water tank. It should be noted that

the auxiliary tank provides the primary source of water supply when the sprinkler system is initiated. A total pipeline length of 35 m (considered a worst case scenario by the Korean Construction Code) and two sprinklers with *K*-factor *K*=50 (MFQ72) were installed. Flow meter (Badger Meter, Magetoflow IOM-074-03) and pressure gauges (HISCOI, P201) were installed accordingly in the pipeline (as shown in Figure 3.1). Water pressure at the pump (WILOPUMP, MHI802EM) inlet (P_1) and outlet (P_2) and near the sprinklers (P_3) were monitored to determine any pressure loss in the pipeline. Pipe length from P_1 to P_2 and P_2 to P_3 are 1 m and 34 m, respectively. Data from the corresponding sensors (flow meter and pressure gauges) were monitored using oscilloscopes and captured using data acquisition module from National Instrument (NI9215 and NI9263).

3.2.2 Fire sprinkler characteristics according to different water pressure

Figure 3.2(a) and 3.2(b) show the water pressures during 10-minute test at corresponding gauges P_1, P_2, and P_3 when two sprinklers with *K*=50 and inlet pipe size of 15A and 25A were used, respectively. As can be expected, due to 1-m distance between P_1 and P_2, the pressure loss appears to be insignificant. In this experiment, the pressure at the main water supply line was 0.157 MPa, in the case of 25A pipe the pressure at point P1 and P2 was about 0.146 MPa while the average pressure at P3 was 0.041 MPa. On the other hand, for the case of 15A pipe the average pressure at P_1 and P_2 was approximately 0.095 MPa while the average pressure at P3 was 0.023 MPa, obviously lower than the case of 25A pipe. With *K*=50 the water flow quantity at one sprinkler can be approximated as $Q_{25} = K\sqrt{10P} = 32.0$ L/min and $Q_{15} = 24.0$ L/min for 25A and 15A pipes,

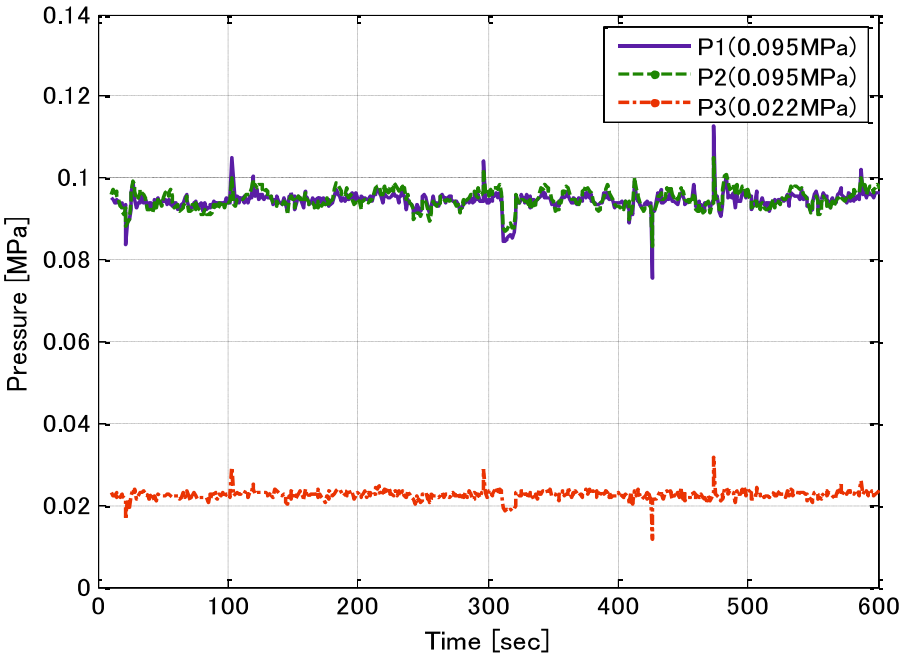

(a)

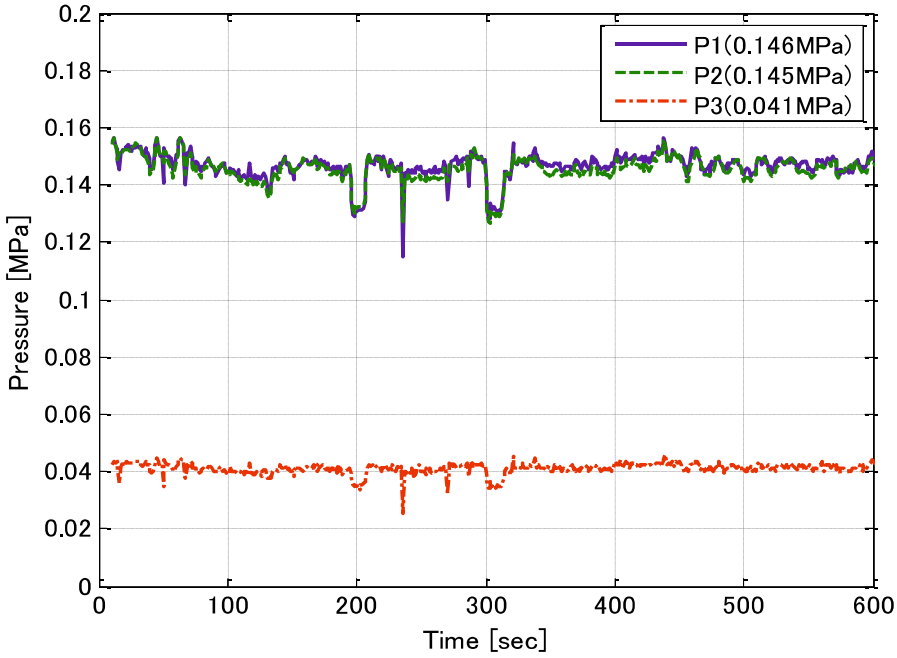

(b)

Figure 3.2 Pressure variations in the pipeline when the sprinkler system is directly connected with: (a) 25A pipe and (b) 15A type water pipe are used

respectively. Accordingly, when two sprinklers were open simultaneously, the discharge flow rates at the head will be twice as much, i.e. 64 L/min and 48 L/min for 25A and 15A pipes, respectively. Korea Fire Code requires sprinklers minimum water discharge at 0.1 MPa at the rate of 50 L/min measured for at least 10-minute continuous discharging time. Thus, considering the minimum requirement of 1.0 m^3 $\left(50\ \text{L/min} \times 2 \times 10\ \text{min} = 1{,}000\ \text{L} = 1.0\ \text{m}^3\right)$, it will take about 16 minutes and 21 minutes for the sprinklers to release the same quantity of water for 25A and 15A pipes, respectively.

3.2.3 Water flow characteristic according to water pressure

Based on the results discussed in the previous section, pipe sizes have been shown to affect water pressure in the sprinkler system. For the case of 25A pipe the discharge pressure at the sprinkler with K=50 is lowered to 0.04 MPa. Obviously, to meet the required standard minimum pressure of 0.1 MPa, installation of a water pressure booster pump is needed. Water pressure booster inverter-driven pump (WILOPUMP MHI802EM, discharge head 46 m, flow rate 160 L/min) was installed. Pump performance was verified by comparing the water flow rates with the pump not operating (not in use) and with the pump operating (in use) at 3,500 rpm. The water flow rates measured over 10 minutes of continuous discharge for both cases are shown in Figure 3.3. When the pump is not operating, the average flow rate was 57.6 L/min closely agreeing with the calculated value of 64.0 L/min while the average flow when the pump was operating was about 84.1 L/min. Furthermore, it was found that the corresponding outlet pressure when the pump was operating was 0.07 MPa (at 84.1 L/min). It was also tested where the pump inlet was connected

with an experimental water tank. In this case, the flow rate was measured as 100 L/min at a pressure of 0.25 MPa. Japan Fire and Disaster Management Agency guidelines require sprinkler discharge pressure of 0.05 MPa with flow rate of 30 L/min measured within a few minutes of continuous water flow. However, Korea's Public Fire Services Act mandates 1.0 m^3 of water storage capacity for the required minimum 10-minute continuous water discharge. With the aim of catering both countries with one fire sprinkler system, it is evident that auxiliary water tank is needed to guarantee that international standard requirements are satisfied.

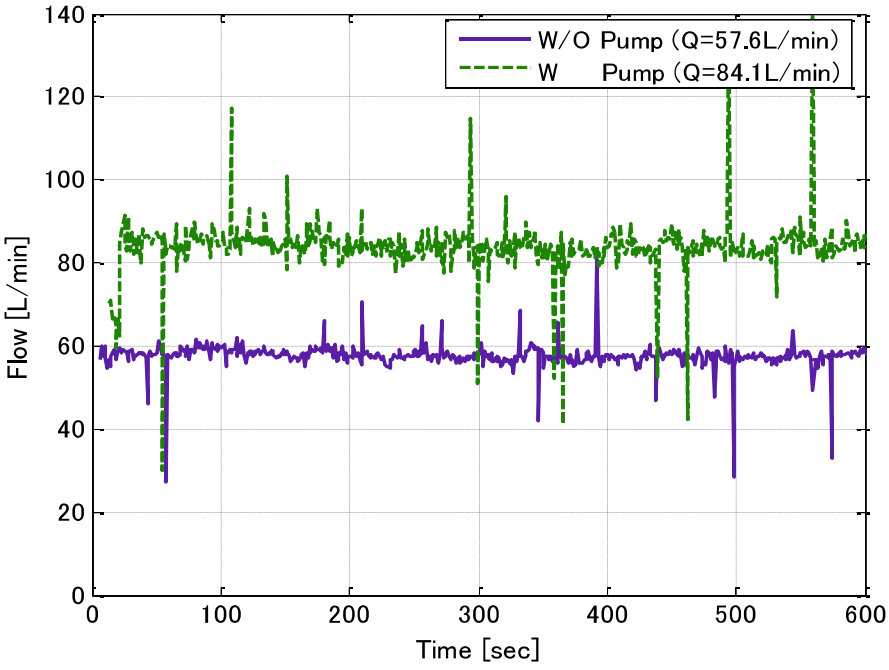

Figure 3.3 Flow results without and with the use of tank and pump

3.2.4 Determination of auxiliary tank capacity by experiment

To minimize extra cost for the sprinkler system, additional auxiliary water tank with minimum volume must be used. A few alternatives are considered while keeping in mind the strict requirement of Japan and Korea for fire sprinkler pressure of 0.1 MPa, water storage capacity of 1.0 m^3 to be discharge in 10 minutes or more. Firstly, 15A pipe together with 230 L experimental water supply tank was tested with the pump operating at 3,500 rpm. The measured water pressures are shown in Figure 3.4. The pressure at the sprinkler was maintained at 0.1 MPa but started to fluctuate after 6 minutes of operating the sprinklers due to insufficient water supply. It was possible to maintain uniform pressure after 6 minutes but it required 600 L of water. Moreover, the pressure at the sprinklers was found to be 0.04 MPa resulting to a flow rate of approximately 31.6 L/min. Therefore, an auxiliary tank with capacity of 368 L is needed to secure a total discharge of 1 m^3 of water in 10 minutes.

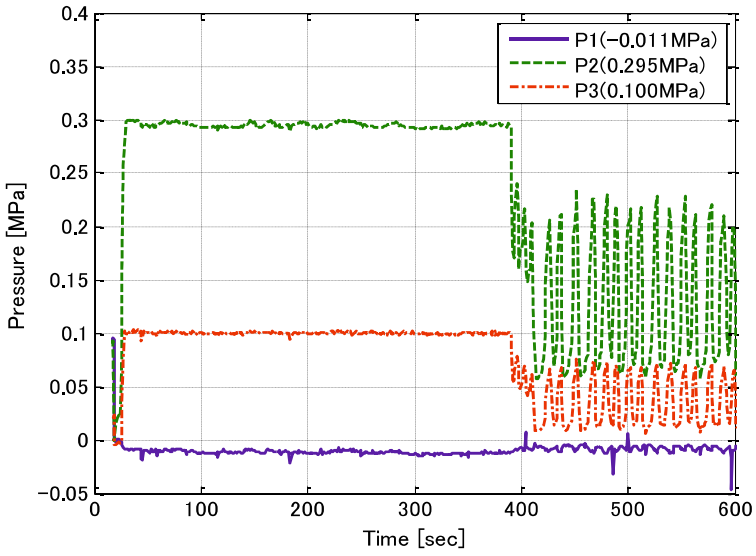

Figure 3.4 Pressure measurements with 230L water in the tank

Next, the combination of 15A pipe and 290 L water tank were considered. It can be seen in Figure 3.5(a) that the water pressure of 0.1 MPa at the sprinkler was maintained for 670 seconds or about 11.16 minutes. Conversely, the size of auxiliary water tank needed to keep the water pressure of 0.1 MPa for 10 minutes is 390 L/11.16 min*10 min = 350 L. Also if pipe 25A was used, as shown in Figure 3.3, the flow rate of 84 L/min at water pressure of 0.1 MPa can be maintained for more than 20 minutes. As such the volume of the auxiliary water tank needed can be calculated as (100L/min-84L/min) x20min = 320L. As experiment, an auxiliary tank with capacity of 370 L was tested. As shown Figure 3.5(b), the pressure at the sprinkler is maintained at 0.1 MPa for 1270 seconds. For the 10-minute requirement, the needed volume for the auxiliary water tank is 370L/21.16minx10min = 175L.

Based on the results, to maintain the water pressure at the sprinkler on the required 0.1 MPa for 10 minutes, water pressure booster pump is needed. Accordingly, using 15A or 25A pipes, auxiliary water tank with water volume capacity of 350 L and 175 L, respectively are needed to satisfy the discharge requirement of 1,000 L.

3.3 Fire suppression test

The effect of water pressure at the sprinkler on the ability of the fire sprinkler system to suppress fire is investigated. Sprinkler types commonly installed in general fire sprinkler system are used. These types of sprinklers require minimum water pressure (at the head) of 0.02 MPa or 0.05 MPa. Noting the huge margin between the mandated water pressure of 0.1 MPa and the minimum water pressure required by

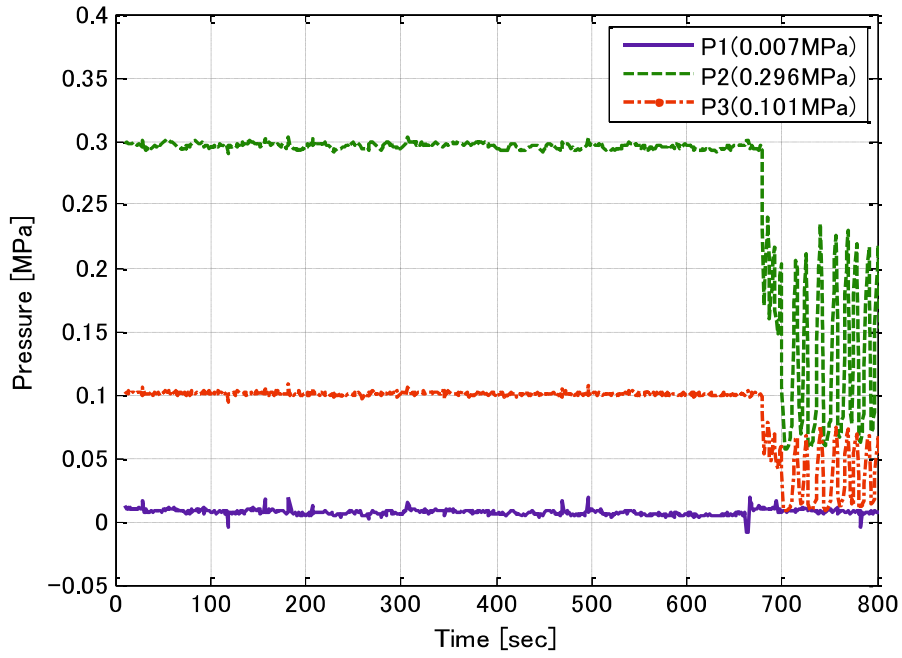

(a)

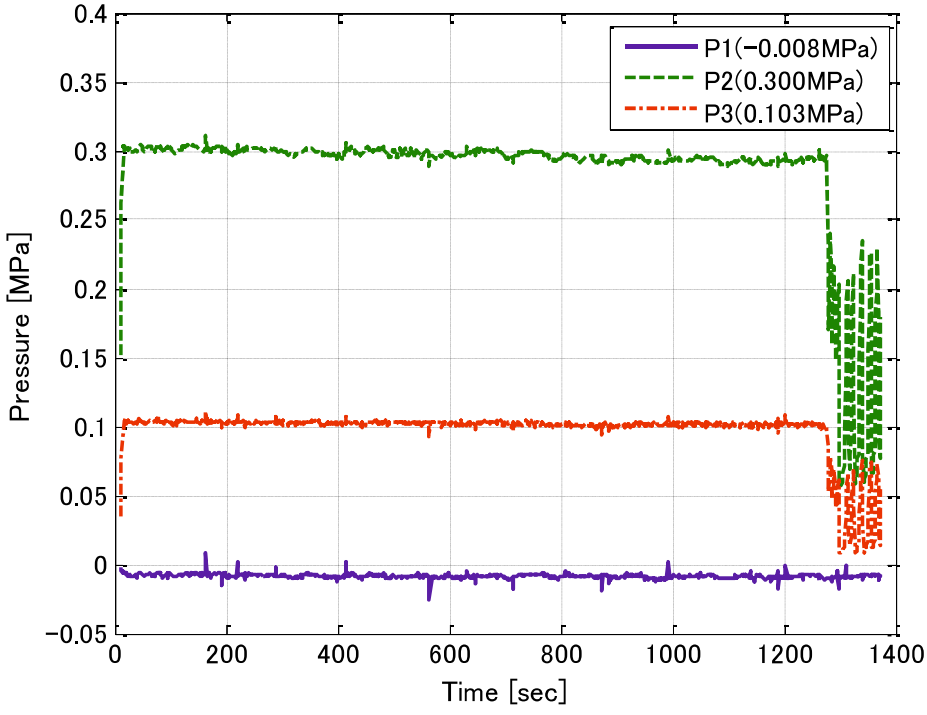

(b)

Figure 3.5 Pressure variations in cases of (a) 15A pipe with 390L water in the tank and (b) 25A pipe with 370L in the tank

the sprinkler (0.02 MPa), the effectiveness of the fire sprinkler system to suppress fire was analyzed by varying the pressure at the head (P3) from 0.02 – 0.1 MPa. Similar with the experiments described in the earlier sections, pump inlet and outlet pressures (P_1 and P_2), pressure at the sprinkler (P3), and the water flow rate were recorded at the same time. Sprinklers with K-factors K-30 and K-50 were used.

The experiments for determining the fire suppression performance of the fire sprinkler system under different pressures were carried out in accordance with residential fire test standard (ISO-6182-10). Particularly, crib fire tests were performed where for the fear of creating large blaze, 25 ml of Heptane was poured into fuel plates instead of using the standard 50 ml. Wooden crib placed 2.2 m below (measured vertically) and 1.5 m away (measured horizontally/radially) from the sprinkler was ignited, set on fire and kept going. When the fire or heat was large enough the sprinklers were automatically activated. For a particular sprinkler pressure and sprinkler type, the fire suppression performance described by the status of the crib was closely monitored using video capture device. Table 3.1 shows the summary of the results from experiment.

Table 3.1 Fire tests setup

Description	Setup values	Measured results	Remarks
Exp.1	P_2 = 0.02 MPa, K–50		Failure to extinguish
Exp.2	P_2 = 0.038 MPa, K–50	P_3 = 0.019 MPa, Q = 22.4 L/min	Half-burned
Exp.3	P_2 = 0.123 MPa, K–50	P_3 = 0.098 MPa, Q = 50.0 L/min	Succeeded
Exp.4	P_2 = 0.062 MPa K–30	P_3 = 0.046 MPa, Q = 20.5 L/min	Almost burned

Images captured during the fire suppression performance experiments are arranged to depict the test procedure and the corresponding outcome as shown in Figure 3.6. Figure 3.6(a) shows the ignition of Heptane contained in the fuel pan which subsequently set the wooden crib on fire. Figure 3.6(b) shows the sprinkler water discharge at P_2 = 0.02 MPa. It was observed that water pressure at the pump outlet of 0.02 MPa was too low and unable to sufficiently spray the water out of the sprinkler – similar to the water flow in faucet. Figure 3.6(c) illustrates the activation of sprinklers wherein water was sprayed. Figure 3.6(d) shows the remaining portion of the wooden crib after 10 minutes of sprinkler operation. It appeared that with discharge pressure of 0.019 MPa (≅ 0.02 MPa) at 22.4 L/min water flow half of the crib was totally burned.

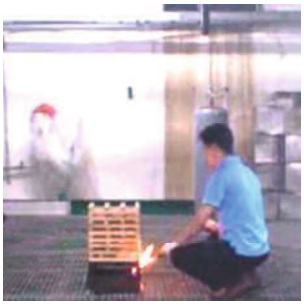

(a) Igniting the crib

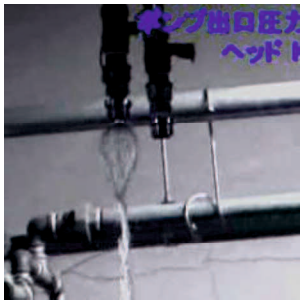

(b) Low-pressure sprinkler discharge in Exp.1

(c) Sprinkler activated (water spray initialize)

(d) Remain in Exp.2

(e) Remain in Exp.3

(f) Remain in Exp.4

Figure 3.6 Images depicting the test procedure and the crib remain conditions at the end of fire test.

In experiment 3 (Exp.3), pressure at the pump outlet and sprinkler were maintained at P2=0.123 MPa and P3=0.1 MPa, respectively with water flow of 50.0 L/min. In this case, the fire was completely suppressed in about 10 minutes. The condition of the crib was checked after 10 minutes and found still intact as whole structure as shown in Figure 3.6(e). At this point, it can be confirmed that based on Japan Fire and Disaster Management Agency guidelines as mentioned earlier, the required minimum 0.02 MPa or 0.05 MPa water pressure at the sprinkler with 30 L/min water flow rate have been sufficiently satisfied. Due to significantly wide margin between the required and the experiment result data, additional experiment was conducted with sprinkler orifice reduced from K=50 to K=30. In the fourth experiment (Exp.4) the pump outlet pressure was set to 1.6 times greater than the pressure in Exp.2., resulting to sprinkler pressure P_3=0.046 MPa. With a flow rate of Q=20.5 L/min, the sprinkler system failed to suppress the fire causing the crib to completely burned within 7 minutes as shown in Figure 3.6 (f).

These results show that sprinkler system condition with sprinkler pressure of P_3=0.02 MPa and flow rate of Q=23.0 L/min is able to suppress fire however with the degree of burn as indicated in the crib test, pressure and flow rate need to be increased for complete fire suppression. Sprinkler pressure of P3=0.1 MPa and flow rate of Q=50.0 L/min or higher guarantee that complete fire suppression can be accomplished.

3.4 Water spray distribution and fire extinguishing capability

Figure 3.7 shows the type of sprinkler used during the fire test. The water spray distribution patterns of the sprinklers used for Exp. 2 (K–50, P_3 = 0.019

Figure 3.7 K-50 sprinkler test specimen

MPa, Q = 22.4 L/min), and Exp. 3 (K–50, P_3 = 0.098 MPa, Q = 50 L/min) are shown in Figure 3.8. It can be seen that for the case of Exp. 2, the water spray pattern is significantly scattered near the region where the fire was located which is 1.5 m radially away from the sprinkler (see Figure 3.8(a)), approximately between 180° and 225°. At 1.5 m radius and 180°, there was almost no (zero) water discharge while at the same radius and 225° water flow rate was about 100 mL/min. Within this region, the quantity of water was not sufficient enough to penetrate and cool the burning wood (fuel). However, large volume of water was discharged at about 0.3 m shorter from the center of fire. The water droplets from the nearby large discharge may have displaced the oxygen resulting to the reduction of fire. This could be the reason why K-50 sprinkler under water pressure of 0.02 MPa and discharge of 22.4 L/min was able to extinguish the fire yet leaving the sample wood (fuel) half-burned. On the other hand, the water spray distribution pattern for the third experiment which was conducted with the same size of sprinkler orifice (K-50) appears to be less scattered compared to that in Exp. 2. Water discharges at regions located before and after the position of fire were significantly higher. In other words, the fire was not only being

directly hit and penetrated by sufficient amount of water but was also surrounded by it as can be seen in Figure 3.8(b). As a result, the fire was successfully and completely extinguished.

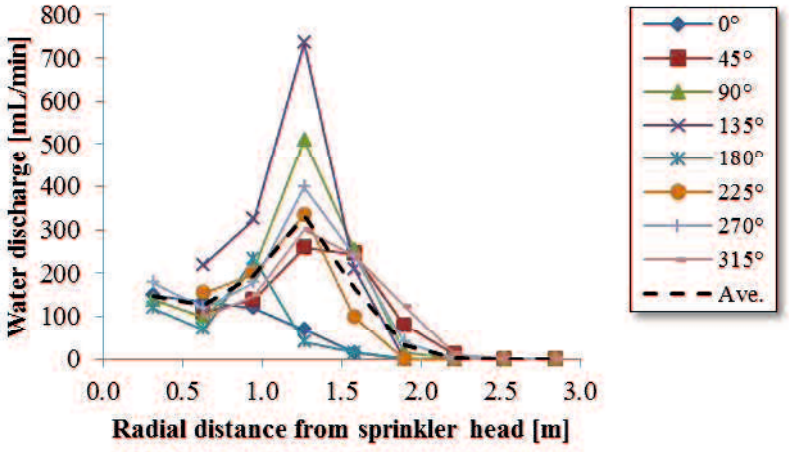

(a) Exp. 2: $P_3 \approx 0.02$ MPa, $Q = 22.4$ L/min

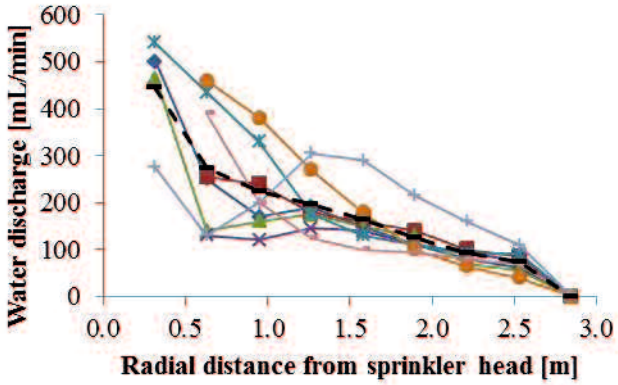

(b) Exp. 3: $P_3 \approx 0.1$ MPa, $Q = 50$ L/min

Figure 3.8 Water spray distribution patterns of sprinkler with fire-extinguishing capability under different pressure and water discharge.

Based from the water spray distribution tests the average water discharge rate for Exp. 2 and Exp. 3 at 1.5 m radius from the sprinkler are 165 mL/min and 156 mL/min, respectively. In practical sense, the difference in the location-wise averages is insignificant relative to fire extinguishing capability. The water discharges surrounding the location of fire should also be considered in assessing the fire extinguishing capability of a sprinkler. As shown earlier, the pressure condition for Exp. 3 (0.1 MPa) enabled spraying of large quantity of water to greater radius, enclosing the fire and providing significant cooling effect. On the other hand, the lower pressure condition in Exp. 2 affected the uniformity of water spray pattern that has resulted to failure to extinguish the fire at early stage leaving the combustible partly burned.

3.5 Package residential fire sprinkler system

Based on the experiment results, a compact fire sprinkler system shown in Figure 3.9 was developed for residential installation. The system is primarily consists of pump, water tank, and fire alarm device. Practically, the system works as follows: in case of fire, the fire sprinkler ① is activated spraying out water and enabling water to flow in the pipeline ②. Once water flow is detected by the sensor ③, it triggers the fire alarm device ④ which can be fitted with communication capability for automatic notification of the fire department. At the same time, the pressure booster pump⑥ is switched ⑤ on to supply water at suitable pressure and flow rate for the sprinkler system. Water level in the tank ⑦ is monitored by the water level sensor ⑧. Once a specified level of water in the tank is reached, the electric ball valve ⑨ automatically opens allowing water from the main supply line to flow into

the tank to replenish the water discharged in the sprinkler. With this setup, it is guaranteed that the required water supply at 0.1 MPa pressure can be delivered and maintained in 10 minutes or over. Taking into account the required water delivery capacity with pump flow rate of 170 L/min, the water tank capacity of 350 L can be specified for the design of the unit. Additionally, the developed system is fitted with rechargeable battery for back-up power source to ensure system operation during main power failure. That is, the pump and electronic devices (control panel, electric ball valve, etc.) are powered through the battery while the battery is connected to the household AC power source.

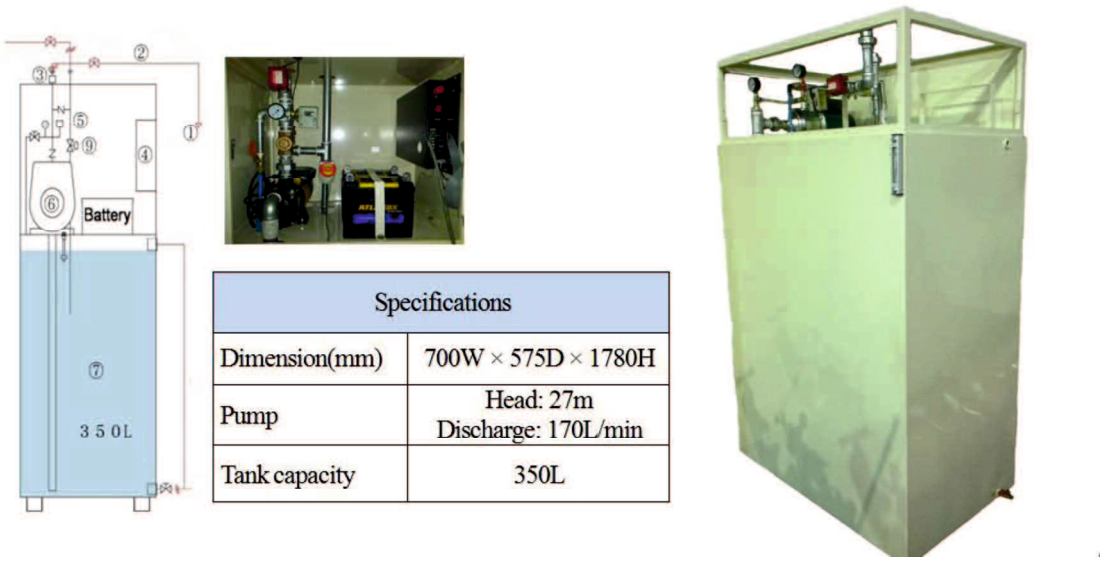

Figure 3.9 Package-type fire sprinkler system

3.6 Other types of residential sprinklers for the developed package system

In the preceding sections it was shown that a residential sprinklers with K-factor of K-50 connected to water delivery line with minimum pressure of 0.1 MPa can discharge water at a rate of 50L/min successfully suppress a fire. This class of sprinklers (K-50) can be fitted with the developed package-type fire sprinkler system for effective fire control or suppression.

Assuming a sprinkler is properly activated, the ability to control or extinguish a fire is significantly affected by its water spray distribution characteristics for a given water pressure and flow rate [4, 36-43]. Several other types of residential sprinklers with K-factor equal to or lower than K-50 that can be installed with the developed package fire extinguishing system were tested for water spray distribution performance. Figure 3.8 shows the images of models for K-30, K-43, and K-50 sprinklers. Their corresponding water spray patterns are shown in Figure 3.10, 3.11, and 3.12 at 0.1 MPa, 0.4 MPa, and 0.7 MPa, respectively.

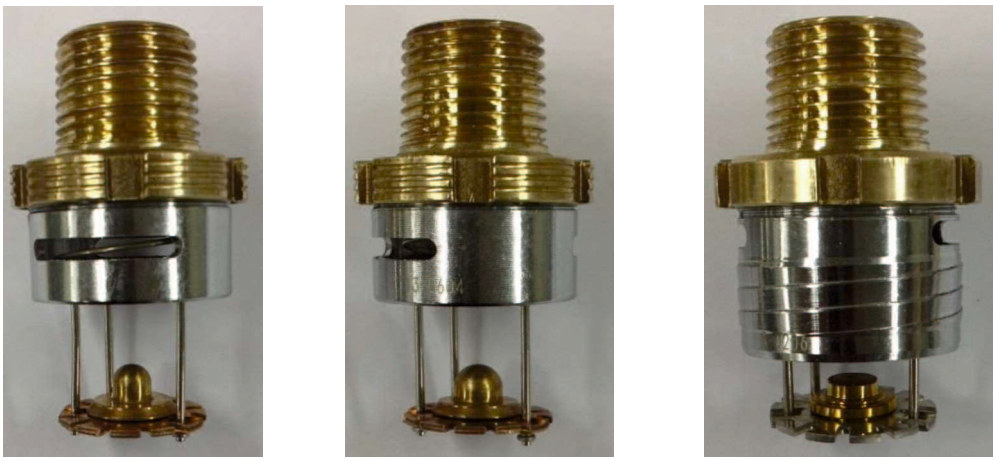

(a) (b) (c)

Figure 3.10 Various types of residential fire sprinklers that can be installed with the developed package fire extinguishing system: (a) K-30, (b) K-43, and (c) K-50.

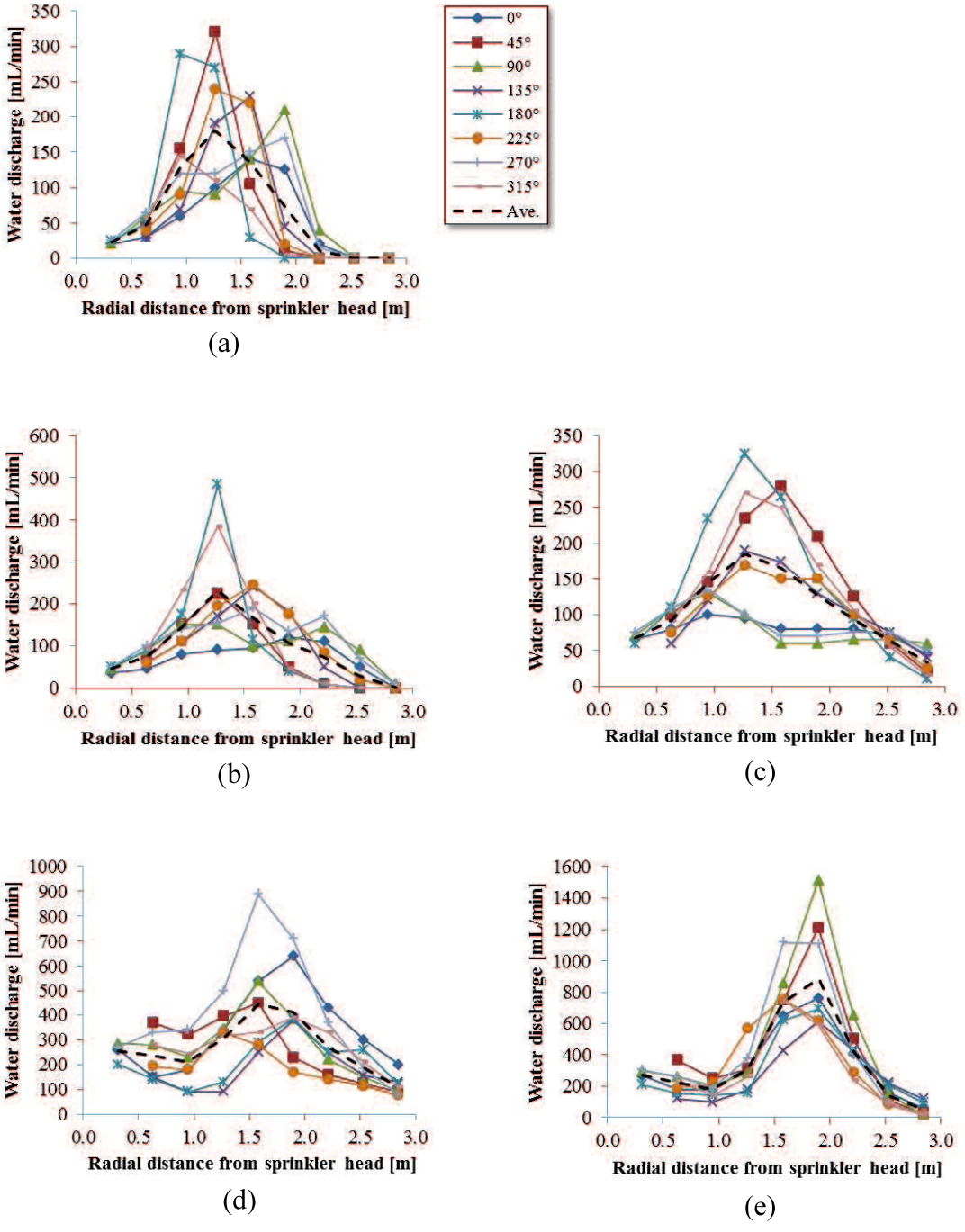

Figure 3.11 Water spray distribution patterns for K-30 sprinkler at (a) 0.02 MPa, (b) 0.05 MPa, (c) 0.1 MPa, (d) 0.4 MPa, and (e) 0.7 MPa.

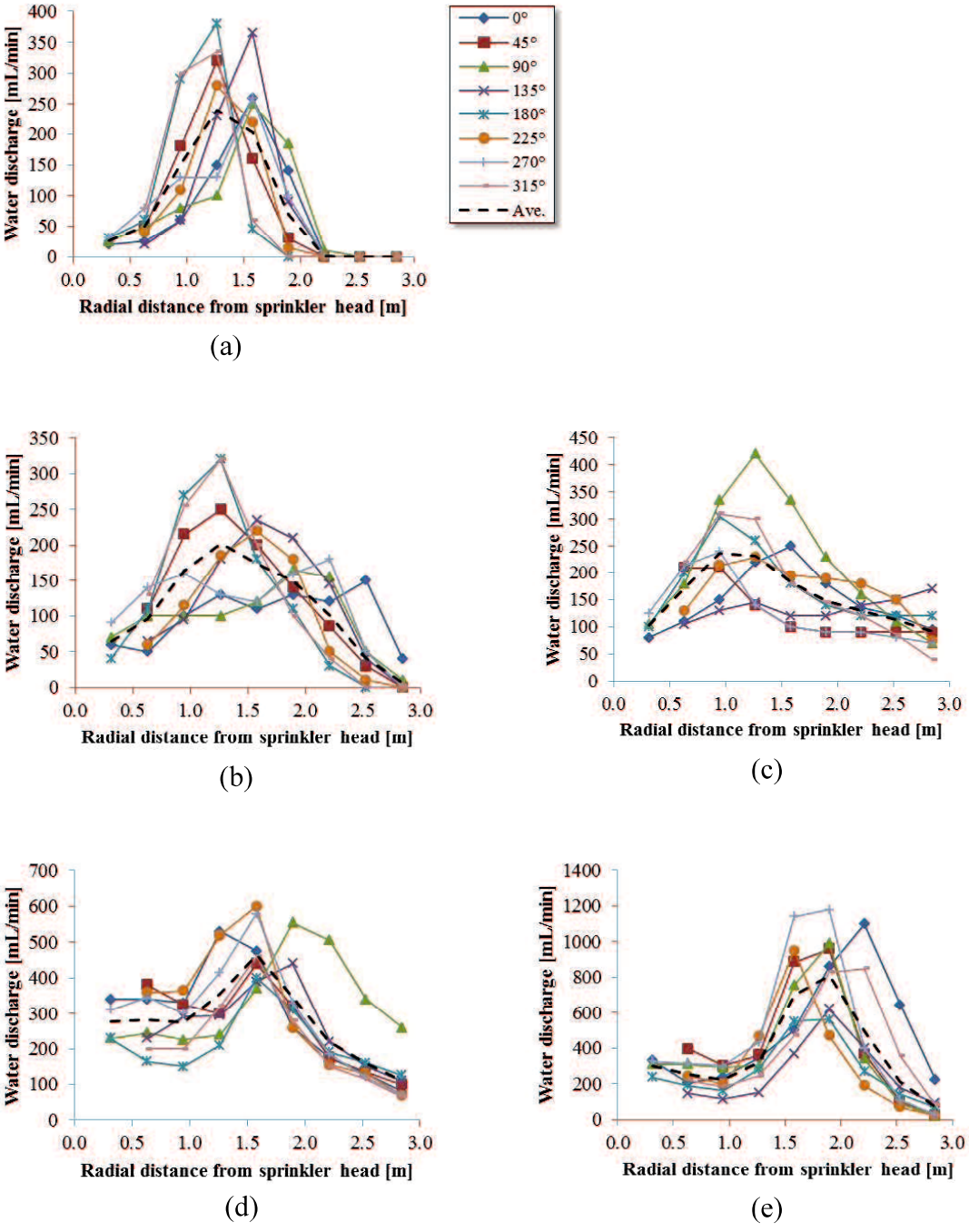

Figure 3.12 Water spray distribution patterns for K-43 sprinkler at (a) 0.02 MPa, (b) 0.05 MPa, (c) 0.1 MPa, (d) 0.4 MPa, and (e) 0.7 MPa.

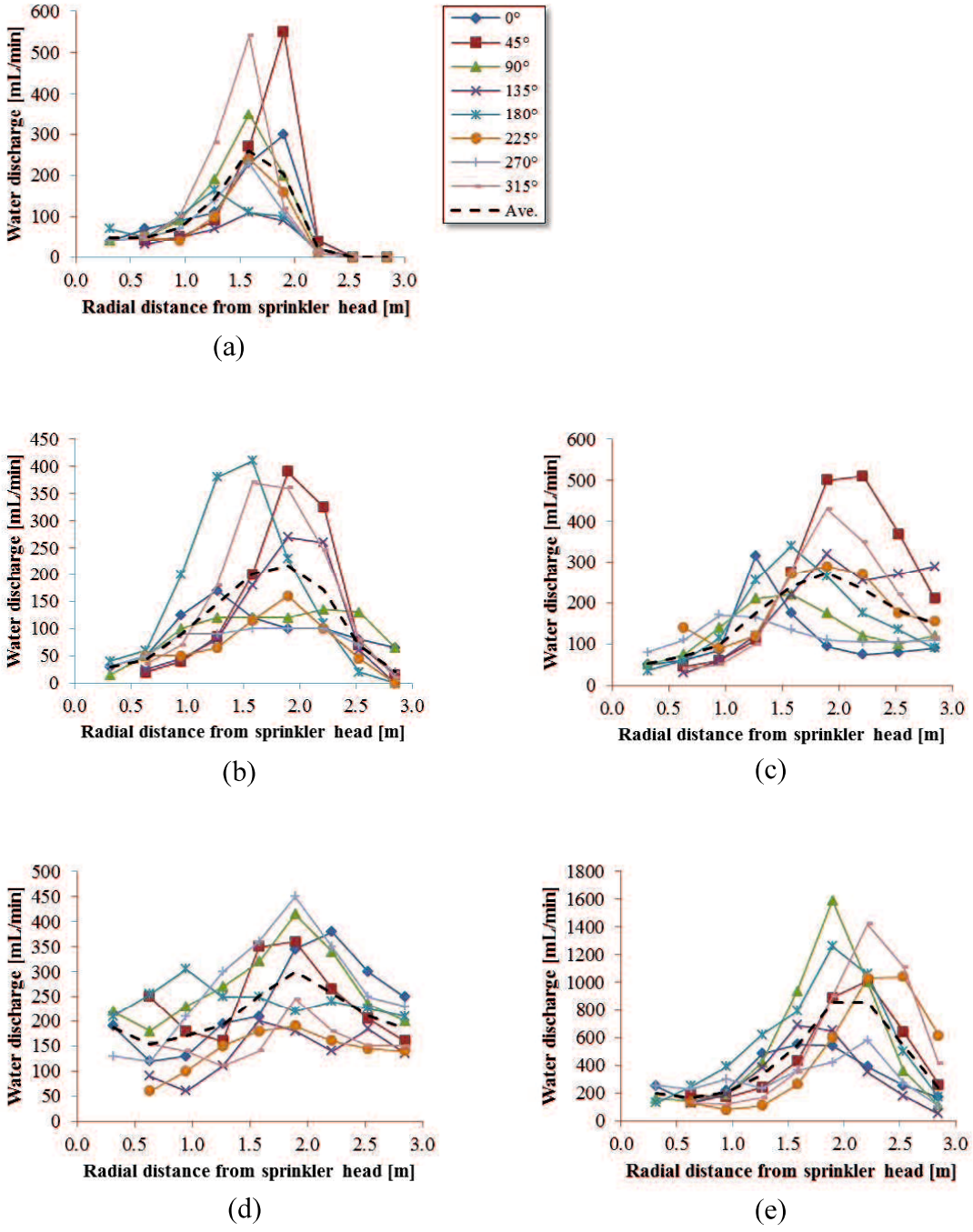

Figure 3.13 Water spray distribution patterns for K-50 sprinkler at (a) 0.02 MPa, (b) 0.05 MPa, (c) 0.1 MPa, (d) 0.4 MPa, and (e) 0.7 MPa.

Chapter 4

RESIDENTIAL SPRINKLER ANALYSIS AND DESIGN

4.1. Overview

A relatively large number of individual components for an existing fusible link, flush type pendent residential sprinkler render complexity of the assembly process. For such type of sprinkler, knowledge of the assembly mechanics is critical for ensuring proper and reliable operation over its intended service life. However, analytical method for predicting the assembly loads and structural response of such sprinkler has neither been well-established nor published in scholarly literature. Furthermore, the existing sprinkler was observed to spray water unevenly. It is hypothesize that the uneven water spray is due to its tripod-mounted deflector as can be related to the study in [37]. The impress screw that is used to provide the required force to seal the nozzle and prevent water leakage is manipulated from the interior of the sprinkler making it difficult to visually check the structural condition during and after assembly process. The large number of individual components also contributes to increased product cost, product rejection rate and high probability of activation malfunction. In this study, an analytical model for predicting the assembly loads and structural response of the sprinkler is developed. Equilibrium force system equations are derived considering load transfer mechanics within several contacting components for the two-step assembly process. Components integration and downsizing which have enabled an innovative design of the deflector with equally-sized spray ports uniformly located around the circumference are proposed. The size of the rectangular ports and the gap between the heat collector and deflector are

taken as design parameters for improving spray pattern and response time index (RTI) characteristics of the sprinkler. Design parameters are explored and corresponding prototypes are tested to verify water spray and RTI performance. The analytical model for predicting assembly loads is verified with experimental testing. Tests revealed that the proposed analytical model agrees significantly with test data. The proposed sprinkler exhibits even spray patterns when tested at different water pressures with RTI that meets standard regulations for residential application. Moreover, the proposed sprinkler is relatively slimmer with seven pieces less components resulting to an over 32% weight reduction compared to existing design.

Images of actual model
(Left: standby, Right: activated)

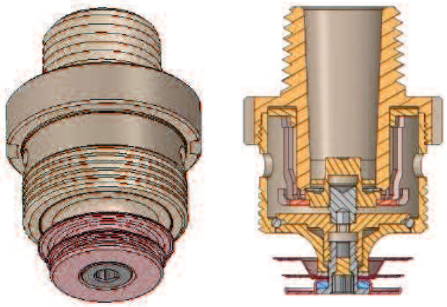

CAD model
(Left: Isometric, Right: Cross section)

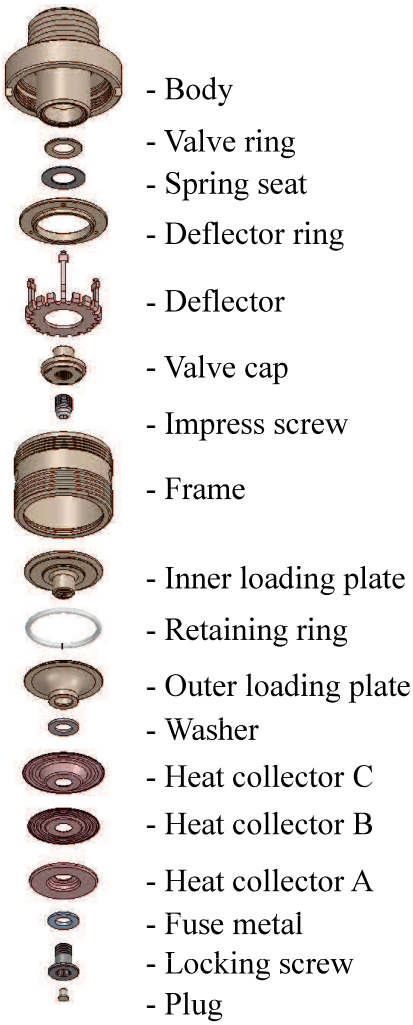

Figure 4.1 Existing residential sprinkler

4.2 Existing sprinkler

The existing fusible flush-type pendent residential sprinkler considered in this study is shown in Figure 4.1. It consists of 18 individual components made of various metallic materials that are highly resistant against corrosion such as brass, copper, stainless steel, titanium alloy, and bismuth-lead alloy. Eight of these components are manufactured by machining and 10 by molding or forming. The components are assembled in sequential manner and held tightly together by means of threaded connections.

4.3 Sprinkler components and their functions

The sprinkler components are categorized into two major sub-assemblies referred to in this study as *first sub-assembly* and *second sub-assembly* as depicted in Figure 4.2. These two sub-assemblies also correspond to the actual production assembly processes whereby the first sub-assembly is performed in its process line and upon completion, is brought into second sub-assembly process line for full assembly.

4.3.1 Heat collectors and fusible element

Heat collector A, B, and C (Figure 4.1.) are used to collect convective heat produced by fire. The collected heat is transferred to the fusible element or fuse metal by heat collector A via heat conduction. The fuse metal is melted when it reached the design temperature, triggering the activation of sprinkler (see Figure 2.1 for illustration of activation process). Since convective heat which is shown to supply over 80 percent of the heat needed for sprinkler activation [44] is carried by flowing

air past the sprinkler, proper arrangement of the heat collectors is crucial for efficient heat collection and sprinkler activation.

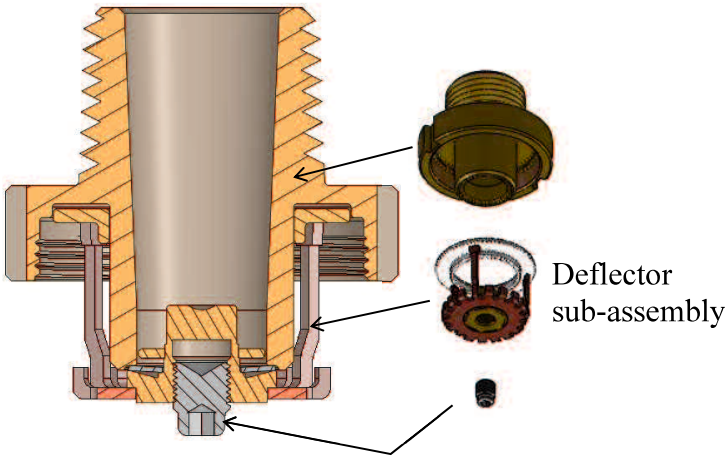

(a) Second sub-assembly components

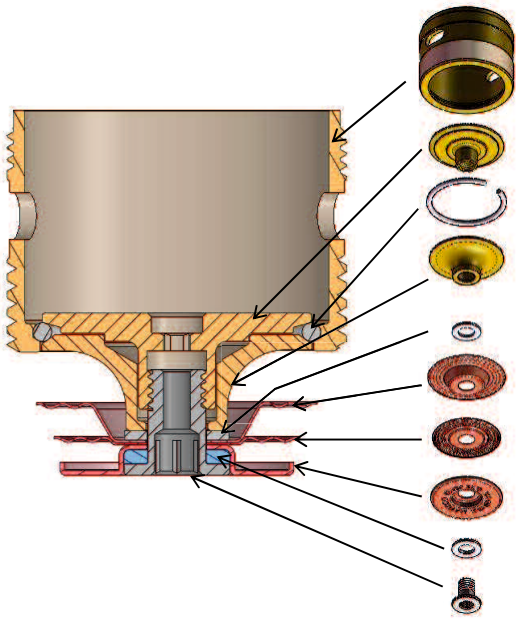

(b) First sub-assembly components

Figure 4.2 Sub-assemblies for the existing sprinkler

4.3.2 Locking devices

In the first sub-assembly (Figure 4.2b), the fuse metal, heat collectors, washer, outer loading plate, and retaining ring are sandwiched between the locking screw and inner loading plate. The locking screw and inner loading plate function as bolt-nut device that secures the sandwiched components altogether as depicted in Figure 4.3. Washer is used to ensure even distribution of bolt-nut pressure over the components being secured and reduce chance of damage on these components. The retaining ring which is installed in the groove of the frame as the locking screw and inner loading plate are tightened securely holds the sandwiched assembly in place. More details are discussed in the succeeding sections.

The impress screw which is a part of the second sub-assembly (Figure 4.2a) also provides locking effect to the sprinkler assembly. When the first and second sub-assemblies are joined together, the impress screw is tightened until enough pressure is generated against the valve cap and inner loading plate. The generated pressure tightly secures the valve cap with the orifice in the body.

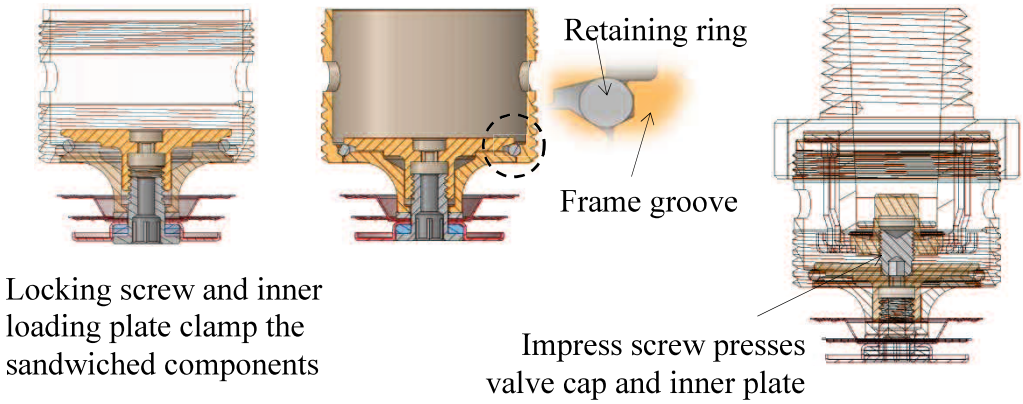

Figure 4.3 Sprinkler components functioning as locking devices

4.3.3 Deflector sub-assembly

The deflector sub-assembly is formed by joining the valve cap, deflector, deflector ring, spring seat and valve ring altogether, as shown in Figure 4.4a (see also Figure 4.2(a)). The valve cap has internal threads that enable the tightening or loosening of the impress screw. As been pointed out above, as the impress screw is tightened, the spring seat is pressed against the orifice, sealing the orifice. The valve ring serves as guide to ensure proper alignment of the deflector sub-assembly with orifice. The deflector ring serves as base support and stopper to the deflector sub-assembly during water discharge. The tripod not only mounts the deflector plate to its base but also provides enough space for generation of water spray.

Upon sprinkler activation, the pressurized water pushes the deflector sub-assembly causing the sandwich assembly (described above) to eject and the deflector sub-assembly with the impress screw attached to it to descend as depicted in Figure 4.4b. Water jet flows out of the orifice and strikes the deflector plate to form droplets which are sprayed over the area. For this reason, the deflector design significantly influences the water spray pattern performance of the sprinkler.

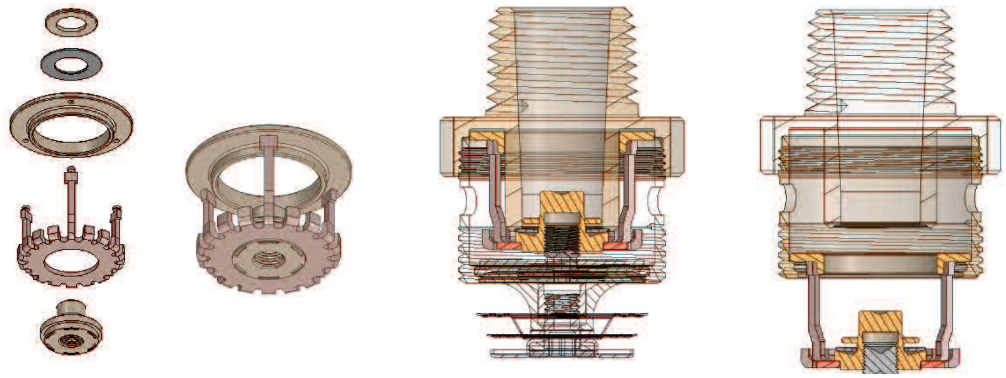

(a) Deflector sub-assembly (b) Deflector sub-assembly seals the orifice and deflects water jet during discharge

Figure 4.4 Deflector sub-assembly functional design

4.3.4. Sprinkler body and frame

The body and frame provides for enclosure, rigid support, and connection of first and second sub-assemblies. The sprinkler is fixed to a discharge terminal of the water distribution piping system through its taper-threaded inlet end. During sprinkler activation and water discharge, the frame supports the deflector sub-assembly through the deflector ring (as pointed out above).

4.4. Analysis of assembly forces and structural response

As been described in the previous sections, the sprinkler components are joined together using threaded connections which ultimately impose compressive force on the fuse metal. During the first sub-assembly process, the fuse metal is subjected to direct compressive force resulting from the clamping of sandwiched components by the locking screw and inner loading plate (see Figure 4.3). After the *second sub-assembly* has been connected with the *first sub-assembly*, the tightening action of the impress screw imposes another compressive force which is observed to reduce the effect of the first compressive force on the fuse metal. The force generated from tightening the locking screw with the inner loading plate is called as the *first assembly force*. Accordingly, the force generated by tightening the impress screw is called the *second assembly force* while the final value of the compressive force on the fuse metal due the counteracting effect of the *second assembly force* is called as the *net compressive force*. A low value of the *first assembly force* may be able to clamp the associated components but may snap loose once the *second assembly force* is applied. On the hand, if excessively high may induce compressive force high enough to produce large deformation of the fuse metal that will trigger sprinkler

activation. The suitable magnitudes of these assembly loads are needed to be determined to ensure water-tight connections and the structural integrity of fuse metal, i.e. significant amount of deformation or strain that may render misoperation or unintended activation of the sprinkler has to be avoided. The development of theoretical methods for the analysis of assembly forces and the corresponding structural response of the fuse metal is presented in the succeeding sections.

4.4.1 First assembly force

The *first assembly force* is analyzed by considering the mechanics of *first sub-assembly* process. Referring to Figure 4.5 (see also Figure 4.3), the fuse metal, heat collector A, B, and C, washer, outer loading plate, and retaining ring are clamped together by the locking screw (as bolt) and inner loading plate (as nut). The clamped components are secured in place by tightening the locking screw with inner loading plate with a sufficient *first assembly torque* T_1 . The *first assembly force* F_1, the force equivalent of T_1, pushes the retaining ring to set tightly into the frame groove to secure the *first sub-assembly.* The completed *first sub-assembly* is shown to the right of Figure 4.5.

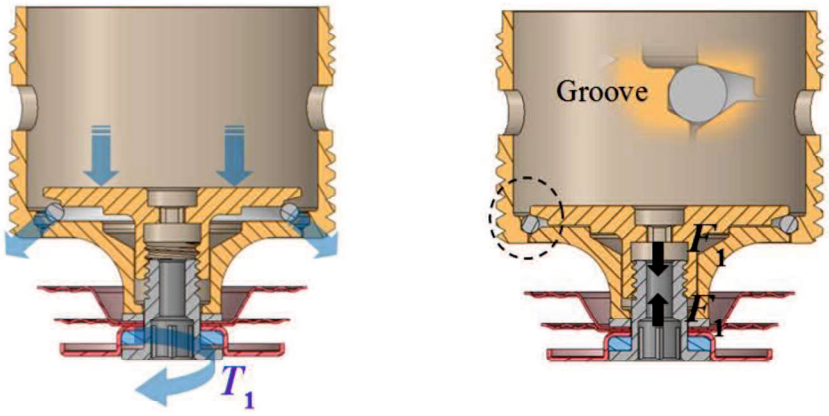

Figure 4.5 First sub-assembly process and the corresponding first assembly load

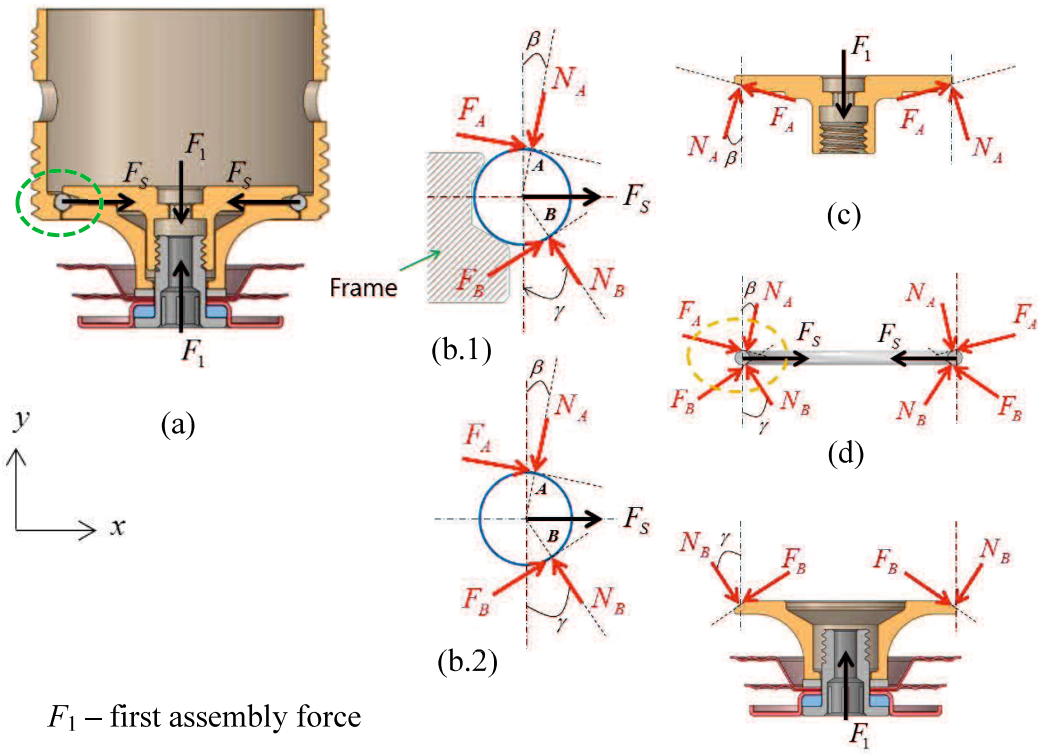

Figure 4.6 Free-body diagrams for first assembly force analysis

The retaining ring which is a kind of spring, generates spring force F_S when it is stretched. In other words, the minimum value of F_1 should be sufficient to overcome F_S and the frictional forces on the contacting surfaces so that the retaining ring can be stretched and secured into the frame groove. Conversely, if F_1 is significantly higher than the minimum value, the retaining ring will be stretched further generating higher F_S. Consequently, the retaining ring can only be stretched within the bounds of sprinkler frame. Regardless how high F_1 becomes the reaction force exerted by the retaining ring should remain unchanged with a value equivalent to the spring force at maximum allowable stretch or change in ring diameter (note the

distinction between ring and wire diameter). In such case, the excess force is imposed on the frame.

Since the system is static, the reaction forces on the retaining ring and frame for different values of F_1 is analyzed using static rigid body mechanics approach. By assuming F_S to represent lumped reaction forces of the retaining ring and frame, a single analytical model can be utilized for various scenarios. The free-body diagrams (FBDs) of the contacting components of the *first sub-assembly* are shown in Figure 4.6 (cross-hatches in the section views are removed for clarity of illustrations).

Considering FBDs in Figure 4.6(c),

$$\left[\Sigma F_y = 0; F_A = \mu N_A\right]:$$

$$N_A = \frac{F_1}{2\left(\cos\beta + \mu\sin\beta\right)} \tag{4.1}$$

where μ is the coefficient of static friction. From Figure 5.6(e),

$$\left[\Sigma F_y = 0; F_B = \mu N_B\right]:$$

$$N_B = \frac{F_1}{2\left(\cos\gamma + \mu\sin\gamma\right)} \tag{4.2}$$

and Figure 5.6(b)

$$\left[\Sigma F_x = 0\right]:$$

$$F_S = \frac{1}{2}\left(\frac{\sin\beta - \mu\cos\beta}{\cos\beta + \mu\sin\beta} + \frac{\sin\gamma - \mu\cos\gamma}{\cos\gamma + \mu\sin\gamma}\right)F_1 \tag{4.3}$$

The relationship between F_1 and F_S is expressed in equation (4.3) and plotted in Figure 4.7 with $\mu = 0.212, \beta = 15°, \gamma = 35°$. Figure 4.7 clearly shows that the assumed lumped reaction force of the retaining ring and frame varies linearly with the *first assembly force*.

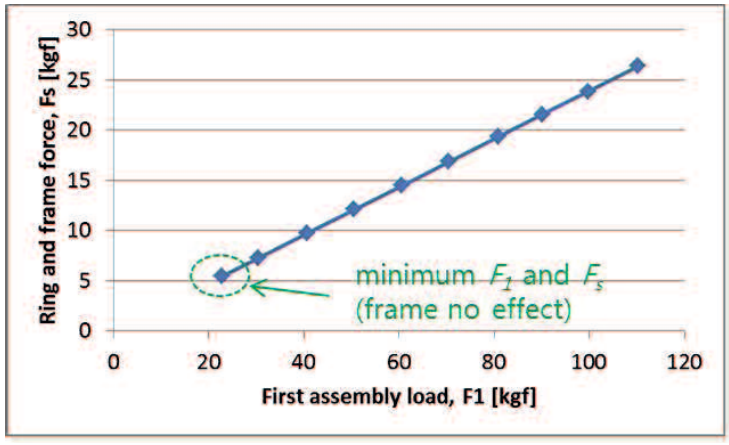

Figure 4.7 Relationship between first assembly force and reaction forces for the existing sprinkler

4.4.2 Retaining ring force

As been pointed out, the minimum F_1 (see Figure 4.7) corresponds to the retaining ring spring force at maximum allowable stretch or change in retaining ring diameter and frictional resistance forces in the contacting surfaces between retaining ring, inner and outer loading plates. The maximum allowable stretching or change in diameter of the retaining ring is depicted in Figure 4.8.

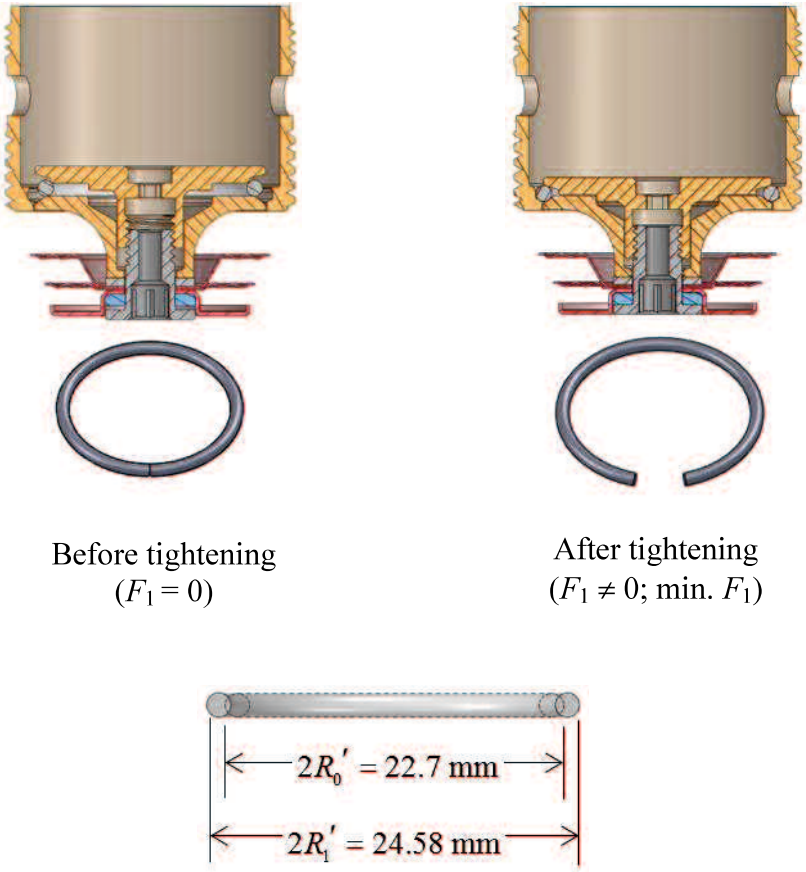

Figure 4.8 Maximum allowable change in retaining ring diameter to prevent unintended sprinkler activation

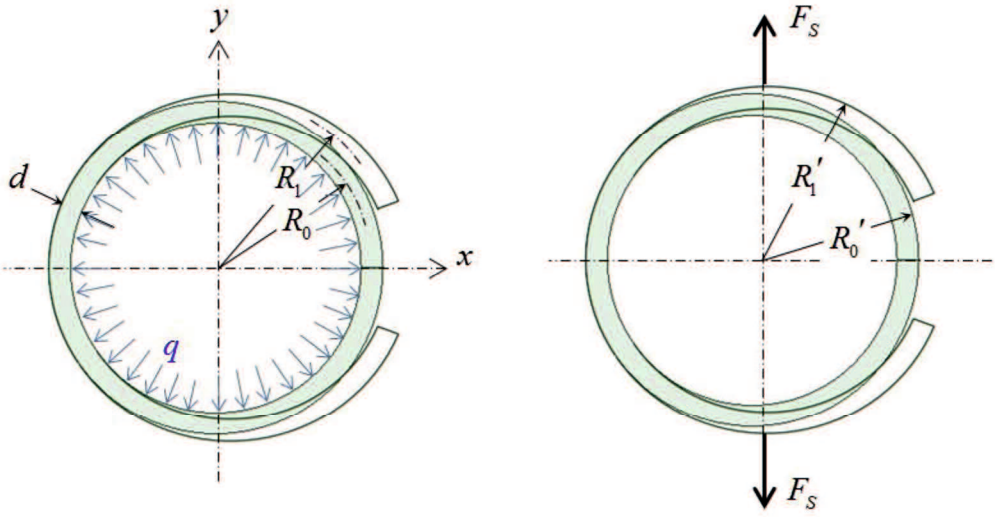

Figure 4.9 Spring force in radially-stretched rings

Referring to Figure 4.9, the formula for calculating the retaining spring force for a given change in ring diameter can be derived as

$$F_S = -EI\left(\frac{1}{R_1^{\,2}} - \frac{1}{R_0^{\,2}}\right) \tag{4.4}$$

where $E = 115\,\text{GPa}$ (Ti-6Al-4V) , $I = \frac{\pi d^4}{64}$, $d = 1.6\,\text{mm}$, $R_0 = R_0' - \frac{d}{2}$, and $R_1 = R_1' - \frac{d}{2}$ giving $F_S = 5.36\,\text{kgf}$.

In equation (4.4), E is the elastic modulus of the retaining ring material (Ti-6Al-4V, titanium alloy), I is the area moment of inertia (of circular wire), d is the wire diameter, R_0 and R_0' are the mean and outer radii of unstretched ring, respectively, R_1 and R_1' are the mean and outer radii of stretched ring. The details for the derivation of equation (4.4) can be found in Appendix.

Using equation (4.4) and noting in Figure 4.8, the values of retaining ring radii R_0' and R_1' for maximum allowable stretching, the corresponding $F_S = 5.36\,\text{kgf}$ is determined. With $F_S = 5.36\,\text{kgf}$ and $\mu = 0.212$, the minimum required $F_1 \approx 22\text{kgf}$ as can be seen in Figure 4.7.

4.4.3 First assembly torque-force conversion

Since the first assembly components are joined together by threaded connection (see Figure 4.5), F_1 is applied in terms of T_1 using torque wrench or driver

devices installed in the assembly line. Although the coefficient of friction may vary widely, the torque required to produce such force can be approximated [45] using

$$F_1 = 2T_1\left[d_m\left(\frac{\tan\lambda + f\sec\alpha}{1 - f\tan\lambda\sec\alpha} \right) + f_c d_c \right]^{-1} \tag{4.5}$$

where

T_1 – first assembly torque
F_1 – first assembly force
d_m – locking screw mean (bolt) diameter
d_c – mean diameter of the fuse metal (collar)
f – locking screw coefficient of friction
f_c – fuse metal coefficient of friction
α – screw helix angle $(\alpha = 30°)$
λ – screw lead angle $\left(\lambda = \tan^{-1} l/\pi d_m\right)$
l – lead $(l = p$; single-threaded; p – pitch$)$

For metric locking screw (used as bolt) and with fuse metal (used as collar) forming an annulus,

$$d_m = d - 0.649519p \tag{4.6}$$

and

$$d_c = \frac{2\left(d_o^{\,3} - d_i^{\,3}\right)}{3\left(d_o^{\,2} - d_i^{\,2}\right)} \tag{4.7}$$

respectively; where d is the nominal outside diameter of the locking screw , d_i and d_o are the inner and outer diameters of the fuse metal.

In the existing sprinkler, the specifications for the locking screw and fuse metal which are used as bolt and collar respectively are illustrated in Figure 4.10. Based on the design specifications, $d_m = 4.48$ mm and $d_c = 7.2$ mm.

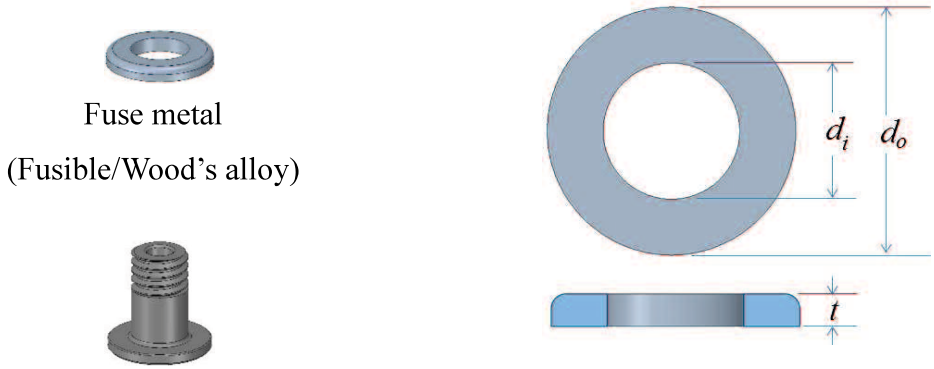

$$d_m = d - 0.649519p$$
$$= 5 - 0.649519(0.8)$$
$$= 4.48 \text{ mm}$$

$$d_c = \frac{2\left(d_o^3 - d_i^3\right)}{3\left(d_o^2 - d_i^2\right)}$$
$$= \frac{2\left(9.1^3 - 5^3\right)}{\left(9.1^2 - 5^2\right)}$$
$$= 7.25 \text{ mm}$$

Figure 4.10 Design specifications for locking screw and fuse metal

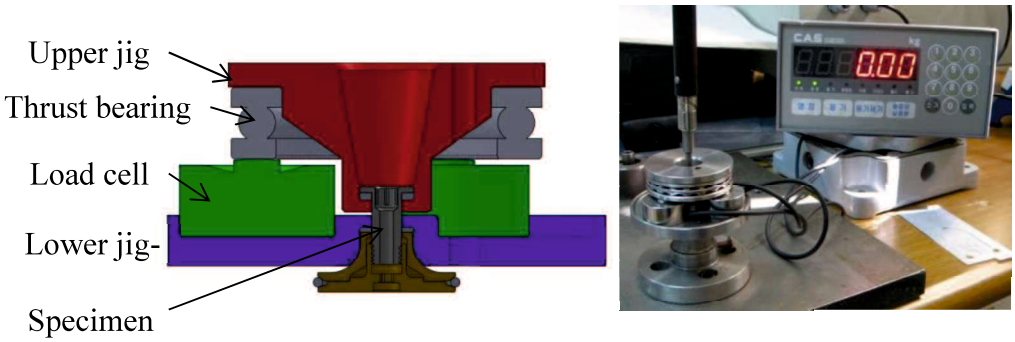

(locking screw, fuse metal, and inner loading plate)

Figure 4.11 Test setup for verification of $T_1 - F_1$ conversion and actual coefficient of friction

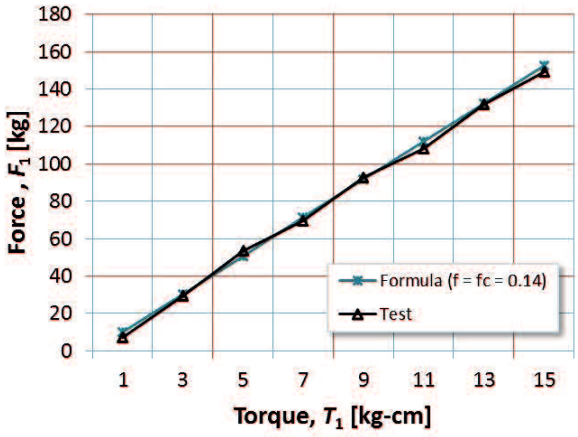

Figure 4.12 First assembly torque-force conversion graph

The coefficient of friction depends upon the surface smoothness, accuracy, and degree of lubrication. However, on the average, $f = f_c = 0.15$ can be assumed [45]. Experimental tests depicted in Figure 4.11 have been performed to establish reference data for $T_1 - F_1$ conversion and to obtain good approximate of the actual value of coefficient of friction $f = f_c$ existing within the first sub-assembly components. Figure 4.12 shows the comparison between theoretical results and experiment. It is noted that $f = f_c = 0.14$ has provided very good agreement between the use of equation (4.5) to convert F_1 to T_1 and test data.

4.4.4 Functional design of fuse metal

Section 4.2.1 has provided brief introduction of the function of fuse metal for the sprinkler assembly. It should be noted that the sprinkler is actually classified as "fusible type" mainly because of its activation mechanism which is initiated by the melting of the fuse metal in contrast to the "bulb type" sprinkler which is activated by the bursting of the bulb.

In another perspective, the fuse metal can be thought of as a device that provides for ensuring that the clamped components in the first sub-assembly are secured in place, otherwise the sub-assembly will dislodge from the frame and ejects, subsequently activating the sprinkler. Figure 4.13 illustrates in detail the functional design of fuse metal (cross-hatches are removed for clarity). Referring to Figure 4.13, when the sprinkler is at standby/normal mode excessive deformation or significant change in thickness of the fuse metal can cause sprinkler activation, thus must be avoided. The maximum allowable fuse metal thickness change can be calculated by analyzing the geometry when the retaining ring is securely installed and when it retracts and moves downward until it dislodges out of the frame groove as shown in Figure 4.14. The maximum change in thickness or normal deformation of the fuse metal is determined as

$$\delta_y = y_1 - y_0 = \left(\tan\beta + \tan\gamma\right)\delta_x \tag{4.8}$$

$$= 0.58 \text{ mm}; \left[\text{for}: \beta = 15^\circ; \gamma = 35^\circ\right]$$

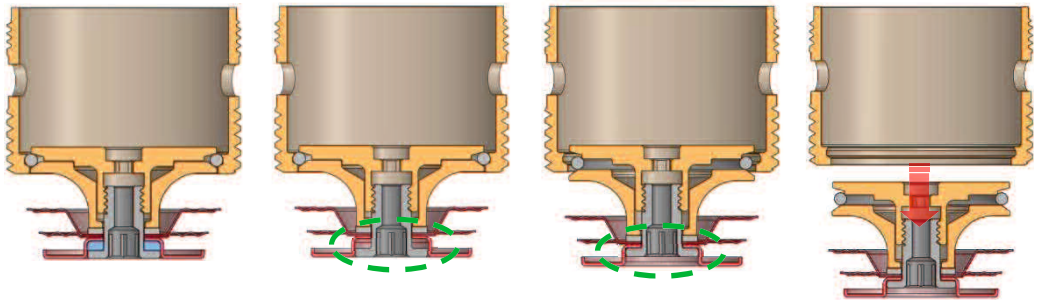

(a) Fuse metal secures components.

(b) Melting/removal of fuse metal.

(c) Sub-assembly loosens, retaining ring retracts.

(d) Sub-assembly ejects, sprinkler activates.

Figure 4.13 Illustrative description of the function of fuse metal in the sprinkler

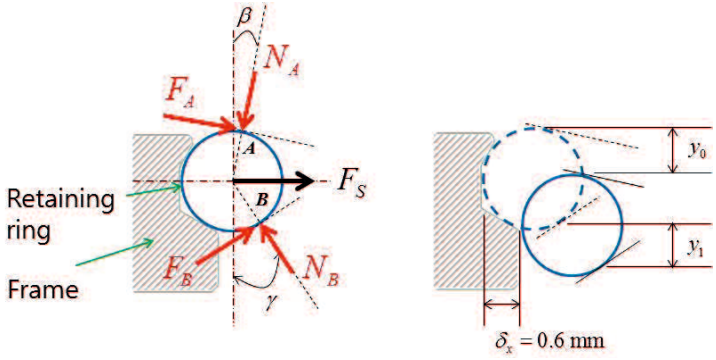

Figure 4.14 Geometric analysis of retaining ring-frame groove connection

4.4.5 Fuse metal response to first assembly force

Fuse metal is made of Wood's (fusible) alloy, a Pb-based alloy which is naturally relatively soft. It has been observed that the fuse metal exhibited deformation that resulted to the significant reduction of compressive force after the first sub-assembly is completed. To avoid excessive loading of the fuse metal the suitable T_1 must be determined. Although, nonlinear response may exist due to the material properties (see Table 4.1) of the fuse metal, simple equations for static, linear assumptions are utilized to approximate the normal deformation and stress in the fuse metal. The deformation and stress in the fuse metal are expressed as

$$\Delta t = \frac{F_1 t}{EA} \tag{4.9}$$

and

$$\sigma = \frac{F_1}{A} \tag{4.10}$$

respectively, where δ is the normal deformation, σ is the normal stress, t is the thickness, E is the elastic modulus, A is the bearing area. Noting that F_1 is a function

of T_1 , the deformation and stress with respect to the first assembly torque are shown in Figure 4.15 and Figure 4.16 respectively. At $T_1 = 11\,\text{kgf-cm}\,(F_1 \approx 110\,\text{kgf})$ the normal stress is about 25 MPa which is slightly less than the σ_y of fuse metal. This condition suggests that the linear analysis assumption appears to be valid up to such value of T_1. Furthermore, at $T_1 = 11\,\text{kgf-cm}\,(F_1 \approx 110\,\text{kgf})$, the normal deformation $\Delta t \approx 0.7 \times 10^{-6}\,\text{m}$ which is by referring to equation (4.8), relatively insignificant.

Table 4.1 Material properties of fuse metal

Material	Wood's alloy
Elastic modulus, E	39.0 GPa
Poisson's ratio, ν	0.4
Yield strength, σ_y	26.0 MPa
Tensile strength, σ_u	42.0 MPa

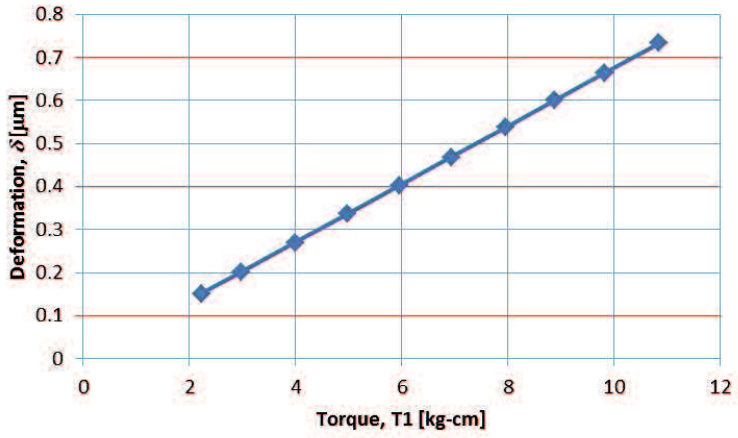

Figure 4.15 Fuse metal deformations during first assembly for the existing sprinkler

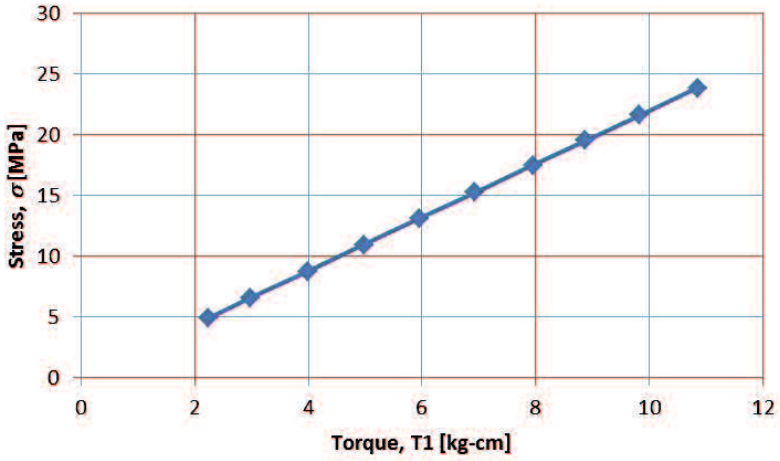

Figure 4.16 Fuse metal stresses first assembly for the existing sprinkler

4.4.6 Second assembly force

Referring to Figure 4.2, the first sub-assembly and second sub-assembly are joined by threaded connections to complete the full sprinkler assembly. Once the connection is secured, the *second assembly force* F_2 is generated by applying *second assembly torque* T_2 to the impress screw. The application of F_2 to the impress screw causes the valve cap to be pressed against the orifice of the orifice and the inner loading plate against the retaining ring as depicted in Figure 4.17. The pressing force should be sufficiently large enough to keep the orifice closed and prevent water leak until the sprinkler is activated. The minimum amount of pressing force generated by the impress screw should be at least equivalent to the hydrostatic test pressure specified by international approval standards.

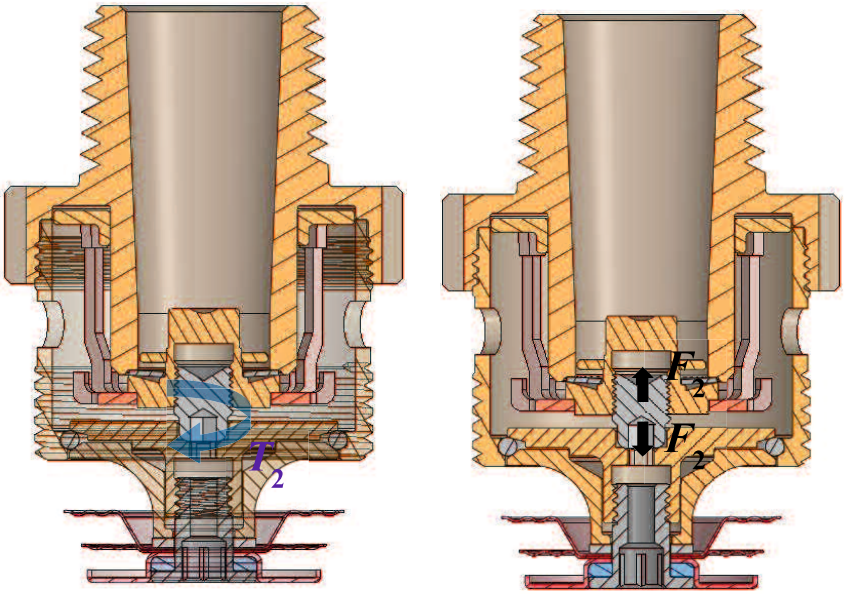

Figure 4.17 Application of second assembly force

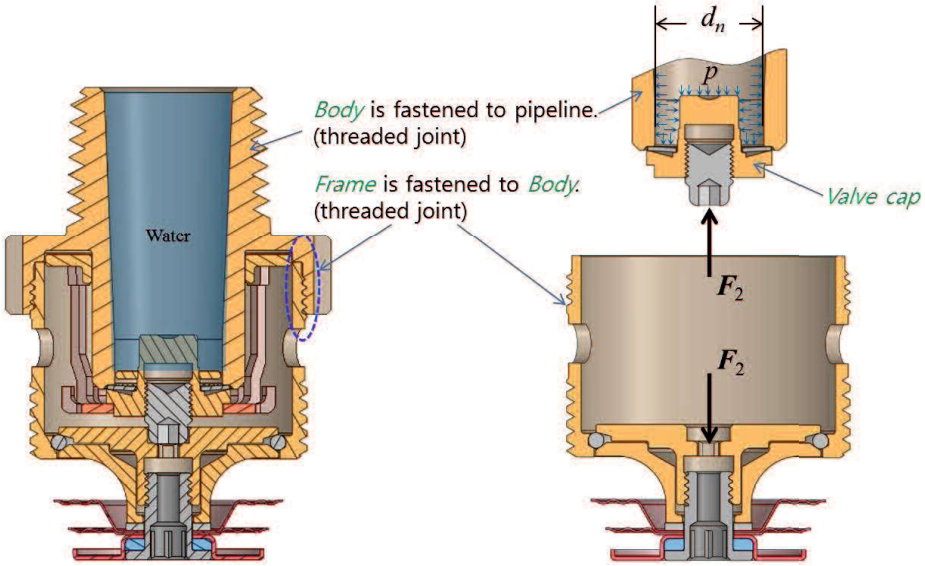

Figure 4.18 Free-body diagram of the sprinkler under hydrostatic pressure

The FBD of the full sprinkler assembly when subjected to hydrostatic test as shown in Figure 4.18 is analyzed in order to determine the required F_2. From the FBD (Figure 4.18, right), the required F_2 is calculated as

$$\left[\Sigma F_y = 0\right]:$$

$$F_2 = \frac{\pi d_r^{\,2}}{4} \cdot p \tag{4.11.1}$$

where d_r is the diameter of orifice and p is the water pressure. UL 199 [17] and FM 2030 [46] standards for automatic residential sprinkler (rated up to 1.2 MPa) specify hydrostatic test pressure of about 4.8 MPa. Hence, to meet such standards F_2 is determined as

$$F_2 = \frac{\pi (11.3)^2 \, 4.8}{4(9.81)} = 49.1 \,\text{kgf} \tag{4.11.2}$$

$F_2 = 60 \,\text{kgf}$ is used to account for safety factor.

The corresponding T_2 that can generate the required F_2 for the impress screw is determined in similar fashion as with the case of locking screw (described in Section 4.4.3). For the case of impress screw, the screw collar is assumed as the head of the impress screw itself. The mean diameter of the collar is calculated using equation (4.7) but setting $d_i = 2.2 \,\text{mm}$ and $d_o = 4.1 \,\text{mm}$. Equations (4.5) and (4.6) are used accordingly with the impress screw specified as single-threaded M5 × 0.5 bolt, and $f = f_c = 0.14$.

4.4.7 Analysis of net compressive force on fuse metal

The application of second assembly force via T_2 presses the valve cap against the orifice at one end of the impress screw, and also presses the inner loading plate against the retaining ring at the other end. The pressing of the inner loading plate against the retaining ring is seen to cause reduction of the effect of F_1 ultimately over the compressive force on the fuse metal. This observation is investigated by analyzing the system of forces that exist in the involved key sprinkler components when F_2 is imposed. The force system for each sprinkler component of interest is established by using FBDs with considerations on the effects of both F_1 and F_2. It should be noted that at this point, the effect of F_1 is internal to the system.

Figure 4.19(a) shows the FBD of *first sub-assembly* components with F_2 representing the action of impress screw on the inner loading plate. It can be seen that the action of F_2 on the inner loading plate is supported by the frame through the retaining ring. The inclined orientation of the frame wall promotes the sliding of retaining ring down and inward. Moreover, the deformation of the inner loading plate can also relieve the pre-load on the locking screw (imposed by F_1). In the current investigation, rigid body static analysis is considered, thus the effect of any deformation is ignored. The remaining or net compressive force F_{net} on the fuse metal is reflected on the FBD of inner and outer loading plates as shown in Figure 4.19(c) and 4.19(e), respectively.

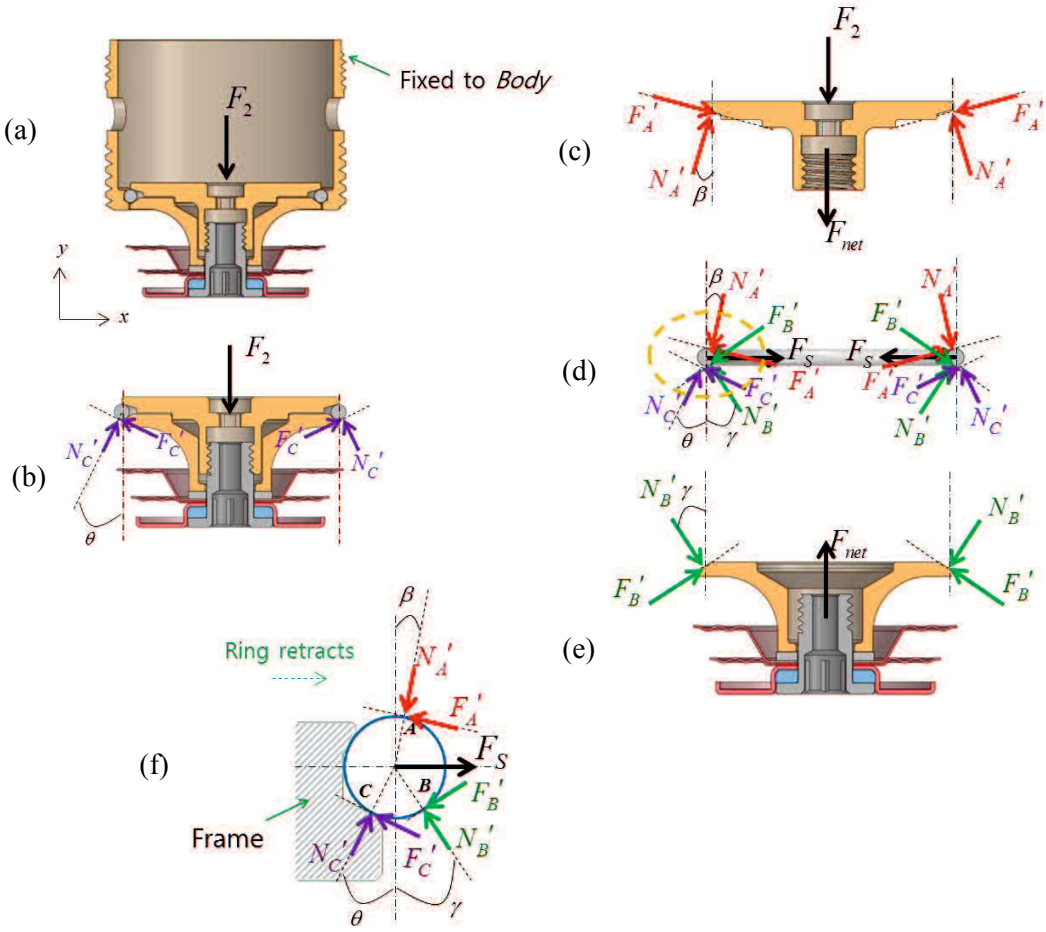

Figure 4.19 System of forces in the sprinkler components considering the effect of assembly forces.

From Figure 4.19(b)

$$\left[\Sigma F_y = 0\right]:$$

$$N_C' = \frac{F_2}{2\left(\cos\theta + \sin\theta\right)} \tag{4.12}$$

and from Figure 4.19(f)

$$\left[\Sigma F_x = 0; F' = \mu N'\right]:$$

$$\left(\sin\beta+\mu\cos\beta\right)N_A{}'+\left(\sin\gamma+\mu\cos\gamma\right)N_B{}'=\left(\sin\theta-\mu\cos\theta\right)N_C{}'+F_S \qquad (4.13)$$

$\left[\Sigma F_y=0\right]$:

$$\left(\cos\beta-\mu\sin\beta\right)N_A{}'+\left(-\cos\gamma+\mu\sin\gamma\right)N_B{}'=\left(\cos\theta+\sin\theta\right)N_C{}' \qquad (4.14)$$

Note in equations (4.13) and (4.14) that $F_S=f\left(F_1\right)$. Using equation (4.12), equations (4.13) and (4.14) can be rewritten respectively as

$$\left(\sin\beta+\mu\cos\beta\right)N_A{}'+\left(\sin\gamma+\mu\cos\gamma\right)N_B{}'=\frac{\left(\sin\theta-\mu\cos\theta\right)}{\left(\cos\theta+\mu\sin\theta\right)}\left(\frac{F_2}{2}\right)+F_S \quad (4.13')$$

$$\left(\cos\beta-\mu\sin\beta\right)N_A{}'+\left(-\cos\gamma+\mu\sin\gamma\right)N_B{}'=\frac{F_2}{2} \qquad (4.14')$$

Considering equations $(4.13')$ and $(4.14')$ simultaneously gives

$$\begin{Bmatrix}N_A{}'\\N_B{}'\end{Bmatrix}=\begin{bmatrix}\left(\sin\beta+\mu\cos\beta\right), & \left(\sin\gamma+\mu\cos\gamma\right)\\\left(\cos\beta-\mu\sin\beta\right), & \left(-\cos\gamma+\mu\sin\gamma\right)\end{bmatrix}^{-1}\begin{Bmatrix}\frac{\left(\sin\theta-\mu\cos\theta\right)}{\left(\cos\theta+\mu\sin\theta\right)}\left(\frac{F_2}{2}\right)+F_S\\\frac{F_2}{2}\end{Bmatrix} \qquad (4.15)$$

where F_S is given in equation (4.3). From Figure 4.19(c) and 4.19(e),

$\left[\Sigma F_y=0\right]$:

$$F_{net}=2*\left\{\left(\cos\beta-\mu\sin\beta\right)N_A{}'-\frac{F_2}{2}\right\} \qquad (4.16.1)$$

$$F_{net} = 2*\left(\cos\gamma - \mu\sin\gamma\right)N_B' \tag{4.16.2}$$

4.4.8 Experimental measurement of net compressive force

Experiments were carried out to measure the corresponding actual F_{net} imposed unto the fuse metal at the end of the sprinkler full assembly process. The schematic of the experimental measurement setup is shown in Figure 4.20. Note that except for the test specimen, the same devices as the ones used for verifying the load-torque conversion (see Section 4.4.3) are used for this experiment. A sample measurement with $T_1 = 12\,\text{kgf}\cdot\text{cm}$ ($F_1 \approx 121\,\text{kgf}$), and $T_2 = 6\,\text{kgf}\cdot\text{cm}$ ($F_1 \approx 61\,\text{kgf}$) proves that there exists a significant reduction in compressive load in the fuse metal when F_2 is applied as shown in Figure 4.21. The sample data also shows that it takes some time for the compressive load due to F_1 to stabilize. This is due to the fact that the fuse metal is relatively soft and will likely experience creep. In this study, creep is not considered therefore the fuse metal was removed during the experimental measurement. Additionally, since the static rigid body condition is assumed in the analysis, the removal of fuse metal could make the measurement consistent with such assumption.

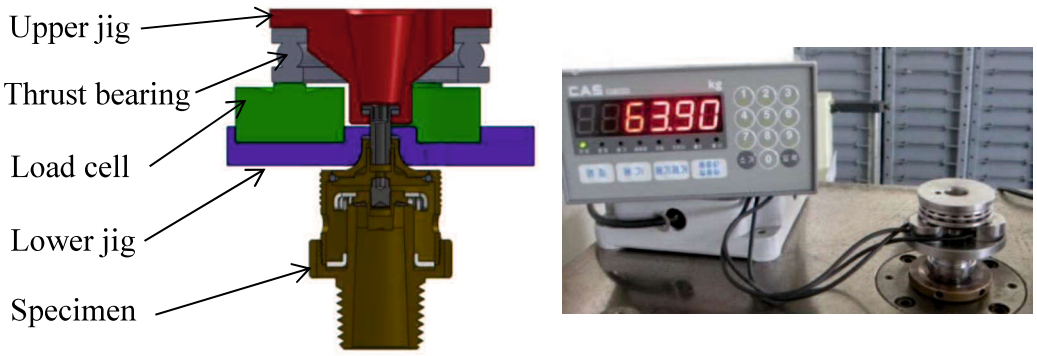

Figure 4.20 Test setup for measuring net compressive force on fuse metal

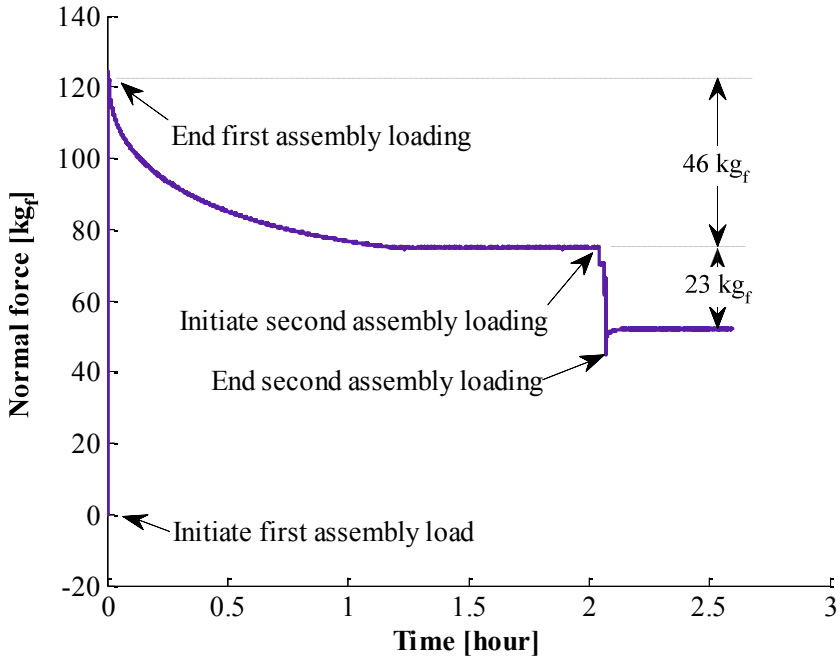

Figure 4.21 Compressive load in the fuse metal as measured experimentally during full assembly process

4.4.9 Analytical model vs. experiment

Using the analytical model for calculating F_{net} as expressed in equations, (4.15), and (4.16), with $\theta = 30°, \gamma = 35°, \beta = 15°$ and certain values of μ, the results are shown in Figure 4.22. T_2 is held constant at $T_2 = 6\,\text{kgf}\cdot\text{cm}$ ($F_1 \approx 61\,\text{kgf}$) for all tests and calculations. It can be noticed from Figure 4.22 that when $\mu = 0.1$, the analytical model agrees significantly with experiment data at lower values of F_1. On the other hand, when $\mu = 0.06$ the model and experiment agrees at higher values of F_1. These results suggest several important points: (1) that there seems to be no single μ for the analytical model that can actually predict corresponding F_{net} at various F_1 (2) values of μ that have enabled significant agreement between the model and experiment are relatively lower compared to the value ($\mu = 0.212$)

considered in the *first assembly force* analysis (see Section 4.4.1), – this could mean that frictional forces are small because the retaining does not actually move or not at the point of impending motion especially when F_1 is greater than its minimum value; (3) as F_1 increases μ decreases – which could be translated into some sort of fact (similar to point (2)) that when F_1 is too large enough to clamp the sandwiched components particularly the retaining ring, the prescribed F_2 is unable to produce any significant effect to the retaining ring that will cause it to slide down and inward; (4) that rigid body mechanics assumption may be insufficient, and effects of components deformation should be considered in the analysis; (5) F_{net} is caused mainly by the deformation of inner loading plate that has enabled the fuse metal to be relieved from the compression of F_1 (locking screw/bolt pre-load relief).

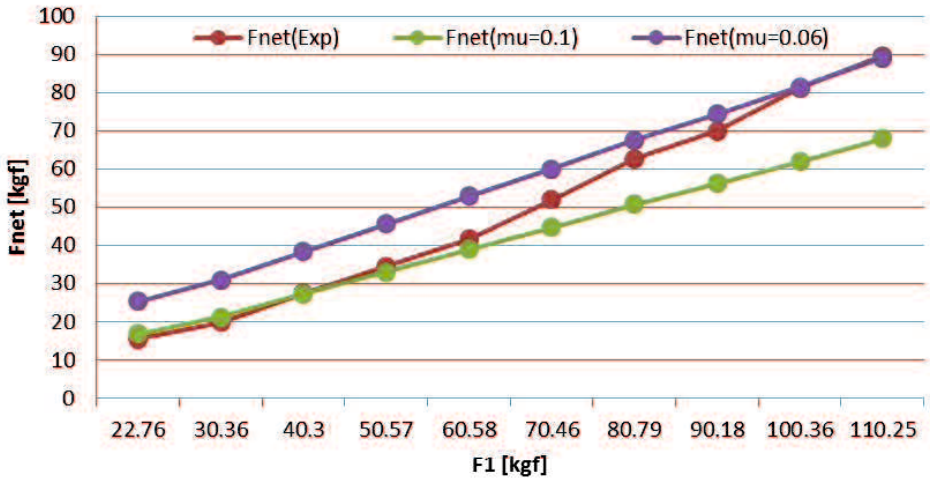

Figure 4.22 Calculated F_{net} for different μ as compared with experiment data

4.4.10 Development and verification of friction model

Based on the preceding discussions, it was pointed out that a single μ to be used with the analytical model in estimating F_{net} at various F_1 does not exist. This non-existent of single μ can be due to the fact that the reaction forces due to a constant F_2 at the contact surfaces vary accordingly with F_1. For instance, at minimum F_1 the retaining ring is stretched and pushed towards the frame groove just enough to secure the sub-assembly in place without causing any additional amount of reaction force from the frame when F_2 is applied. On the other hand, when F_1 is large the retaining ring is pushed against the frame wall causing contact with more surfaces of the groove and generating a different set of reaction forces even when the same F_2 is applied. Accordingly, the magnitude and direction of different sets of reaction forces would change with F_1. In the analysis however, these conditions were ignored and that only one contact point (points C, see Figure 4.19) in the frame is considered regardless the value of F_1. At low value of F_1 the assumption is valid since the retaining ring will be able to retract and slide down the frame wall when F_2 is applied. But such may not hold true for large F_1 as already been pointed out. Considering the above conditions means that an analysis model has to be developed for each and every considered value of F_1 which seems to be an impractical approach. Alternatively, considering the effect of deformation of sprinkler components to F_{net} seems to be a viable option but can be a tedious analysis undertaking due to the complexity associated with a few number of involved components.

In this study, since experimental data are readily available, the analytical model formulated in the previous section (Section 4.4.8) is improved by introducing additional assumptions that take into account the influencing factor. In this case, the influencing factors are related with the reaction forces due to F_1 which are resolved into components normal and tangent to the contact surfaces. The reaction force component tangent to the surface is the frictional force. When the orientation of the contact surfaces changes due to the deformation of the components, the direction and magnitude of the normal and frictional forces would change accordingly even with the same coefficient of friction μ as depicted in Figure 4.23. The corresponding change in direction and magnitude of normal and frictional forces in all contact surfaces are quite complex to be considered simultaneously. Since frictional force F is a product of μ and normal force N, the variation of such reaction forces with F_1 can be modeled by manipulating the value of μ instead.

Theoretically, the proposed method (discussed above) seems to violate the definition of μ (coefficient of friction) since the material for the components remains unchanged. However, by closely examining the basic equation for frictional force which is simply $F = \mu N$, it can be seen (in Figure 4.23) that a change in the value of N by a certain factor k due to deformation resulting from the application of F_1 can be expressed as

$$\tilde{F} = \mu\tilde{N} = \mu kN \tag{4.17.1}$$

where $\tilde{F}$ and $\tilde{N}$ are the corresponding frictional and normal forces, respectively associated with the deformation of inner and outer loading plates. By coupling k with μ gives a similar form of frictional force equation as

$$\tilde{F} = \tilde{\mu} N \tag{4.17.2}$$

Hence, the coefficient of friction is actually not changed but the forces associated with it. Equation (4.17.2) implies that the contact reaction forces and ultimately F_{net} at the deformed states of sprinkler (due to F_1) can be approximated by using the rigid-body static force system analysis in the undeformed states i.e. by replacing the μ by $\tilde{\mu}$ in equations (4.13) to (4.16).

Since the changes in reaction forces are all dependent on F_1, the friction model is formulated from the relationship between F_1 and μ. Using least squares method, the linear model for the coefficient of friction $\tilde{\mu}$ as a function of first assembly force F_1 is shown in Figure 4.24. When the friction model (called the $\mu-$model), expressed as

$$\tilde{\mu} = -0.000623 * F_1 + 0.1264 \tag{4.18}$$

is used with equations (4.15) and (4.16), very good agreement between the analytical model and experiment is obtained as can be seen in Figure 4.25. The maximum relative difference between the improved analytical model and experiment is about 3%.

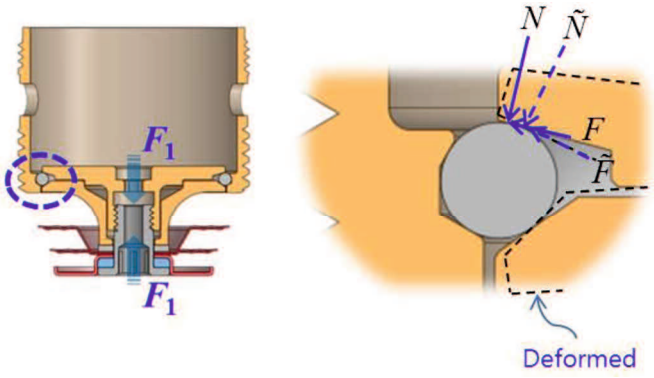

Figure 4.23 Change in orientation of contact forces due to the deformation of sprinkler during assembly

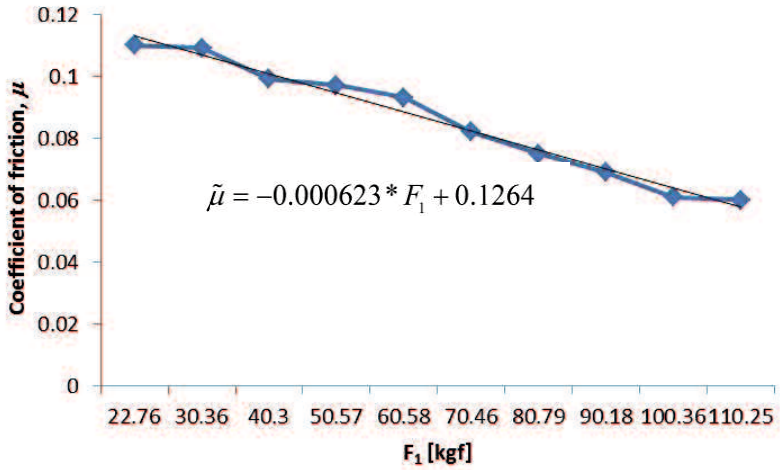

Figure 4.24 Linear friction model ($\mu-$model) using least squares method

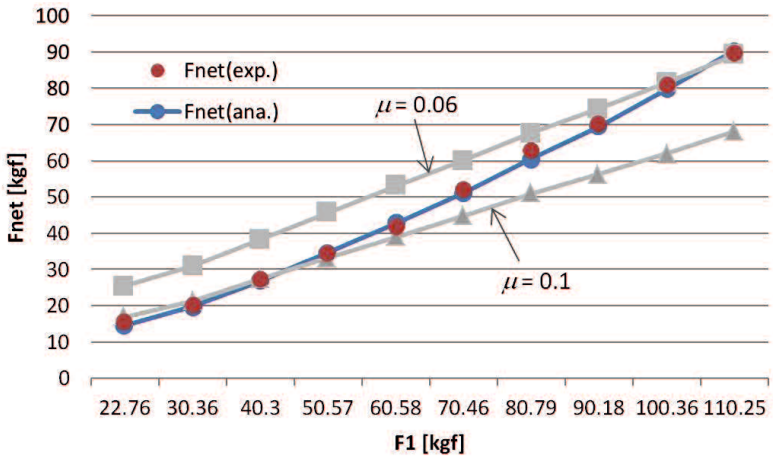

Figure 4.25 F_{net} with the proposed $\mu-$model compared with experiment data and rigid-body static analysis

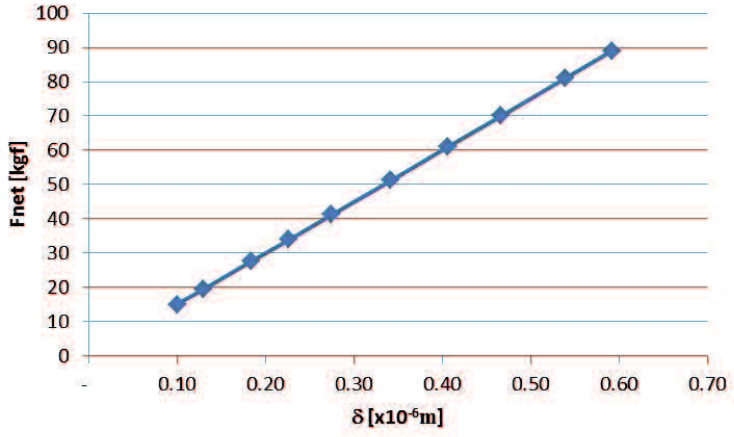

Figure 4.26 Fuse metal deformations due to F_{net} calculated with the proposed $\mu-$model.

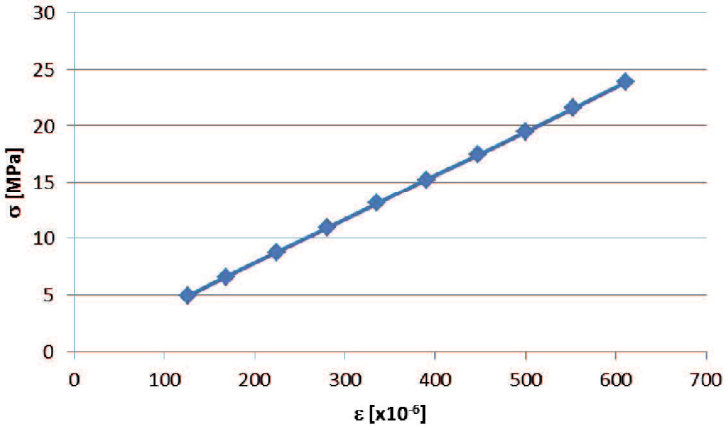

(a) After 1st assembly load F_1

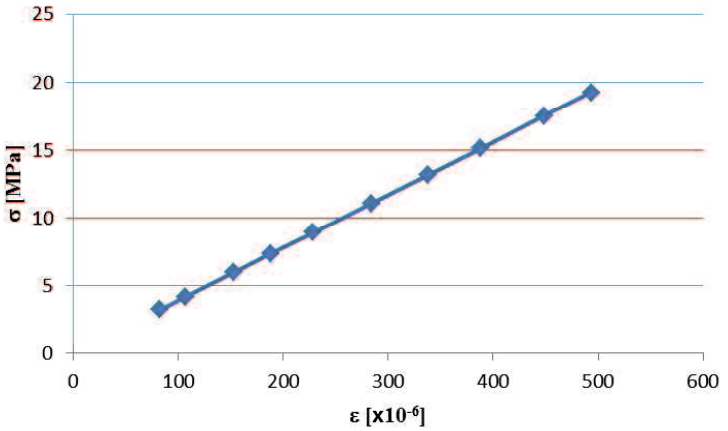

(b) After 2nd (full) assembly with F_{net} calculated using μ-model

Figure 4.27 Stress–strain in the fuse metal during assembly process

Structural responses of the fuse metal to F_{net} calculated with the proposed $\mu-$model are shown in Figure 4.26 and Figure 4.27. As can be expected, the deformations and stresses in the fuse metal due to F_{net} are relatively lower than due to F_1. This reduction of deformations and stresses in the fuse metal at the end of sprinkler full assembly imply that load or stress relieving or relaxation exists. The magnitude of load relaxation on the fuse metal for such class of sprinklers can be accurately predicted using the analytical model developed herein.

4.5 Application of the proposed analytical model to sprinkler design

The analytical model for the determination of sprinkler assembly forces can be applied for design improvement or to help conceptualize new design. In this section, structural response of sprinklers according to changes in the identified design parameters is evaluated using the proposed analytical model.

For the same class of sprinklers (the one considered in this study), the angular orientation of the contact surfaces of the inner loading plate (β), outer loading plate (γ), and frame (θ) as shown in Figure 4.28 (c.f. Figure 4.19) are critical to the proper operation of the sprinkler. For instance, if the surfaces in the inner and outer loading plates are horizontally flat or at zero degree (with respect to horizontal plane), the sub-assembly cannot be secured with the frame due to the absence of force component that will stretch the retaining ring and push it to frame groove. In other words, the components cannot be sub-assembled. If the angles of the surfaces are too steep, the sprinkler may not activate or delay its activation since the surfaces of the loading plates will tend to block the retraction of the retaining ring and will

remain in the frame groove, preventing the heat collector sub-assembly (first sub-assembly without the frame) from ejecting and the deflector assembly from descending. Additionally, depending on the values of these angles, F_{net} , and consequently deformation and stress of the fuse metal will change. Table 4.2 shows the summary of structural response for the existing design corresponding the design parameter settings and assembly loads.

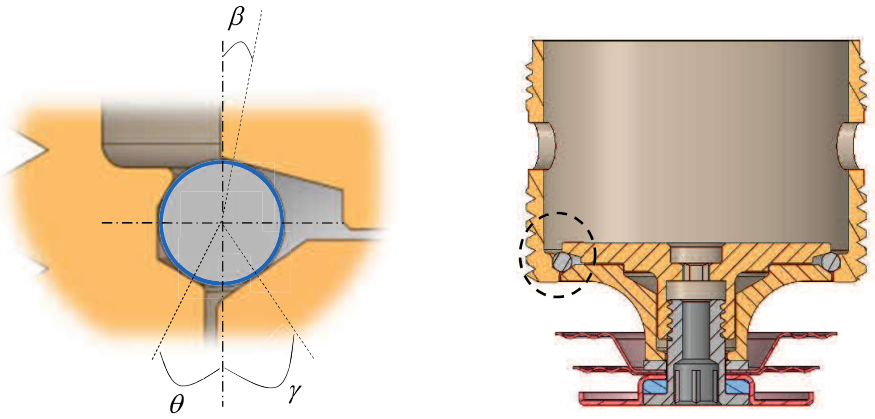

Figure 4.28 Design parameters affecting sprinkler structural performance

Table 4.2 Design parameter settings and structural response for the existing sprinkler

Design parameters [°]			Assembly loads [kgf]		Structural response		
θ	γ	β	F_1	F_2	F_{net} [kgf]	σ [MPa]	$\delta \times 10^{-6}$[m]
30	35	15	100	60	79.38	17.15	0.528

4.6 New sprinkler design

4.6.1 Problems with existing sprinkler design

The existing sprinkler has been observed to spray water into the area unevenly [47]. Such spray pattern characteristics can be disadvantageous for controlling or extinguishing a fire. For instance, at areas where water distribution is relatively less, temperature may not be lowered quickly and significantly to control the fire and prevent its growth. Based on this characteristic, sprinklers have to be installed with suitable spacing to ensure effective protection from fire. For this case, it implies closely-spaced sprinklers – a need for many sprinklers.

Moreover, the existing sprinkler is thought to have too many components. Consequently, it requires more materials and cost for manufacturing.

4.6.2 Proposed new sprinkler design

Based on the observed problems of the existing sprinkler as discussed in the preceding section, new sprinkler design is proposed. The proposed design is mainly driven by the following major ideas: (1) to improve water spray distribution pattern i.e. to discharge the water to the area as even as possibly, (2) to reduce the number of components, and (3) and to obtain a relatively slimmer sprinkler. Moreover, to classify the proposed sprinkler design as residential sprinkler, the RTI of $50\ (\text{meters}\cdot\text{seconds})^{1/2}$ or less is imposed as design constraint.

The proposed sprinkler design is illustrated in Figure 4.29. In the proposed design, the essential features related to the process or mechanism for activating the existing sprinkler is maintained i.e. the opening of the orifice is triggered by the release of the retainer ring resulting from the melting of fuse metal.

The number of components is reduced by integrating several components into a single component and designing its geometry according to the functions of the merged components. In the proposed sprinkler design, the frame assembly and deflector are integrated wherein unlike the existing sprinkler in which the deflector assembly descends during activation, the proposed deflector is fixed with the body, therefore, static. The valve cap which is an individual component in the existing design is integrated with the inner loading plate. This sprinkler configuration has eliminated the necessity for impress screw, thus it has been removed in the proposed design. Figure 4.30 illustrates the component integration design concept that has enabled the reduction of assembly components for the proposed sprinkler.

In order to produce even water spray distribution, the shape of the deflector is designed to have equally-spaced same size rectangular holes. This way, the deflector can provide uniformly-sized openings for water discharge. Hence, uniform or even water distribution over the area can be obtained.

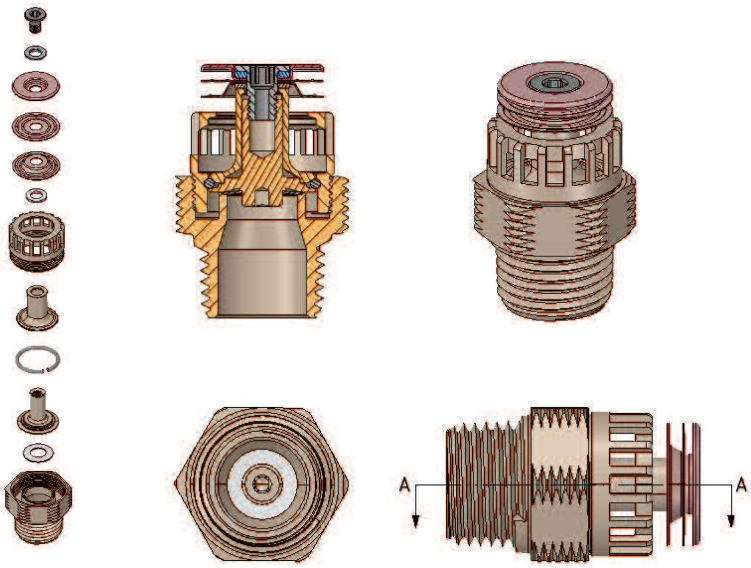

Figure 4.29 The proposed design of new residential fire sprinkler

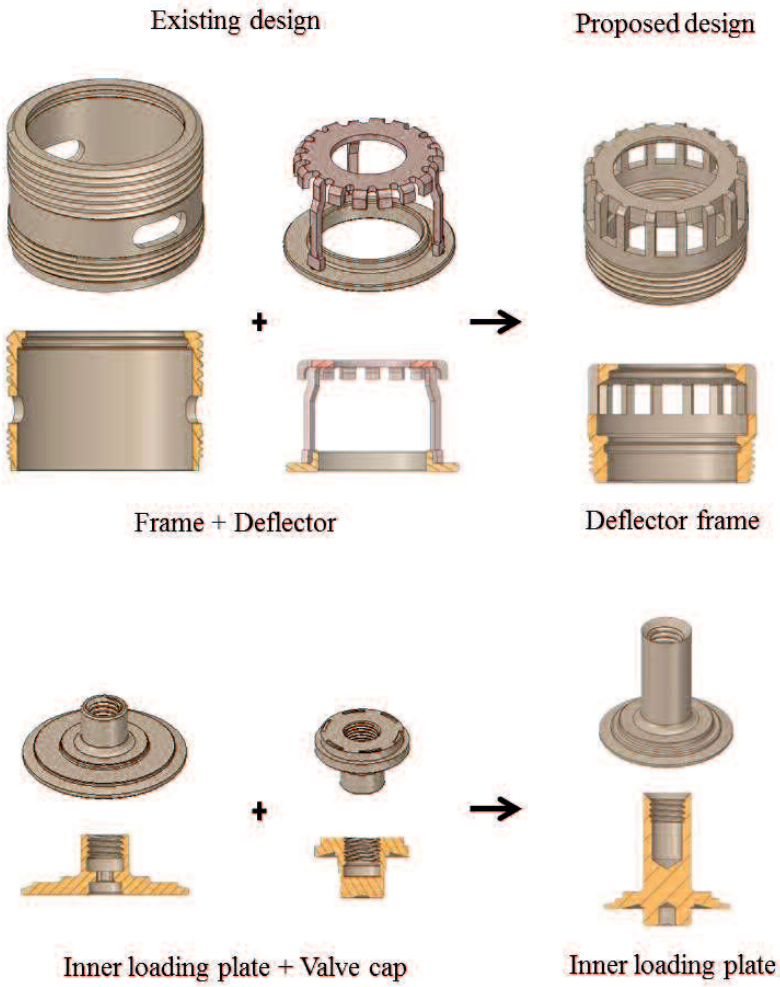

Figure 4.30 Component integration for the proposed sprinkler design

4.6.3 Assembly forces for the proposed new sprinkler

The total number of components for the proposed new residential sprinkler is 12, compared to 18 for the existing design. These components can be assembled in two essential steps in manners which are quite similar with that of the existing sprinkler. Figure 4.31 shows the complete and identified components for the proposed sprinkler and how they are assembled. As in the case of existing sprinkler, fuse metal, heat collectors and outer loading plate are joined or clamped together by the locking screw and inner loading plate during the first step of assembly process.

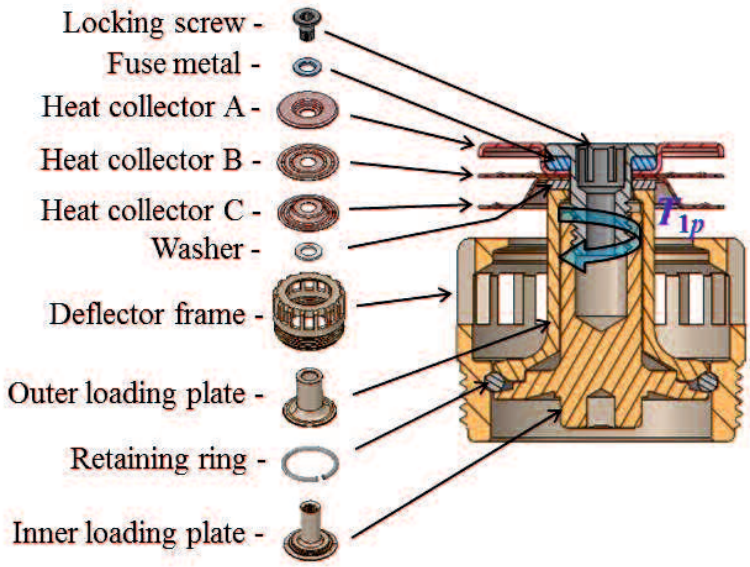

(a) **First assembly force**: Torque T_{1p} is applied in similar manner and purpose as the existing sprinkler

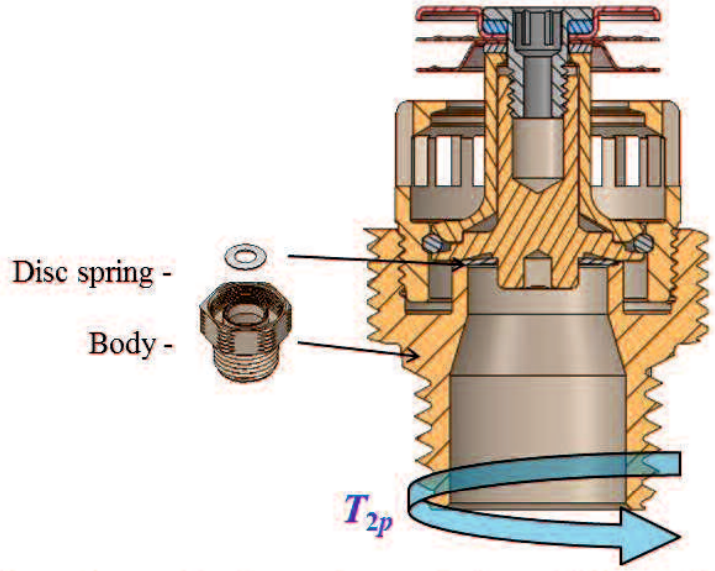

(a) **Second assembly force**: Torque T_{2p} is applied to tighten the Deflector frame with the Body, in effect the Disc spring is pressed against the nozzle to shut the opening and prevent water leakage.

Figure 4.31 Assembly sequence and corresponding forces for the proposed sprinkler

The clamping effect is created by applying suitable torque or *first assembly torque*, T_{1p} to the locking screw (bolt) against the inner loading plate (nut). In the second step, the sprinkler body is tightened with the deflector frame by applying the *second assembly torque*, T_{2p}. While the second assembly load is applied, the disc spring is pressed against the orifice to tightly close the orifice and prevent water leakage or discharge until the sprinkler is activated.

4.6.4 Friction model for the proposed new sprinkler

In terms of structural response aspect, the major difference between the existing and new sprinkler is the size of the retaining ring. The retaining ring diameter of the new design is about 5 mm smaller than the existing sprinkler. For the same wire diameter, the spring force exhibited by the ring with smaller ring diameter is higher than the one with larger ring diameter, i.e. the new design requires greater first assembly force than the existing design. Accordingly, the reaction forces will behave differently for the new sprinkler.

The procedures for the formulation of analytical model for the existing design have been implemented for the design of the proposed sprinkler. The verified friction model for the proposed sprinkler is shown in Figure 4.32.

4.6.5 Design parameter settings for the proposed new sprinkler

In such case, the effect on net compressive load on the fuse metal for the new design can be regulated by selecting the suitable values for the design parameters β, γ, and θ (angles for inner loading plate, outer loading plate, and frame, respectively). Table 4.3 shows the options for the design parameters for the proposed

design. Based on the structural performances of several design options, New 3 option was chosen.

4.7 Water spray pattern of the existing sprinkler

One of the performance requirements for sprinklers intended for residential protection is its water spray distribution pattern or spray pattern. The sprinklers spray pattern is designed for control of fire growth and prevent flashover in the space where fire starts by wetting of the area and the combustibles. The water spray distribution pattern dictates the importance of sprinkler spacing. Thus, it is imperative that this performance be known prior to putting the sprinkler to actual service. In this study, residential sprinkler with K-factor of K-50 were tested for spray pattern performance. Figure 4.33 shows the spray pattern characteristics for two different water pressures of 0.02 MPa and 0.05 MPa. It can be seen that water distribution varies significantly at position or points located at the same radial distance from the point vertically below the sprinkler. This uneven water distribution can be attributed to the geometric design of the deflector and may affect the ability of the sprinkler to control or extinguish the fire.

4.8 Response time index (RTI) of the existing sprinkler

A sprinkler with low RTI indicates that it is fast or quick response type. There exist specific ranges of RTI for sprinklers to be classified as fast or quick response, special response or standard response type. For residential application, sprinklers must be of quick response types which have RTI of $50\,(\text{meters}\cdot\text{seconds})^{1/2}$ or less. Four samples of the existing K-50 sprinklers were subjected for RTI test using the

sensitivity test oven. The average RTI of $44.8\,(\text{meters}\cdot\text{seconds})^{1/2}$ suggests that the considered existing K-50 sprinkler is acceptable for residential application. Details of the test results are shown in Table 4.4.

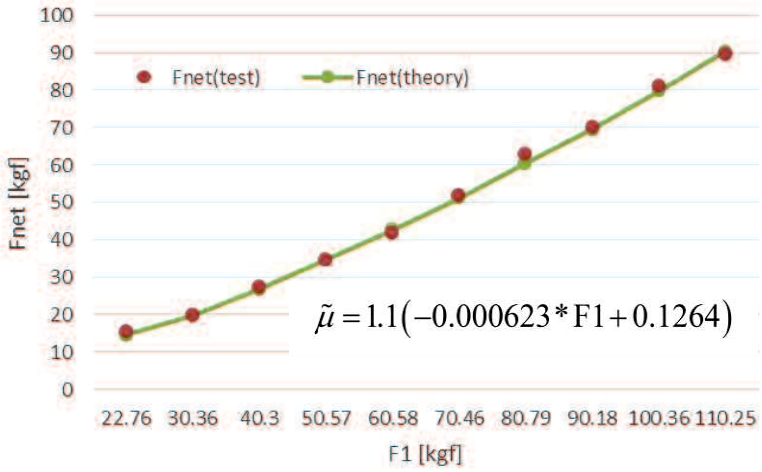

Figure 4.32 Verified friction model for the new sprinkler design

Table 4.3 Design parameter settings and structural response for the proposed new sprinkler

Sprinkler	Design parameters [°]			Assembly loads [kgf]		Structural response		
	θ	γ	β	F_1	F_2	F_{net} [kgf]	σ [MPa]	$\delta\times10^{-6}$[m]
Existing	30	35	15	100	60	79.38	17.15	0.528
New 1	30	35	15	100	60	76.06	16.44	0.505
New 2	30	35	10	100	60	79.84	17.25	0.531
New 3	30	30	15	100	60	75.08	16.22	0.499
New 4	30	30	10	100	60	79.58	17.14	0.5272

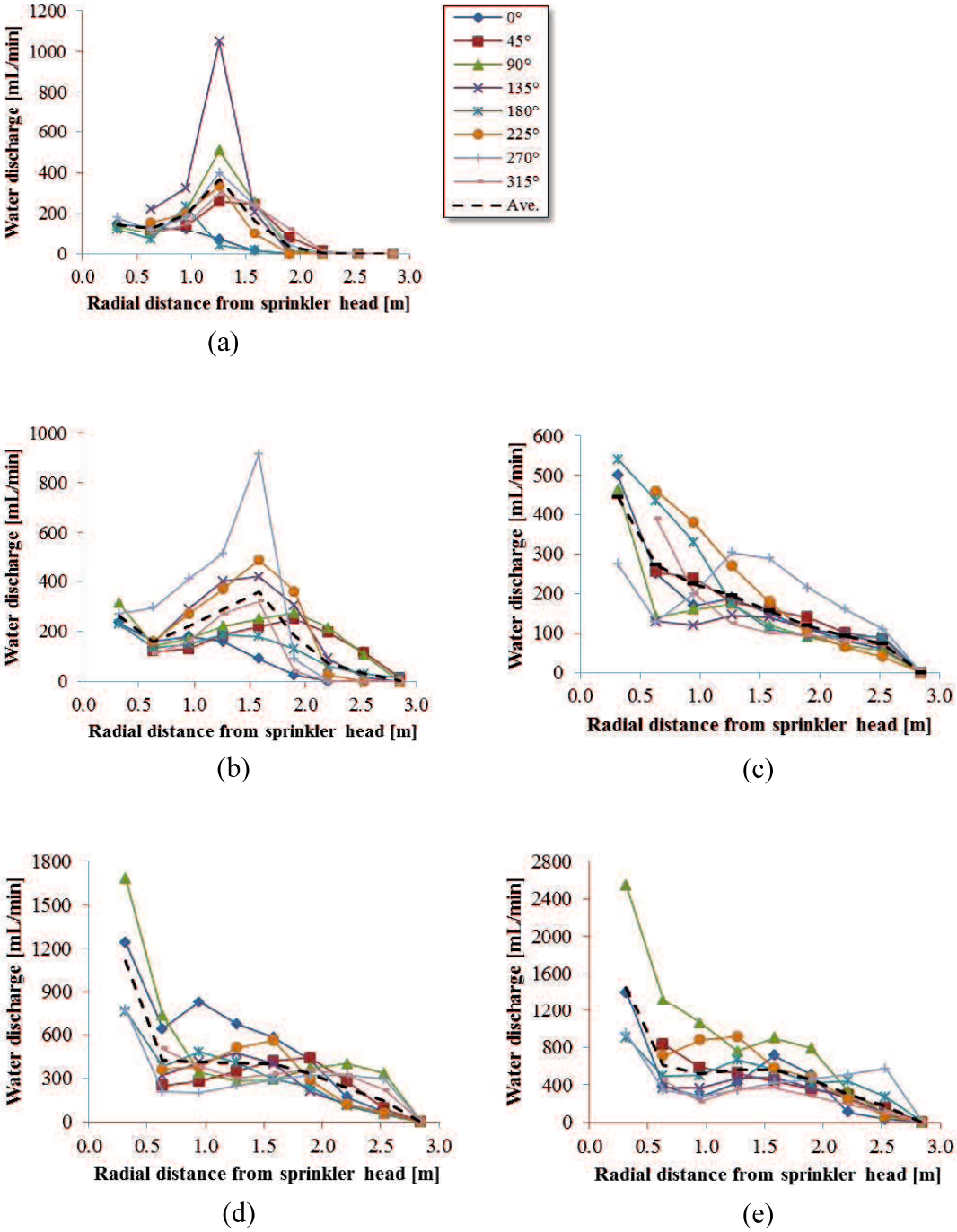

Figure 4.33 Spray patterns for the *existing sprinkler* with K-50 at (a) 0.02 MPa, (b) 0.05, (c) 0.1 MPa, (d) 0.4 MPa, and (e) 0.7 MPa water pressures.

Table 4.4 RTI for the existing sprinkler with K-factor K-50

Sample	Air temp. [°C]	Air speed [m/s]	Operating time [sec]	RTI
1	136.2	1.7	21.0	46.0
2	136.4	1.7	21.0	46.0
3	136.5	1.7	21.0	46.0
4	136.5	1.7	19.0	41.0
Average				**44.8**

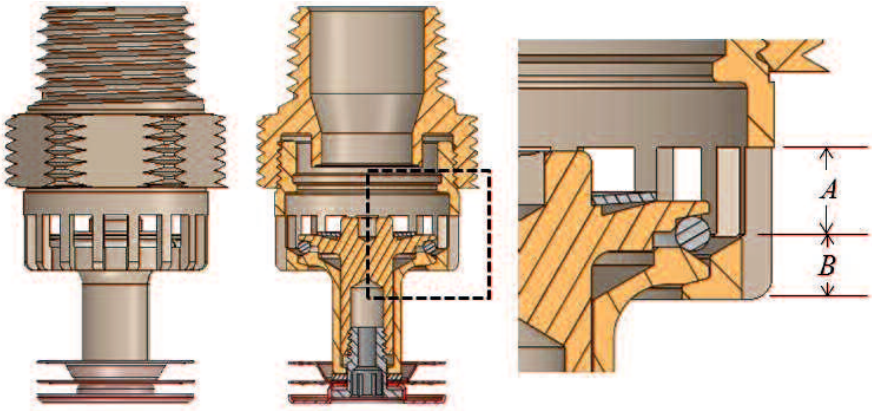

(a) Position of activated sprinkler head and the considered design parameters for water spray distribution pattern assessment.

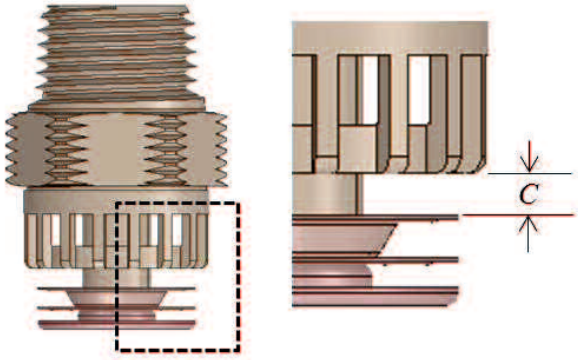

(b) Position of sprinkler head on standby mode and the considered design parameters for response time index (RTI) assessment.

Figure 4.34 Proposed sprinkler design exploration parameters for spray pattern and RTI assessment

4.9 Design exploration for spray and RTI performance

Several prototypes with different design configurations were manufactured and tested for sprinkler characteristics or performance evaluation. The design aspects that are assumed to affect water spray distribution pattern and response time are taken as design parameters.

The height of the rectangular opening or discharge ports of the deflector is varied and corresponding prototypes were tested for spray pattern characteristics. Figure 4.34(a) illustrates the design parameters for spray pattern testing. For the case of RTI, obviously the greater volume of hot air (used in RTI testing device) passing through the heat collectors will transfer more heat, melting the fuse metal quickly. Hence, the distance between the heat collector C and the deflector frame is chosen as the design variable as illustrated in Figure 4.34(b). Accordingly corresponding prototypes were also tested.

The extent of design parameters exploration (trial-and-error) is constrained by the minimum performance required by standard regulations. That is, the average water spray distribution at 0.1 MPa must be above the regulation curve and $RTI \leq 50$.

4.10 Water spray pattern of the proposed sprinkler

Prototypes of sprinklers with K-factor of K-50 and varied values of the design parameters A and B were tested for spray pattern characteristics. Design parameters $A = 4.2\,\text{mm}$ and $B = 3.0\,\text{mm}$ were found to exhibit acceptable spray pattern performance. At water pressures of 0.02 MPa and 0.05 MPa, the spray patterns appear to be even for points at the same radial distance from the sprinkler as shown

in Figure 4.35. Results from tests at higher pressures of 0.1 MPa, 0.4 MPa, and 0.7 MPa, show that the performance of *proposed sprinkler* is accordance with standard regulation for a minimum water pressure of 0.1 MPa as can be seen in Figure 4.36. Although the regulation is only set for 0.1 MPa, for the purpose of visual verification the regulation curve is also shown in higher test pressures.

4.11. RTI of the proposed sprinkler

Several samples of the proposed sprinklers with $A = 4.2$ mm, $B = 3.0$ mm and varied values for the design parameter C were subjected to RTI testing. Table 4.5 shows the RTI of three samples for each design exploration. Here, design exploration 3 with $C = 3.3$ mm and average RTI of 48 is chosen. Although performance-wise sprinkler design with $C = 4.3$ mm is better however, one of the considerations for the design is practically to minimize the amount of material – large C means longer loading plates. So, the least value for C that can produce RTI 50 or less is preferred.

Table 4.5. RTI for the proposed sprinkler with K-factor K-50

Exploration		RTI			
		Sample 1	Sample 2	Sample 3	Ave.
1	C = 2.0 mm	59	59	66	61
2	C = 2.3 mm	59	55	50	54
3	C = 3.3 mm	48	48	47	48
4	C = 4.3 mm	44	44	48	45

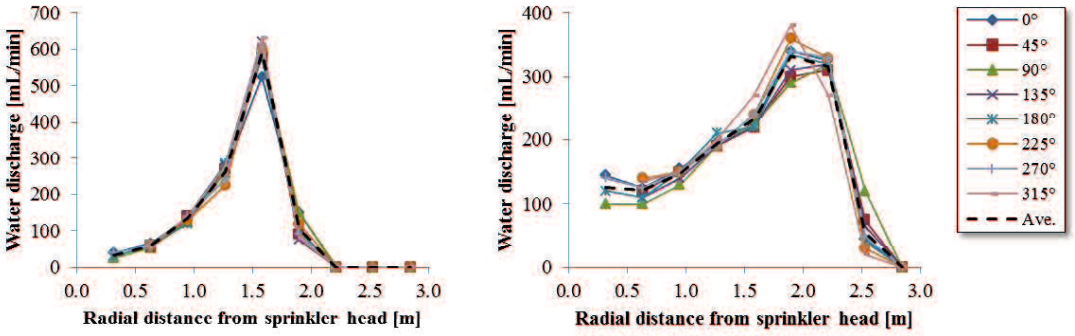

(a) (b)

Figure 4.35 Spray patterns for the *proposed sprinkler* with K-50 at (a) 0.02 MPa and (b) 0.05 MPa water pressures

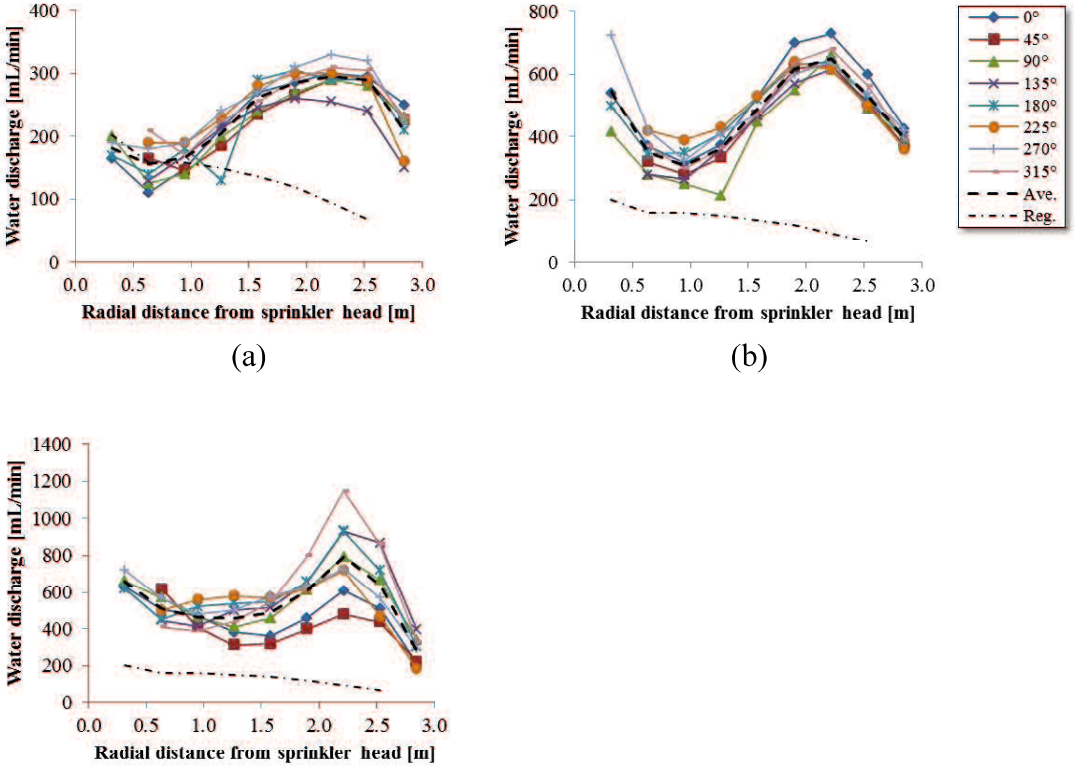

(a) (b)

(c)

Figure 4.36 Spray patterns for the *proposed sprinkler* with K-50 at (a) 0.1 MPa, (b) 0.4 MPa, and (c) 0.7 MPa water pressures.

4.12 Sprinkler design summary

Summary of the key physical features of the existing and proposed sprinkler designs is presented in Figure 4.37. The proposed sprinkler design is relatively slimmer, consists of six-piece less number of components and over 32% lighter than the existing design. Experiments show that the proposed sprinkler can distribute water evenly and meets standard regulation for water pressure of 0.1 MPa or higher. The RTI of the proposed design is $48\,(\text{meters}\cdot\text{seconds})^{1/2}$ and therefore qualifies as quick response residential type sprinkler.

A closer look at the sprinkler performances, interestingly the average RTI for the existing design is $44.8\,(\text{meters}\cdot\text{seconds})^{1/2}$ compared to the proposed design of $48\,(\text{meters}\cdot\text{seconds})^{1/2}$. Thus, it can be said that existing sprinkler will activate and discharge water into the fire area faster than the proposed final design. The faster response characteristic of existing sprinkler can compensate its relatively slight weakness in water spray distribution performance. Therefore, the proposed sprinkler can be taken as an alternative not a total replacement of the existing design. Then, marketing of these two variants of residential sprinklers can be challenging, however it is outside the scope of this study.

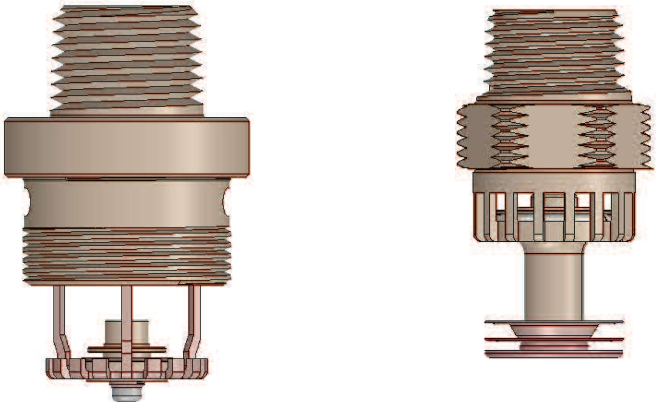

(a) Position of activated sprinklers; existing (left) and proposed (right)

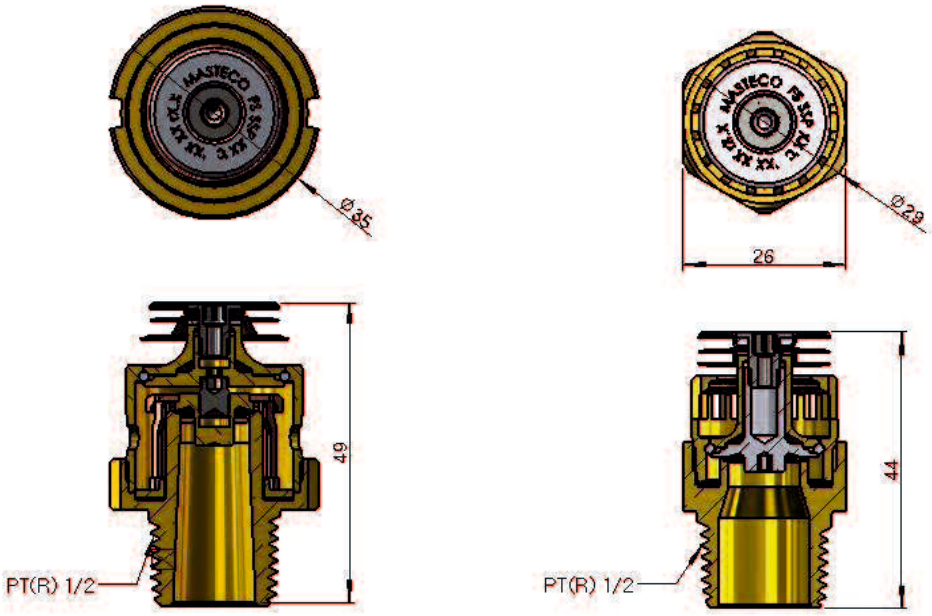

(b) External dimension of sprinklers; existing (left) and proposed (right)

Figure 4.37 Key physical features of the existing and proposed sprinkler designs

Chapter 5

SMART RESIDENTIAL FIRE PROTECTION SYSTEM

5.1 Overview

Embedded system is applied for the development of smart residential fire detection and extinguishing system. Wireless communication capability is integrated into various fire sensors and alarm devices. The system activates the fire alarm to warn occupants, executes emergency and rescue calls to remote residents and fire-fighting facility in an intelligent way. The effective location of extra sprinklers within the space of interest for the fire extinguishing system is also investigated. Actual fire test suggests that the developed wireless system for the smart residential fire protection system is reliable in terms of sensors and their communication linkage.

5.2 System workflow

In residential structures, a potential fire can be indicated by the presence of smoke, heat, gas or their combination. The smart fire protection system presented in this article is initiated upon the detection of these early indicators of fire. Generally, the presence of fire indicators is detected using sensors [28, 48-51]. The sensors trigger the alarm system when the concentration of detected smoke, carbon monoxide (CO), liquefied natural gas (LNG), or liquefied petroleum gas (LPG) has met the criteria for alarm activation i.e. above threshold values. These sensors are interfaced with the control system so an automatic fire notification system is executed at the instant the fire alarm is activated. Telephone networking is included in the control system thereby automatic notification call or message is sent to the fire

department and residence owners who are off the premises. In an unlikely event of fire, the sprinkler system is activated allowing water to flow out of the sprinklers to extinguish the fire. Since the residential sprinklers are temperature-activated, only the sprinkler closest to the fire source is set off thus, reducing damage to properties. Water pressure information in the sprinkler line is sent into the control system through the standalone type alarm valve. The water pressure required to extinguish the ongoing fire is supplied by a water pump that is also interfaced with the control system. When fire is totally suppressed, the water supply is automatically shut off. In case of LNG or LPG leakage is detected which is attributed by the gas concentration above the preset limits of the sensor, the gas line is automatically shut off and the gas bureau and residence owner are instantaneously notified. Essentially, the system operation is illustrated in Figure 5.1.

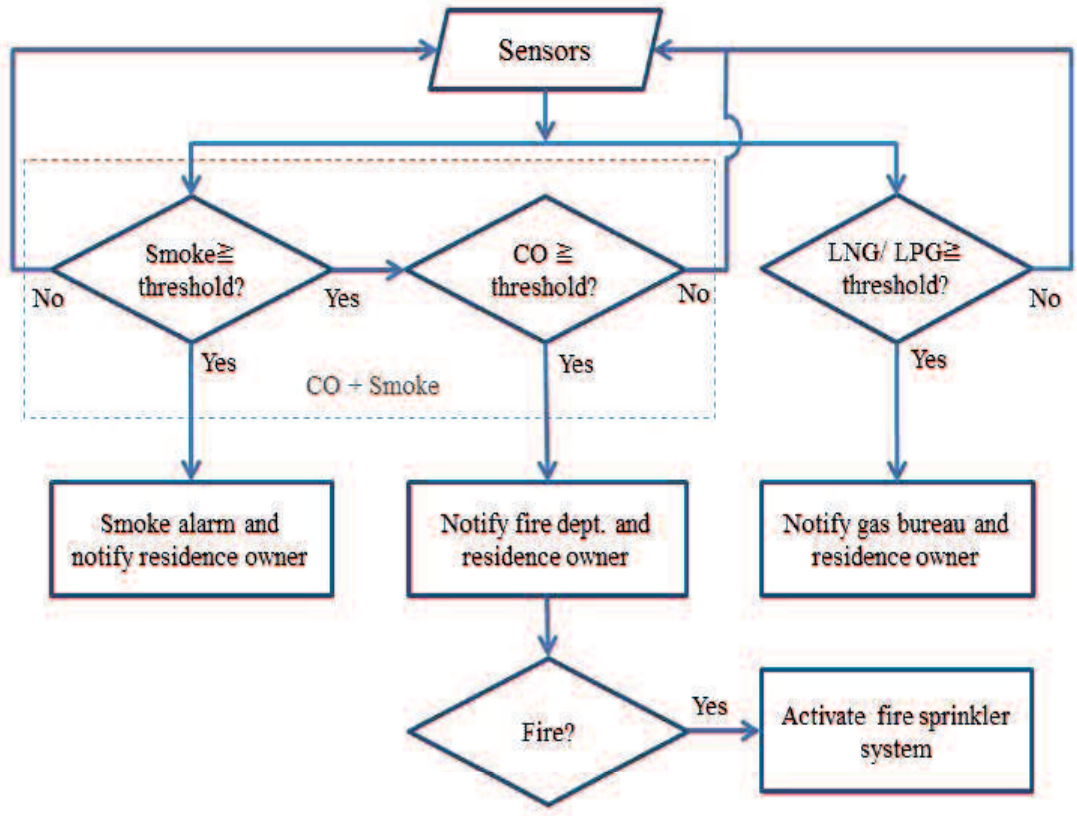

Figure 5.1 Fire protection system operation schematic

To minimize false fire alarm and rescue calls, the smart system has particularly utilized an integrated CO+Smoke sensor which follows an algorithm for identifying actual fire based on the combination of detected smoke and CO concentration. This is mainly based on the fact that CO is a product of an incomplete combustion that is characterized by the presence of smoke. In other words, the amount of CO present in the detected smoke is a determining factor for fire detection, fire extinguishing system activation, and subsequent notification calls. Various other algorithms for similar kind of sensor integration for fire detection are available in the literature (see [26, 29, 49, 52] among others). In the developed residential fire detection and extinguishing system presented herein the corresponding sensor triggers the alarm when threshold value is reached (as depicted in Figure 5.1). These threshold values are preset by the manufacturer. Additionally, the CO+Smoke sensors installed in the whole area can be wirelessly interconnected with each other, so that if one detects smoke or confirms fire, the alarm will sound on all sensors in the network. This setup improves the ability to get the residents alerted either they are on closed-door bedrooms or living two floors away from the location. Wireless linkage and networking of the CO+Smoke, LNG/LPG and water pressure sensors with the control system is implemented using ZigBee technology as depicted in Figure 5.2. By having the sensors wirelessly interconnected, the technology allows the sensors to be retrofitted in a residential building without costly wire installations.

Conventional sprinkler system often gets its water supply from an overhead water reservoir or through connection to commercial water line which may need pump to maintain the required water pressure. The sprinkler system for this proposed

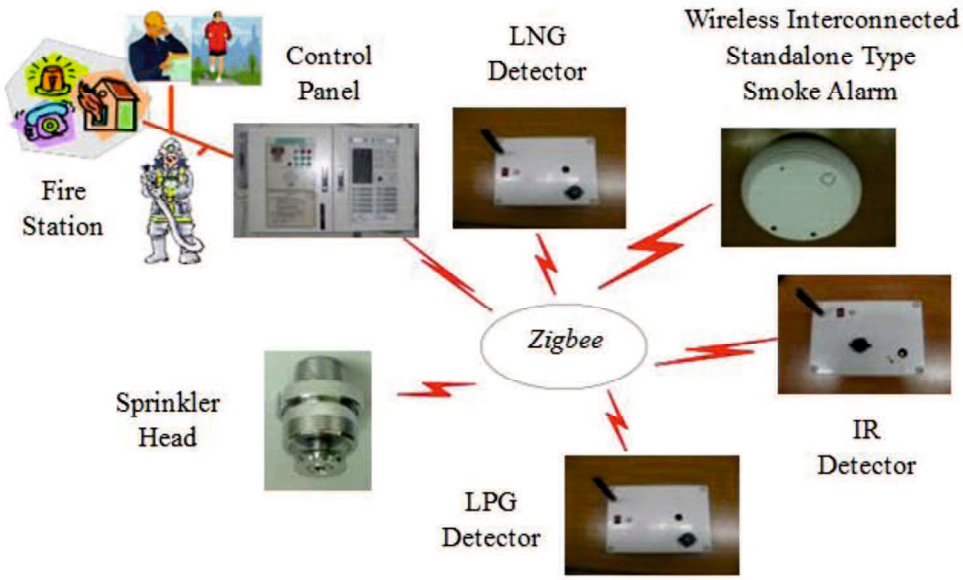

Figure 5.2 Wireless linkage system

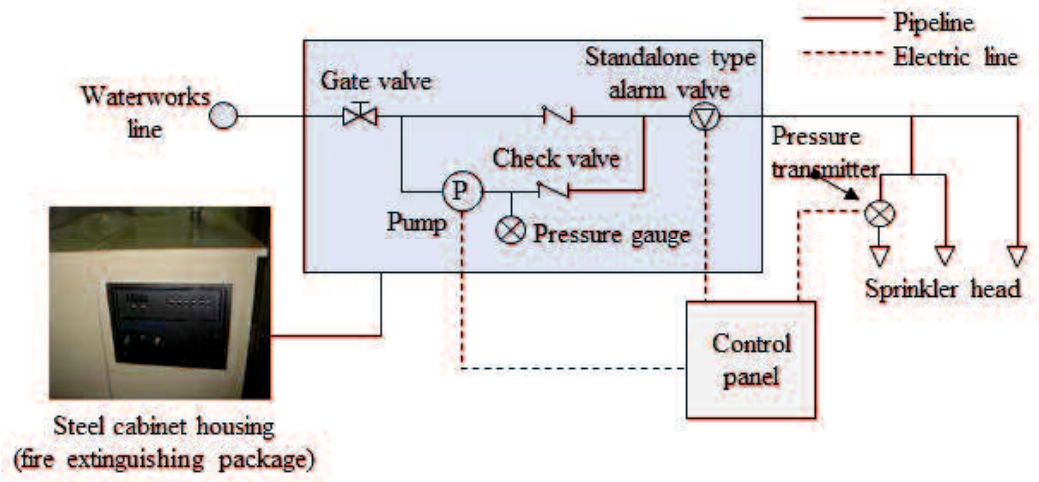

Figure 5.3 Sprinkler system connection with the control system

smart fire protection system has implemented a compact cabinet-type design. That is except for the sprinklers and the corresponding water pipe lines, all components of the sprinkler system such as water tank, pumps, pressure gauges, valves etc., and even the control panel are housed in a steel cabinet. This feature has made the system highly mobile, can be conveniently installed in residential buildings and transferred from one property to another. The fire extinguishing sprinkler system is depicted in Figure 5.3.

The smartness of the developed system can be described by its ability to discriminate or make decisions when to trigger the necessary alarms, execute notification calls, or activate and regulate the fire extinguishing system automatically. Furthermore, it is capable of monitoring and storing information of all events in the system.

5.3 System components

5.3.1 CO+Smoke sensor

Existing standalone alarm type fire sensor is basically capable of fire detection through smoke sensors with local alarm. In this study, wireless CO+Smoke sensor used for the proposed fire protection system enables wireless interconnection with other sensors which has added safety feature as has been described in the preceding section. It is basically consists of two sensors, CO and infra-red (IR) smoke sensors packed into a single unit. As a result less expensive compared to having two separate sensors for the same purpose. Wireless buzzer is added to activate sound alarm once detection is confirmed. Table 5.1 shows the specification of the CO+smoke sensor.

Table 5.1 Specifications of the CO+Smoke sensor

Sensor	CO	IR Smoke
Threshold	0.055% (550 ppm)	15% obs./m
Alarm	Buzzer (1 mW, 54 mA)	
Transmission	ZigBee (2.4 GHz, 9600 bps)	
Size (mm)	50H x 120D	

Table 5.2 Specifications of the LNG and LPG sensor

Sensor	LNG	LPG
Threshold	1.25%	0.45%
Current	120 mA	
Transmission	ZigBee (2.4 GHz, 9600 bps)	
Size (mm)	180W x 130H x 35D	

Table 5.3 Specifications of the Wireless I/O and TCP/IP module

Module	I/O	TCP/IP
Current	100 mA	200 mA
Transmission	Zigbee	Serial
Size	53W x 40D	65W x 18H x 42D

5.3.2 LNG/LPG IR sensor

LNG or LPG leakage in the residential buildings is potentially hazardous. For instance, natural gas leaks can cause immediate death if high concentration is inhaled. These gases are highly flammable. The developed system includes LNG and LPG IR sensors. Table 5.2 shows the specification of the LNG and LPG sensors.

5.3.3 Wireless I/O and TCP/IP interface

Wireless sensors are linked with the control panel through wireless I/O module. Zigbee wireless technology is used to receive wireless signal from each sensors and

initiate the alarm system in case of fire. The test result obtained with the communication program indicates that the wireless module can cover area within 7-meter radius. The notification system is connected with the control panel through serial ports. Through telephone line the system automatically calls the fire department for notification and fire extinguishing assistance if needed. Subsequently the residence owners are also automatically notified. Emergency notification system includes voice transmission, manual call, and communication recorder. Table 5.3 shows the wireless I/O and TCP/IP module specifications.

The CO+Smoke sensor with the wireless module was tested at a house fire environment. It was still operational and works stable when the temperature was over 400 °C. Furthermore, the wireless model has installed the reciprocal checking function and they will communicate with each other periodically. If there is no response from the neighbor sensor a notification will be sent to the residents or owner. If one sensor module is in alarm status the other alarms will be activated also.

5.3.4 Sprinkler system

Existing sprinkler system is used for the proposed residential fire protection system. For the purpose of testing, flush type sprinklers are used. Figure 5.4 shows example of the flush type sprinkler and its activation mechanism (fuse metal melts at known temperature, set off the heat collector and discharges pressurized water).

5.4 System testing

5.4.1 Wireless communication linkage test

Figure 5.5 shows the location configuration of the sensors and control panel installed for wireless communication linkage test. A monitoring program was

developed for testing purpose. To test the functionality of the devices described earlier, smoke and gas were introduced into each area where corresponding sensors were installed. Once the triggering substance is detected wireless signal was received and the fire alarm was activated. The test has shown to confirm the wireless communication capability of the system. In the fire test with a single-floor three-bedroom residential building, four CO+smoke sensors and one LNG/LPG sensor were found to be the optimal configuration. In such sensor location configuration wireless communication can be established within 7-meter radius.

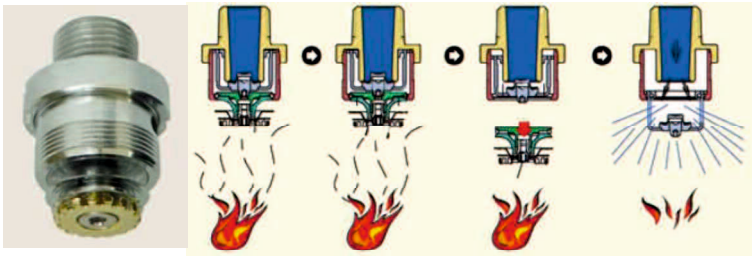

Figure 5.4 Flush type sprinklers (leftmost) and its activation mechanism during fire

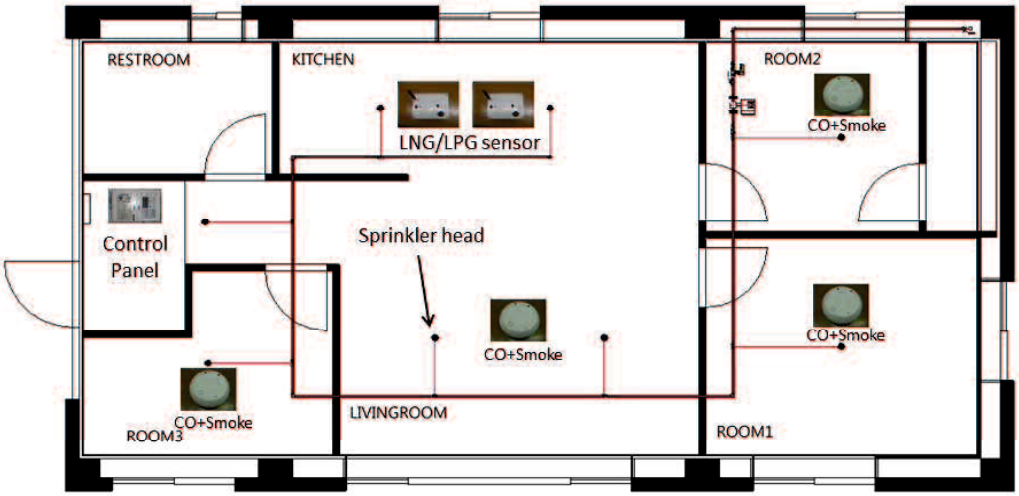

Figure 5.5 Test room configuration for wireless linkage and sprinkler system test

5.4.2 Fire and wireless linkage test.

At high temperature environment, the operational reliability of the sensors and linkage capability are highly critical. Hence, the system linkage test was carried out with fire occurrence scenario. In this study, computer program was developed for the room fire monitoring test. The program also facilitates the connection between the fire detection system and automatic fire notification system. Figure 5.5 shows the layout of the sprinklers in the test room. Wooden materials commonly found in residential buildings were contained in a metallic bin situated in the room as shown in the leftmost of Figure 5.6. The wooden material (fuel) was manually ignited. As the smoke ascended and spread into the ceiling and reached the CO+Smoke 52 seconds after ignition the fire alarm was triggered. The status monitor reported an

Figure 5.6 Fire ignition and suppression sequence during the actual fire test

active status (active = 1; standby = 0) of the CO+smoke sensor. The fusible material in the nearby sprinkler melted when ceiling temperature reached 405º C opening the head and allowing water to spray down into the fire source. Figure 5.6 depicts a sequence of fire build-up, sprinkler activation and finally fire suppression.

As can be seen in Figure 5.7(a), smoke detection status continued to be reported while the fire was ongoing with temperature over 400 °C which appear to indicate that the CO+Smoke sensor linkage was operational and stable at such

critical condition. Due to water flow in the pipe line, standalone alarm type valve sent pressure signal to the control panel. The control panel automatically adjusted the pump speed so that the required instantaneous water flow and pressure were supplied into the sprinkler. As the fire temperature gone down which indicated fire suppression, the amount of water being discharged was properly regulated. Test revealed that fire is completely extinguished within 247 sec (4.11 minutes) as shown in Figure 5.7.

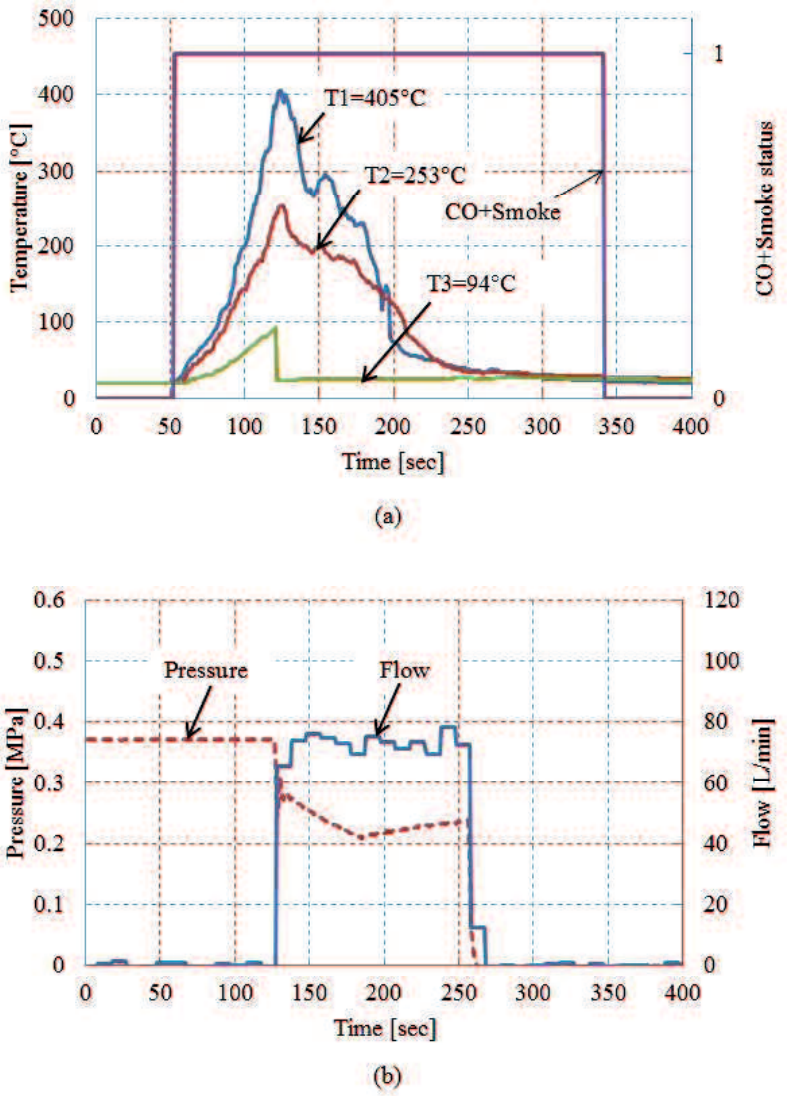

Figure 5.7 (a) Temperatures at various test points during fire suppression with the corresponding CO+smoke sensor status monitor (1-active; 0-standby) and (b)Water pressure and flow-rate data at fire suppression

5.5 Sprinkler types for the smart residential sprinkler system

In Chapter 3, different types of sprinklers were tested for water spray distribution performance. For a given water supply pressure, it was shown that a particular type of sprinkler characterized by its K-factor can be located with suitable spacing in the protected area for effective fire control or extinguishing. For instance referring to Figure 5.8(a), sprinklers having identical deflectors but different K-factors, K-30 (SR-30A) and K-50 (SR-50A), under the same water pressure of 0.01 MPa, the K-30 sprinkler can extinguish a fire within 1.3 m radius, while K-50 within about 1.9 m. Based on the spray patterns, the effective regions for fire control or extinguishing are characterized by the location of maximum water discharges. Figure 5.8 shows the images of the corresponding residential sprinklers tested for water spray patterns shown Figure 5.9. Based on water spray pattern characteristics, the recommended installation of these classes of residential sprinklers (shown in Figure 5.8) according to floor dimensions (area) of residential buildings or facilities can be determined.

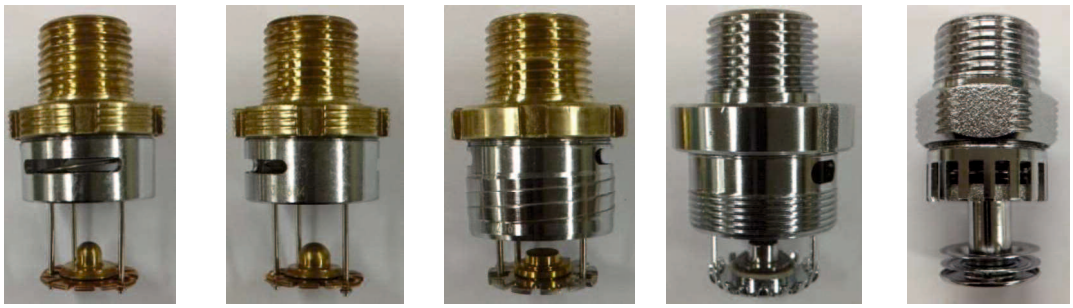

SR-30A SR-43A SR-50A MFQK50 MFQSK50

Figure 5.8 Classes of residential sprinklers for installation with the smart fire extinguishing system

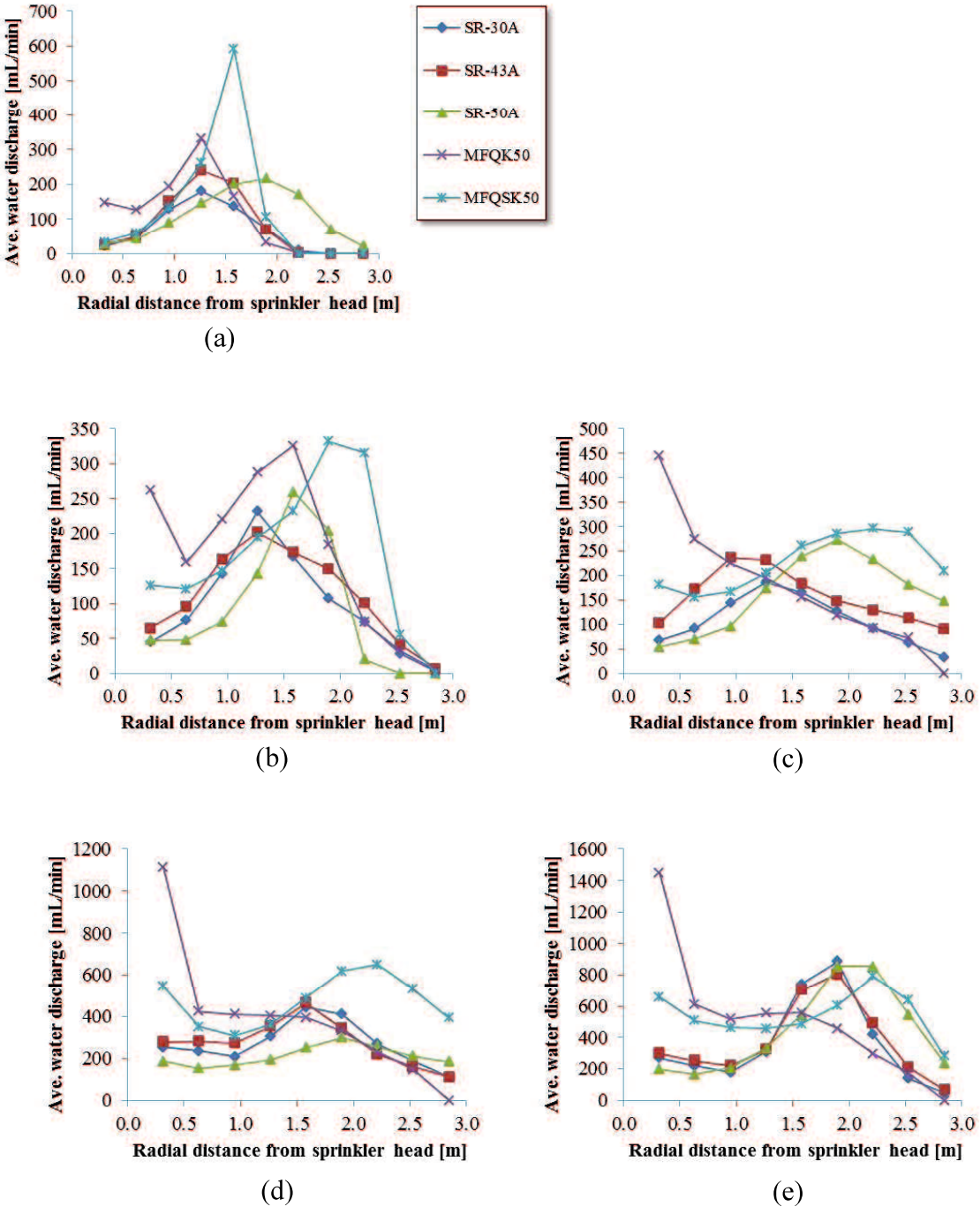

Figure 5.9 Water spray distribution patterns of sprinklers for the smart residential fire extinguishing system at (a) 0.02 MPa, (b) 0.02 MPa, (c) 0.1 MPa, (d) 0.4 MPa and (e) 0.7 MPa discharge pressures

Chapter 6

CONCLUSIONS

In Chapter 3, basic experiments were carried out to determine auxiliary tank capacity and operating pressure for a class of pipe sizes and sprinkler types for effective fire suppression. Data found after detailed examination of the results inspired the development of a low-cost, easy-to-install residential package fire extinguishing system. Conclusions are summarized as follows:

Water supply pressure and flow rate depend on the pipe sizes installed in residential facility. When water pressure is less than 0.1 MPa, auxiliary water tank and pressure booster pump are needed. The minimum required auxiliary tank capacity depends on the sprinkler type and water pressure at the sprinkler.

Sprinkler water pressure of 0.02 MPa with flow rate of 22.0 L/min or less fail to suppress the fire in crib fire test. On the other hand, water pressure of 0.1 MPa and flow rate of 50.0 L/min or over, likely to completely suppress a fire.

Simple, easy-to-install-in-houses fire sprinkler system was developed. The capacity of the auxiliary tank was determined based on various considerations such as the installed sprinkler type, pressure at the sprinkler, of water line pipe diameter, space, and cost.

In Chapter 4, rigid-body static analysis approach was developed for the analysis and design of fusible, flush, pendent, multi-component sprinkler. The proposed analysis approach is able to accurately predict the reaction forces at contact surfaces in the sprinkler for some values of first assembly loads. With the introduction of friction model, the improved analytical model becomes more generic

such that the reaction forces and ultimately the compressive load in the fuse metal for any value of first assembly load can be accurately predicted. The analytical approach is an efficient tool for exploring new designs of the same class of sprinklers. The effectiveness of the analytical tool is demonstrated in the design exploration of an alternative sprinkler. Several design parameters were explored quickly and easily using the analysis tool and prototypes are tested to ensure that the final design has met the standard regulations in terms of water spray pattern and response time index (RTI). The proposed final sprinkler design is relatively slimmer, consists of six-piece less assembly components and over 32% lighter than the existing design. Tests show that the proposed design sprays water evenly into the area and have an RTI value that meets the requirement for residential sprinkler.

In Chapter 5, the development of wireless fire detection and extinguishing system for residential application was presented. Wireless connectivity and communication capability were added to the basic features of various kinds of fire sensors using Zigbee wireless technology. The developed system allows wireless home networking that can send fire notification to residents and fire department automatically. Through actual fire test, the performance of the integrated wireless fire detection and extinguishing system has been verified even at critical condition – high temperature condition. Wireless communication among devices in the fire test room was established within 7-meter radius. The improved compact fire extinguishing system has the ability to suppress fire at the early onset within less than 5 minutes. The result of this study can be used for the development of smart, effective and efficient fire safety and fire-fighting system to address the related demands of a modern society.

REFERENCES

[1] In, 2013, "Fire Sprinklers," Fire Sprinkler Scotland.

[2] In, 2013, "Industrial Fire Sprinklers," Fire Safety Advice Center.

[3] NFPA, 2010, "Standard for the Installation of Sprinkler Systems," NFPA 13.

[4] Grant, G., Brenton, J., and Drysdale, D., 2000, "Fire Suppression by Water Sprays," Progress in Energy and Combustion Science, 26(2), pp. 79-130.

[5] NFPA, 2010, "Standard for the Installation of Sprinkler Systems in One- and Two-Family Dwellings and Manufactured Homes," NFPA 13D.

[6] Butry, D., 2009, "Economic Performance of Residential Fire Sprinkler Systems," Fire Technol, 45(1), pp. 117-143.

[7] Butry, D. T., 2012, "Comparing the Performance of Residential Fire Sprinklers with other Life-Safety Technologies," Accident Analysis & Prevention, 48(0), pp. 480-494.

[8] Madrzykowski, D., and Fleming, R., 2008, "Residential Sprinkler Systems," Fire Protection Handbook, 2008 Edition, NFPA.

[9] Wotapka, D., 2010, "Builders Smokin' Mad Over New Sprinkler Rules," The Wall Street Journal.

[10] FEMA, 2013, "Home Fire Sprinklers Save Lives."

[11] Chow, W. K., and Shek, L. C., 1993, "Phyical Properties of a Sprinkler Water Spray," Fire and Materials, 17, pp. 279-292.

[12] Melinek, S. J., 1993, "Effectiveness of Sprinklers in Reducing Fire Severity," Fire Safety Journal, 21(4), pp. 299-311.

[13] Li, K. Y., Hu, L. H., Huo, R., Li, Y. Z., Chen, Z. B., Li, S. C., and Sun, X. Q., 2009, "A Mathematical Model on Interaction of Smoke Layer with Sprinkler Spray," Fire Safety Journal, 44(1), pp. 96-105.

[14] Ren, N., Baum, H. R., and Marshall, A. W., 2011, "A Comprehensive Methodology for Characterizing Sprinkler Sprays," Proceedings of the Combustion Institute, 33(2), pp. 2547-2554.

[15] Widmann, J. F., 2001, "Phase Doppler Interferometry Measurements in Water Sprays Produced by Residential Fire Sprinklers," Fire Safety Journal, 36(6), pp. 545-567.

[16] Wu, D., Guillemin, D., and Marshall, A. W., 2007, "A Modeling Basis for Predicting the Initial Sprinkler Spray," Fire Safety Journal, 42(4), pp. 283-294.

[17] UL, 2005, "Automatic Sprinklers for Fire-Protection Service," UL 199.

[18] Tsang, N., 2004, "Study on the Response Time Index of Sprinklers," International Journal on Engineering Performance-Based Fire Codes, 6(4), pp. 234-241.

[19] Brushlinsky, N. N., Sokolov, S. V., Wagner, P., and Hall, J. R., 2006, "World Fire Statistics, Report No. 10," Center of Fire Statistics, Geneve, Switzerland.

[20] FDMA, 2013, "Fire Statistics 2012 (in Japanese)," Fire and Disaster Management Agency (FDMA), Tokyo, Japan.

[21] Karter, M. J., September 2013, "Fire Loss in the United State During 2012, Full Report," National Fire Protection Association, Quncy, MA.

[22] Sayer, G., June 2013, "Fire Statistics Monitor: England April 2012 to March 2013," UK National Statistics, England.

[23] Athens, M., 2012, "Home Structures Fires," National Fire Protection Association.

[24] Hall, J., 2012, "U. S. Experience with Sprinklers," National Fire Protection Association.

[25] In, 2012, "Fire Statistics," National Statistics, Department for Communities and Local Government.

[26] Chen, S.-J., Hovde, D. C., Peterson, K. A., and Marshall, A. W., 2007, "Fire Detection Using Smoke and Gas Sensors," Fire Safety Journal, 42(8), pp. 507-515.

[27] Ko, B., Cheong, K.-H., and Nam, J.-Y., 2010, "Early Fire Detection Algorithm Based on Irregular Patterns of Flames and Hierarchical Bayesian Networks," Fire Safety Journal, 45(4), pp. 262-270.

[28] Gutmacher, D., Foelmli, C., Vollenweider, W., Hoefer, U., and Wöllenstein, J., 2011, "Comparison of Gas Sensor Technologies for Fire Gas Detection," Procedia Engineering, 25(0), pp. 1121-1124.

[29] Gottuk, D. T., Peatross, M. J., Roby, R. J., and Beyler, C. L., 2002, "Advanced Fire Detection Using Multi-Signature Alarm Algorithms," Fire Safety Journal, 37(4), pp. 381-394.

[30] Derbel, F., 2004, "Performance Improvement of fire Detectors by Means of Gas Sensors and Neural Networks," Fire Safety Journal, 39(5), pp. 383-398.

[31] Sinopoli, J., 2010, "Fire Alarm and Mass Notification Systems," Smart Buildings Systems for Architects, Owners and Builders, J. Sinopoli, ed., Butterworth-Heinemann, Boston, pp. 103-112.

[32] Minnesota, 2009, "International Residential Code and Residential Fire Sprinklers," Minnesota Governor's on Fire Prevention and Control.

[33] Huang, L.-C., Chang, H.-C., Chen, C.-C., and Kuo, C.-C., 2011, "A ZigBee-Based Monitoring and Protection System for Building Electrical Safety," Energy and Buildings, 43(6), pp. 1418-1426.

[34] Lee, W., Cheon, M., Hyun, C.-H., and Park, M., 2013, "Development of Building Fire Safety System with Automatic Security Firm Monitoring Capability," Fire Safety Journal, 58(0), pp. 65-73.

[35] Oh, J., Jiang, Z., and Panganiban, H., 2013, "Development of Smart Residential Fire Protection System," Advances in Mechanical Engineering, Vol. 2013, pp.1-6.

[36] Zhou, X., D'Aniello, S. P., and Yu, H.-Z., 2012, "Spray Characterization Measurements of a Pendent Fire Sprinkler," Fire Safety Journal, 54(0), pp. 36-48.

[37] Zhou, X., and Yu, H.-Z., 2011, "Experimental Investigation of Spray Formation as Affected by Sprinkler Geometry," Fire Safety Journal, 46(3), pp. 140-150.

[38] Lai, C.-m., Su, H.-C., Tsai, M.-J., Chen, C.-J., Tzeng, C.-T., and Lin, T.-H., 2010, "Influence of Fire Source Locations on the Actuation of Wet-Type Sprinklers in an Office Fire," Building and Environment, 45(1), pp. 107-114.

[39] Zhu, N., and Chow, W. K., "A Brief Review on Design and Operation Principle for Nozzles Discharging Water Mist," Proc. 6th Asia-Oceana Symposium on Fire Science and Technology, International Association of Fire Science.

[40] Tanner, J., and Knasiak, K., "Spray Characterization of Typical Fire Suppression Nozzles," Proc. Third International Water Mist Conference.

[41] Sheppard, D. T., 2002, "Spray Characteristics of Fire Sprinklers," PhD Dissertation, Northwestern University.

[42] Prahl, J. M., and Wendt, B., 1988, "Discharge Distribution Performance for an Axisymmetric Model of a Fire Sprinkler," Fire Safety Journal, 14(1–2), pp.101-111.

[43] Yao, C., and Kalelkar, A. S., 1970, "Effect of Drop Size on Sprinkler Performance," Fire Technol, 6(4), pp. 254-268.

[44] In, 2001, "Heat Collector," Quick Response.

[45] Shigley, J., Mischke, C., and Budynas, R., 2004, Mechanical Engineering Design, 7th ed., McGraw-Hill, Singapore.

[46] FM, 2009, "Approval Standard for Residential Automatic Sprinklers for Fire Protection," FM 2030.

[47] Oh, J., Jiang, Z., Chung, T.-J., Panganiban, H., and Kim, M.-S., 2013, "Residential Sprinkler Design Improvement by Parametric Exploration," Innovative Application Research and Education, pp. 70-73.

[48] Marbach, G., Loepfe, M., and Brupbacher, T., 2006, "An Image Processing Technique for Fire Detection in Video Images," Fire Safety Journal, 41(4), pp. 285-289.

[49] Geiman, J., and Gottuk, D., "Alarm Threshold for Smoke Detector Modeling," Proc. 7th International Symposium on Fire Safety Science, International Association for Fire Safety Science.

[50] Gutmacher, D., Hoefer, U., and Wöllenstein, J., 2012, "Gas Sensor Technologies for Fire Detection," Sensors and Actuators B: Chemical, 175(0), pp. 40-45.

[51] Nolan, D. P., 2011, "Fire and Gas Detection and Alarm Systems," Handbook of Fire and Explosion Protection Engineering Principles (Second Edition), D. P. Nolan, ed., William Andrew Publishing, Oxford, pp. 181-201.

[52] Yu, C., Mei, Z., and Zhang, X., 2013, "A Real-time Video Fire Flame and Smoke Detection Algorithm," Procedia Engineering, 62(0), pp. 891-898.

APPENDIX

Derivation of Retaining Ring Force

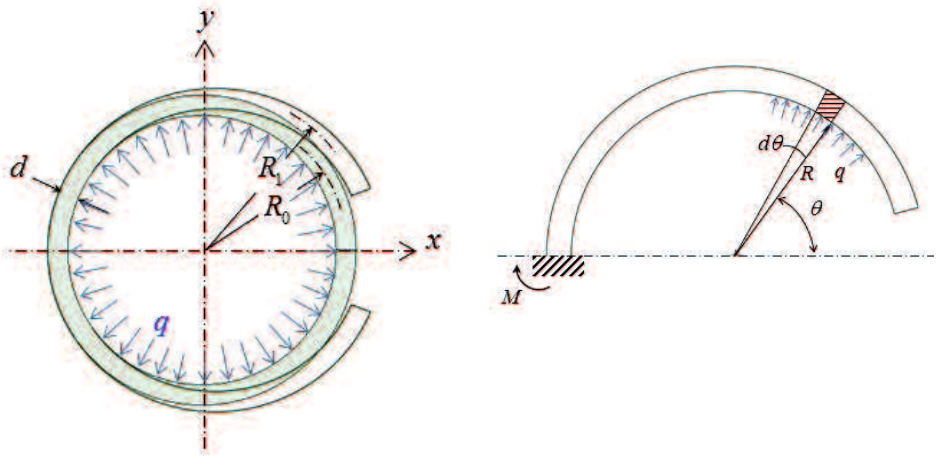

(a) (b)

Figure A.1 Retaining ring subjected to uniformly distributed outward force.

Consider a retaining ring subjected to uniformly distributed force per unit circumferential length, q as shown in the Figure A.1(a). Due to symmetry, take a half-ring and let R be the instantaneous radius of the ring or the radius of curvature as shown in Figure A.1(b). Using Euler-Bernoulli beam equation the bending moment in the ring can be expressed as

$$M = -EI\frac{\partial^2 y}{\partial x^2} \tag{A.1}$$

where E is the elastic modulus of the material and I is the area moment of inertia of the circular wire. Using Cauchy's definition of radius of curvature as

$$\frac{1}{R} = \frac{\partial^2 y}{\partial x^2} \tag{A.2}$$

equation (A.1) can be written as

$$M = -\frac{EI}{R} \tag{A.3}$$

Referring to Figure A.1(b),

$$M = \int_0^{\pi} qRd\theta R\sin\theta = -qR^2\cos\theta\Big|_0^{\pi} = -2qR^2 \tag{A.4}$$

$$N = \int_0^{\pi} q\sin\theta Rd\theta = -qR\cos\theta\Big|_0^{\pi} = -2qR \tag{A.5}$$

where N is the equivalent vertical force (along the *y*-axis). From equations (A.4) and (A.5), it can be seen that

$$M = NR \tag{A.6}$$

$$N = -\frac{EI}{R^2} \tag{A.7}$$

The derivative of equation (A.7) is

$$\frac{dN}{dR} = -\frac{2EI}{R^3} \tag{A.8}$$

or

$$\Delta N = -\frac{2EI}{R^3}\Delta R \tag{A.8′}$$

as $R: R_0 \to R_1$, $\Delta R = R_1 - R_0$, and $\frac{1}{R_0^2 - R_1^2} = \frac{(R_0 + R_1)}{R_0^2 R_1^2}\Delta R = \frac{2\Delta R}{R_0^3}$ equation (A.8′) can be approximated as

$$\Delta N = -EI\left(\frac{1}{R_1^2} - \frac{1}{R_0^2}\right) \tag{A.9}$$

where ΔN represents the outward force that will stretch the retaining ring changing its radius from R_0 to R_1 as illustrated in Figure A.1(a). In this study, ΔN referred to as the retaining ring force F_S.

ACKNOWLEDGMENT

The research presented in this dissertation was carried out at the Systems Design and Engineering, Graduate School of Science and Engineering, Yamaguchi University, Ube, Japan.

I was very fortunate to have Professor Zhongwei JIANG as my research adviser. I am sincerely grateful for his constant encouragement and skillful guidance throughout this study. His profound knowledge and exceptional scientific mindset are extremely beneficial for me and will continue to serve as my motivation for future undertakings.

I would like to thank Professor Kanya TANAKA, Professor Yasuo KATOH, Professor Shinsuke MOCHIZUKI, and Assistant Professor Minoru MORITA for their review of this dissertation, valuable comments and suggestions.

Special thanks to the members of Technology Institute, Masteco Industry Co., Ltd., Incheon Korea, for their valuable assistance in carrying out the experiments and preparation of this dissertation.

Finally, my graduate education would not have been possible without the sincere love, patience, support and encouragement of my wife, children, mother-in-law, brothers and friends.